INVESTIGATING MANAGEMENT AND GENETICS OF SOYBEAN SUDDEN DEATH SYNDROME PATHOGENS *FUSARIUM VIRGULIFORME* AND *F. BRASILIENSE*

By

Mitchell G. Roth

A DISSERTATION

Submitted to
Michigan State University
in partial fulfillment of the requirements
for the degree of

Genetics – Doctor of Philosophy
Plant Pathology – Dual Major

2019

ABSTRACT

INVESTIGATING MANAGEMENT AND GENETICS OF SOYBEAN SUDDEN DEATH SYNDROME PATHOGENS *FUSARIUM VIRGULIFORME* AND *F. BRASILIENSE*

By

Mitchell G. Roth

Annual soybean production in the U.S. is worth nearly $40 billion, valued for its oils and protein content. Many pathogens and pests cause significant soybean yield losses each year, but one of the top threats is sudden death syndrome (SDS). At least five fungal species cause soybean SDS globally, but only two have been found in the U.S.; *Fusarium virguliforme* and *F. brasiliense*. These soil-borne pathogens infect root tissues and cause root rot, with continued infection leading to foliar interveinal chlorosis, interveinal necrosis, leaf drop, and yield loss. The pathogens are strong saprophytes that can overwinter in soybean and corn residue, so successful management is difficult. Long-term crop rotations and seed treatments with fungicides show some efficacy, but these strategies can be costly for growers. Growers desire genetic resistance to SDS, but no soybean germplasm has shown 100% resistance to SDS to date. Therefore, the overall goals of projects presented in this dissertation were to help improve SDS management and explore the biology and genetics of *F. virguliforme* and *F. brasiliense*.

To achieve these goals, I developed a risk prediction tool for integration with current SDS management strategies (Chapter 2). This study revealed that pathogen data collected from soil at-planting can be used to accurately model spatial distributions pathogens and model future SDS development and yield loss at a field level. This risk prediction study used a qPCR assay specific for *F. virguliforme*, but a similar qPCR assay for *F. brasiliense* did not exist. Therefore, I developed a qPCR assay that can distinguish *F. brasiliense* from close relatives (Chapter 3).

This tool that can be used to generate SDS-prediction models for *F. brasiliense* and I predict will be valuable in diagnostic labs across the country to distinguish between these two species.

To advance our understanding of the biology and genetics of these pathogens, I developed a new protoplast generation and transformation method to generate fluorescent strains of each pathogen (Chapter 4). This chapter is the first to report genetic transformation in *F. brasiliense*. Furthermore, I used the fluorescent strains to investigate the synergistic role of soil-borne nematodes in SDS (Chapter 5). The interactions between these fungal pathogens and nematodes *in vitro* show that *F. virguliforme* and *F. brasiliense* can colonize immobile nematodes, but suggest that they are not actively vectored into soybean roots by nematodes.

The genetic mechanisms of SDS development are poorly understood, so I developed high quality genome sequences for *F. virguliforme* and *F. brasiliense* (Chapter 6) and investigated two recognized effector proteins; FvTox1 and FvNIS1 (Chapter 7). The genome assemblies developed here have significantly improved continuity, with improved genome assembly metrics like contig length (N50) and contig number. However, whole-genome alignments between *F. virguliforme* and *F. brasiliense* from soybean (*Glycine max*) or dry bean (*Phaseolus vulgaris*) did not reveal obvious mobile pathogenicity chromosomes that have been observed in the close relative *F. oxysporum*. However, these genome resources should facilitate discovery of new fungal effector proteins like FvTox1 and FvNIS1. Interestingly, my results show that FvNIS1 is able to induce a hypersensitive response in tobacco, while FvTox1 is not, suggesting a conserved mechanism between soybean and tobacco for FvNIS1 recognition.

Overall, this work provides valuable tools for managing and studying SDS-causing fungi, while also revealing insights into the genetics and genomics of the SDS-causing pathogens *F. virguliforme* and *F. brasiliense*.

I first want to thank my Lord and Savior Jesus Christ for the courage, persistence, and patience You provided me throughout my many failures during graduate school.

I dedicate this dissertation to my father, who was the first to show me what a passion for agriculture looks like. You also showed me how to work hard, acknowledge a job well done, and have fun all along the way. I also dedicate this dissertation to my mother. You are a marvelous teacher, and I have you to thank for my teaching skills today. You showed me how to approach complex problems with a clear mind and a full effort, skills that are critical to success in graduate school. I also dedicate this dissertation to my sister. You were the first person to truly inspire me to avoid excuses and always put in the effort to be the best possible version of myself. You have always been my biggest fan, the first to celebrate with me and the first to hear my complaints. Finally, I also dedicate this dissertation to my beautiful wife. You have helped shoulder my graduate school burden and supported me with three different titles; girlfriend, fiancé, and wife. Your endless encouragement, fresh perspectives, and supreme confidence in me are the biggest reasons for my success in graduate school.

Each of you have fueled my desire to push the boundaries of my understanding and become the best scientist I can be. Without the love, support, and prayers from all of you, I would not have become the person I am today, nor a successful scientist. My gratitude to all of you is beyond measure.

ACKNOWLEDGEMENTS

I would like to acknowledge my advisor, Dr. Martin I. Chilvers, for his patience, understanding, and guidance throughout all of the uncertainty that comes with earning a Ph.D. Though things did not always go as planned, you always kept a level head and provided sensible suggestions for future directions.

I would like to thank my committee members Drs. Brad Day, Frances Trail, Jonathan Walton, and Jaime Willbur for guidance and mentorship throughout my research. Without your expertise and helpful discussions, the quality of my work would be significantly lower. As I progressed through graduate school, I came to realize how valuable time is to a scientist, and I truly appreciate the time that you sacrificed to help me achieve my goals.

I would like to thank all of my fellow lab members, past and present. In particular, I want to thank Dr. Alejandro Rojas and Dr. Jie Wang for their endless patience with my naïve questions, which made my transition into graduate school very smooth. I want to thank Zachary Noel for the professional and personal support throughout the countless hours we have spent together. I value the friendships that I have with each of you and am thankful that our common research interests brought us together.

I would like to acknowledge the Genetics Graduate Program and its director Dr. Cathy Ernst for constant support in scientific and personal endeavors. The time and effort put into each student has made being part of this program an incredible experience.

Finally, I want to thank the Michigan Soybean Promotion Committee for funding a large portion of my work. I hope that my research will always have a beneficial impact on growers and commodity groups.

TABLE OF CONTENTS

LIST OF TABLES

LIST OF FIGURES

CHAPTER 1: LITERATURE REVIEW

By

Mitchell G. Roth

Introduction

The causal agent of soybean sudden death syndrome (SDS) in the U.S. was identified in 1971 in Arkansas as *Fusarium solani* f. sp. *glycines* (Rupe 1989; Roy et al., 1989, 1997). Historically, soybean SDS has also been a problem in the South American soybean producing countries Brazil and Argentina. Formal genetic and morphological studies have shown that the *forma speciales* is composed of multiple distinct species. To date, six named and one un-named SDS-causing species have been identified within clade II of the *Fusarium solani* species complex (FSSC); *Fusarium virguliforme* (Aoki et al., 2003), *F. tucumaniae* (Aoki et al., 2003), *F. brasiliense* (Aoki et al., 2005), *F. cuneirostrum* (Aoki et al., 2005), *F. crassistipitatum* (Aoki et al., 2012a), *F. azukicola* (Aoki et al., 2012b), and an unnamed species in South Africa (Tewoldemedhin et al., 2017). Another FSSC clade II species is described as causing root rot; *F. phaseoli* (Aoki et al., 2003). Many of these species had been found in countries outside of the U.S., so it was previously thought that only *F. virguliforme* was present in the U.S. However, recent surveys have identified *F. brasiliense* and *F. cuneirostrum* in Michigan, although *F. virguliforme* remains the most prominent species (Jacobs et al., 2018; Wang et al., 2018).

In the U.S., soybean SDS caused an average 27.7 million bushel yield loss between 2004 and 2009, and an average 41.9 million bushel yield loss between 2010 and 2014 (Wrather and Koenning 2009; Koenning and Wrather 2010; Allen et al., 2017). With current soybean values worth approximately $9 per bushel, the economic loss due to SDS between 2010 and 2014 is estimated at $377 million. SDS-causing pathogens cause soybean yield loss through two-phases

of symptom development. First, initial symptoms of SDS appear in at the site of infection in the roots as discoloration and rotting (Fig. 1-1). Second, foliar symptoms develop as infection progresses which is marked by interveinal chlorosis that turns to interveinal necrosis, which leads to premature leaf drop and pod abortion (Fig. 1-1) (Hartman et al., 2015). These foliar symptoms typically occur much later in the growing season around flowering (Hartman et al., 2015), though they can develop prior to flowering.

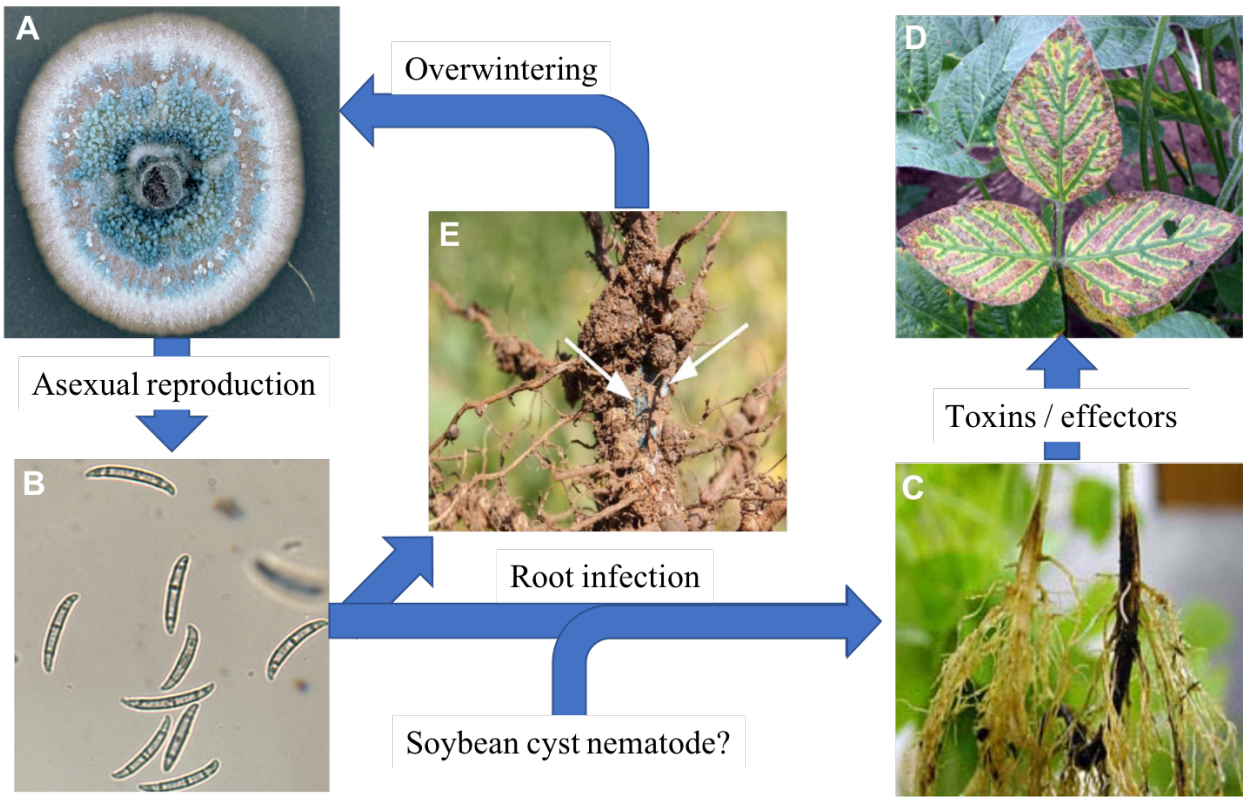

Figure 1-1. Soybean sudden death syndrome (SDS) disease cycle caused by the fungal pathogen *Fusarium virguliforme*. The pathogen grows in culture producing sporodochia with blue pigmentation (**A**) full of asexually produced conidia (**B**). The conidia germinate in the soil and infect roots causing root rot (**C**, from Navi and Yang 2008), with a potential interaction with the soybean cyst nematode. After colonization of the xylem tissues, foliar symptoms of interveinal chlorosis and necrosis can develop (**D**). However, *F. virguliforme* remains in the root system where it can overwinter in fungal masses on plant residue (**E**, white arrows).

SDS Management Strategies

Since its discovery in Arkansas in 1971, SDS has spread to all soybean producing states in the U.S. (Hartman et al., 2015). To date, all studies investigating management strategies for soybean SDS have focused solely on *F. virguliforme*. To manage *F. virguliforme*, researchers have examined soil tillage, crop rotations, fungicide seed treatments, and genetically resistant cultivars. Investigating soil tillage practices revealed that soil compaction with no-till strategies significantly enhances SDS severity, while subsoil tillage between 25-45 cm significantly reduced SDS severity (Vick et al., 2003, 2006). However, no-till strategies have become very popular among growers because it minimizes erosion and fuel costs while enhancing soil moisture and microbial communities (Uri 2000).

Long-term and diverse crop rotations (3 to 4 years) can reduce *F. virguliforme* populations five-fold compared to the commonly used 2-year corn-soybean rotation used by growers (Leandro et al., 2018). However, this reduction in pathogen population is dependent on the crops used in the rotation and weed pressure, as *F. virguliforme* has been shown to colonize at least 15 other crop and weed species including dry bean, alfalfa, pea, sugar beet, canola, and wheat (Kolander et al. 2012), and can survive long-term in corn residue (Navi and Yang 2016). Due to the high value of corn and soybean, growers do not commonly adopt long-term crop rotations with diverse crops.

Fungicide seed treatments and resistant cultivars have been the primary management strategies that growers have relied upon to manage SDS. Fungicide chemistries classified as succinate dehydrogenase inhibitors (SDHI), like fluopyram, have shown efficacy against SDS-pathogens *in vitro* (Wang et al., 2017; Sang et al., 2018). When formulated as a seed treatment, fluopyram has shown reductions in *F. virguliforme* and SDS while also providing yield increases

(Kandel et al., 2016, 2017, 2018), but other chemistries formulated as seed treatments have not shown the same benefit (Weems et al., 2015).

Genetic resistance to SDS is highly desirable, yet many studies have determined that resistance to SDS is complex and controlled by quantitative trait loci (QTLs) (Chang et al., 2018). In addition, each QTL can contribute to separate aspects of SDS-development; e.g., root rot or foliar symptoms (Kazi et al., 2008; Luckew et al., 2013). Lastly, some SDS QTLs overlap with other QTLs known for soybean resistance to other diseases, so understanding the full contribution of each QTL to SDS-specific resistance is challenging (Hughes et al., 2004; Meksem et al., 1999; Srour et al., 2012; Swaminathan et al., 2018). However, progress towards developing genetically resistant varieties has been successful, as certain varieties do tolerate SDS better than others in field settings (Kandel et al., 2016, 2017).

Foliar SDS symptoms are hypothesized to contribute primarily to yield loss (Luo et al., 2000), and no other hosts of *F. virguliforme* display true SDS foliar symptoms (Kolander et al., 2012). Therefore, these alternate hosts may employ some mechanism of resistance that could be transferred to soybean. Ideally, these alternate hosts employ mechanisms that could be transferred to soybean to prevent *F. virguliforme* infection of the roots altogether. Since *F. virguliforme* can cause root rot on many of these alternate hosts, this type of resistance mechanism is not likely (Kolander et al., 2012). Theoretically, there are at least four other possible resistance mechanisms (Fig. 1-2); expression of *F. virguliforme* effectors could be suppressed by alternate hosts, *F. virguliforme* is not able to penetrate to the xylem tissue to release effectors as it does in soybean (Abeysekara and Bhattacharyya 2014; Navi and Yang 2008), effectors are degraded by enzymes in the xylem, or effectors targets in foliar tissues are absent or highly diverged, rendering the effectors ineffective. Each mechanism could be a

potential avenue for intervention through transgenic approaches. Other transgenic approaches have shown some success in limiting *F. virguliforme* abundance and SDS development, including transgenic expression of killer proteins (Lightfoot 2015) and receptor-like kinases (Srour et al., 2012) in soybean. Further understanding of the mechanistic methods of SDS effectors should provide additional insights for transgenic approaches to control SDS.

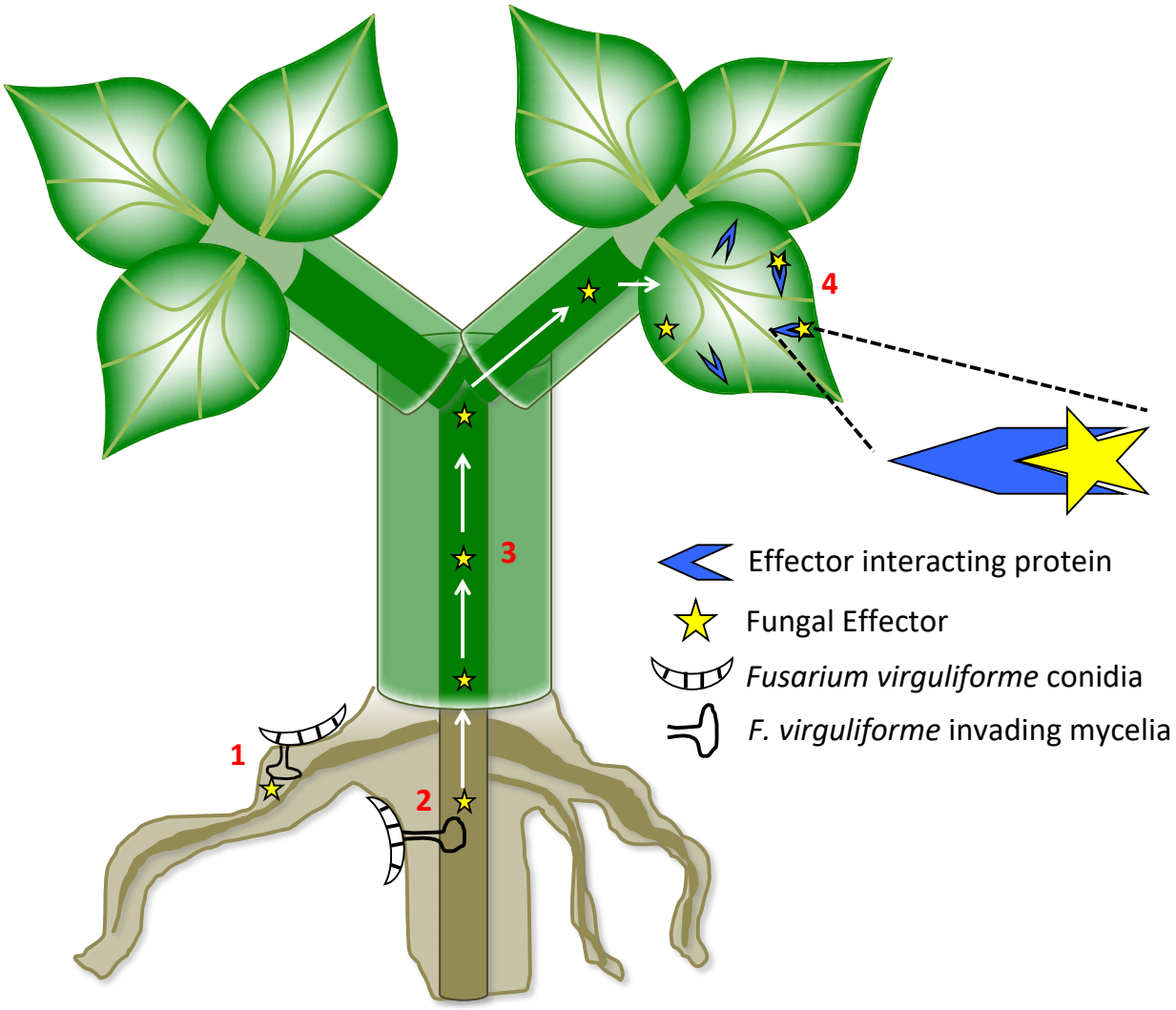

Figure 1-2. Schematic model of four potential modes of resistance to *F. virguliforme* effectors in other hosts. 1) Some *F. virguliforme* effectors may not be expressed in other hosts, or expression is suppressed. 2) *F. virguliforme* may not penetrate to the xylem tissue in non-soybean hosts, which is necessary for effector translocation. 3) Effectors are degraded by enzymes in the xylem of alternate hosts. 4) Effectors reach foliar tissues in alternate hosts, but the effector target is absent or too highly diverged to induce SDS-like symptoms.

Risk prediction is not commonly used for most soybean diseases. Many states encourage growers to submit soil samples to test for SCN population levels, which can assist in the selection of SCN resistant soybean germplasm, if necessary. In fact, some states provide free SCN testing through checkoff dollars. However, SCN was the only pathogen for which risk prediction was commonly used until recent studies on white mold caused by *Sclerotinia sclerotiorum* (Willbur et al., 2018a, 2018b). Other regional risk prediction models have been developed for Asian soybean rust and soybean SDS (Del Ponte et al., 2006; Scherm and Yang 1999), but they have not been widely implemented as disease management strategies.

Fusarium virguliforme infection and interaction with nematodes

To enter plant roots, many fungal pathogens generate specialized hyphae called an appressorium to build up turgor pressure, forcing a hyphal penetration peg between the cells of a plant host (Howard et al., 1991; Howard and Valent 1996). Once inside the host, fungal pathogens typically do one of three things; develop hyphae that remain in the extracellular apoplast, develop intracellular invasive hyphae, or develop specialized feeding structures called haustoria that also invade plant cells (Giraldo and Valent 2013). Scanning electron microscopy of *F. virguliforme* indicates appressoria formation on soybean root surfaces (Navi and Yang 2008), though the appressorium does not appear as large and distinct as those produced by aerial pathogens (Howard and Valent 1996). Indeed, appressorium development in *Fusarium* relatives (*F. oxysporum*, *F. graminearum*, and *F. verticillioides*) either develop intermittent appressorium-like structures (Czymmek et al., 2007), lobate appressoria (Boenisch and Schäfer 2011) or no appressoria at all (Bluhm et al., 2007; Zhang et al., 2011).

Genomic analysis and gene prediction algorithms of the *F. virguliforme* genome have also indicated a significant arsenal of cell-wall degrading enzymes (Chang et al., 2016b). These enzymes are likely expressed and used in addition to appressoria to gain entry into soybean root tissues. Inside the root system, *F. virguliforme* colonization can reach the vascular tissues, as supported by cross sections of infected soybean roots (Islam et al., 2017a, 2017b; Navi and Yang 2008). It is thought that colonization of the vascular tissues is associated with the development of foliar symptoms, where effector proteins can be released into the xylem and translocated to the foliar tissues. Fungal-derived proteins have been identified in soybean xylem sap of *F. virguliforme* infected soybeans, as has the plant defense response compound pipecolic acid (Abeysekara and Bhattacharyya 2014; Abeysekara et al., 2016).

A more efficient mode of entry into soybean roots would be through a mobile vector such as the soybean cyst nematode (SCN) (Fig. 1-1). Independently, SCN is a major threat to soybean production throughout the U.S., but *F. virguliforme* and SCN are commonly found in the same fields (Rupe et al., 1993). Soybean fields with both pathogens often develop significantly worse SDS than fields with *F. virguliforme* only (Brzostowski et al., 2018; McLean and Lawrence 1995; Westphal et al., 2014), leading to the suggestion that the two act synergistically to enhance SDS severity (Xing and Westphal 2013). However, other studies have failed to find this association between the presence of SCN and enhanced SDS severity (Hershman et al., 1990; Marburger et al., 2014; Rupe et al., 1993). There are multiple hypotheses surrounding the interactions between *F. virguliforme* and SCN that could enhance SDS severity. First, the two pathogens may be able to directly interact with one another prior to reaching a soybean root. Second, interactions within the soybean root could facilitate unique physiological responses by the soybean that increases susceptibility to SDS. Both hypotheses surrounding *F. virguliforme*

and SCN interactions could be synergistic or antagonistic. Early studies suggested an antagonistic relationship because *F. virguliforme* was isolated from infected and parasitized SCN cysts and eggs (Donald et al., 1993; McLean and Lawrence 1995). Some *Fusarium* species have been shown to colonize and kill the model nematode *Caenorhabditis elegans* (Muhammed et al., 2012b); hence, it is reasonable to hypothesize that *F. virguliforme* may be able to colonize and kill SCN, increasing in abundance and leading to increased risk of SDS. Additional studies have shown that the presence of *F. virguliforme* decreases SCN reproduction, which also suggests an antagonistic relationship (Gao et al., 2006). However, SDS caused by *F. virguliforme* was only enhanced by SCN, and was not enhanced in the presence of the root knot nematode *Meloidogyne incognita* (Xing and Westphal 2013), suggesting a synergistic effect on SDS due to the presence of SCN. The discrepancies regarding the role of SCN on SDS development could be due to differences in *F. virguliforme* isolates, SCN races, and soybean cultivars used in each study.

Fusarium virguliforme **effectors**

The mechanisms employed by *F. virguliforme* to cause root rot symptoms are unknown and have not been studied at a molecular level. *In silico* analyses and QTL mapping studies have revealed many xylanases, polygalacturonases, and hydrolases in the genome of *F. virguliforme*, which likely play a role in root entry (Chang et al., 2016b; Sahu et al., 2017). These proteins are likely involved in root entry and root rot symptom development, though classical genetic evidence of this is still missing. In contrast, classical genetic approaches have been used to identify specific effector proteins involved in foliar SDS development. The first report providing evidence that *F. virguliforme* secreted toxic compounds and proteins came in the late 1990's, where a pair of publications showed that spent *F. virguliforme* broth, or "cell-free culture

filtrate" caused browning of soybean callus tissue (Jin et al., 1996b), and that a single partially-purified protein from this culture filtrate was sufficient to cause necrosis on detached soybean leaves (Jin et al., 1996a). These studies were also the first to propose the hypothesis that *F. virguliforme* secretes proteins that may translocate into the xylem to the foliar tissues (Jin et al., 1996b). Though these findings were significant, but the gene(s) encoding this protein has not been identified, and thus, characterization of this process is incomplete. A subsequent study has demonstrated that light is required for SDS symptom development, and symptoms are associated with the degradation of the large subunit of Rubisco (Ji et al., 2006).

Additional searches for *F. virguliforme* effectors identified two different proteins, both of which are small proteins with putative secretion signals. The first effector is FvTox1, a 172 amino acid protein that has a predicted 19 amino acid N-terminal secretion signal (Brar et al., 2011). When expressed, purified, and vacuum infiltrated into soybean leaf discs, FvTox1 caused a significant reduction in chlorophyll content (Brar et al., 2011). Some studies have speculated that FvTox1 localizes to chloroplasts, and could be associated with the degradation of Rubisco (Wang et al., 2015; Abeysekara et al., 2016), though a formal colocalization study has not been performed. Similarly, the ToxA protein produced by *Pyrenophora tritici-repentis* also requires light to cause disease symptoms in wheat and functions by direct interaction with a chloroplast protein, which disrupts chloroplast function (Ciuffetti et al., 2010; Manning and Ciuffetti 2005; Manning et al., 2007). The predicted structure of mature FvTox1 (lacking the secretion signal) does not show homology to ToxA, and in fact shows poor structural homology to any known protein models. The Phyre2 protein homology software identifies homology between FvTox1 and a calcium binding protein, but the confidence score is only 78.7. Still, mutant *fvtox1* knockout strains are reduced in their ability to induce foliar SDS in stem-cut assays, indicating a

significant role of FvTox1 in foliar SDS development (Pudake et al., 2013). The second effector is FvNIS1, a 152 amino acid protein with an 18 amino acid N-terminal secretion signal (Armenteros et al., 2019; Chang et al., 2016a). The Phyre2 predicted structure of mature FvNIS1 (lacking the secretion signal) shows a strong homology to the *Neurospora crassa* PMO-2 protein, with 96.1% confidence (data not shown). The *N. crassa* PMO-2 protein is a polysaccharide monooxygenase that enzymatically cleaves cellulose (Li et al., 2012). Assuming FvNIS1 acts in a similar manner to PMO-2, one would expect a significant role for FvNIS1 in plant virulence. Indeed, overexpression of FvNIS1 in soybean leaves with soybean mosaic virus induces SDS-like symptoms, and *fvnis1* knockout mutants are significantly less virulent than wild type *F. virguliforme* (Chang et al., 2016a).

A large number of cysteine residues is commonly found in fungal effectors (Stergiopoulos and de Wit 2009). In some cases, these cysteine residues can comprise up to 16% of amino acid residues (Liu et al., 2012). These cysteine residues are hypothesized to promote disulfide bonding, a chemical feature which strengthens the tertiary structure of proteins and enhances protein stability (Liu et al., 2012). Given the support for the hypothesis that *F. virguliforme* secretes proteins into soybean xylem, (Abeysekara and Bhattacharyya 2014), cysteine residues may be important to *F. virguliforme* effectors. A well characterized example of fungal-derived proteins in plant xylem tissues are the secreted in xylem (SIX) proteins from *F. oxysporum*, which are also cysteine rich (Rep et al., 2004; Takken and Rep 2010). In addition, effectors from *Cladosporium fulvum, Stagonospora nodorum*, and *Phakopsora pachyrhizi* have also shown high cysteine content (Liu et al., 2012; Qi et al., 2016; Stergiopoulos and de Wit 2009). Interestingly, FvTox1 is cysteine-rich (9 of 172), while FvNIS1 is relatively cysteine-poor (2 of 152).

Fungal proteins that induce plant disease symptoms are typically referred to in the literature as host selective toxins (HSTs), or effectors. For example, the previously mentioned ToxA protein from *P. tritici-repentis*, along with ToxB and ToxC, are reported as HSTs (Ciuffetti et al., 2010; Manning and Ciuffetti 2005; Manning et al., 2007). By definition, HSTs are fungal low-molecular-weight metabolites or proteins that play an active role in colonization and symptom development of host plants, and in most cases, host sensitivity to the HST is conferred by a single gene (Wolpert et al., 2002). However, this definition is nearly identical to the gene-for-gene model proposed by (Flor 1946, 1971), where a pathogen-derived and host-derived protein act in a dominant, compatible fashion to induce susceptibility in the host (Ciuffetti et al., 2010; Wolpert et al., 2002). For simplicity, small fungal proteins that trigger either avirulence or host susceptibility should be called one name, either effectors or HSTs. Given the volume of work needed to determine if a single protein is specific to a given host, the term "effector" should be adopted over "HST" for all fungal proteins involved in plant-pathogen interactions (Varden et al., 2017). However, in addition to secreted, virulence-associated proteins, *F. virguliforme* is also capable of producing toxic secondary metabolites like radicicol (i.e., monorden), fusaric acid, and citrinin that can accumulate and cause cell death in soybean leaves (Chang et al., 2016a). Similarly, other fungal plant pathogens produce non-protein compounds that aid plant pathogenicity, like polyketides (Baker et al., 2006; Gaffoor et al., 2005). Though they are not proteinaceous in nature, these compounds still have an effect on plant host immunity, so "effector" is an appropriate term over "HST" for these compounds as well. For simplicity, all fungal-derived compounds that effect plant pathogenicity will be called "effectors" in this work. To date, no studies have investigated whether the symptoms produced by FvTox1 and FvNIS1 effectors are soybean-specific.

One of the key goals of effector-based research has been to define the mechanisms by which effectors control plant processes. As an analogy for this work, if an effector functions as a key and a host susceptibility factor functions as a lock, then it follows that an in-depth understanding of the structure and function of the effector (key) could be used to fine-tune host processes (change the locks) and prevent pathogen manipulation of the plant host. While many other pathosystems have made progress in identifying and characterizing several "lock and key" mechanisms, *F. virguliforme* effector studies have primarily focused on developing synthetic peptides or mammalian-derived antibodies that bind to FvTox1 (Brar and Bhattacharyya 2012; B. Wang et al., 2015). However, artificially binding FvTox1 does not necessarily inhibit its function, and synthetic constructs need to be validated *in planta* before they can be deemed safe and effective. In addition, mammalian-derived transgenes in plant tissues make them unfit for human consumption under the current USDA regulations. Instead, an approach that aims to understand the effector mode-of-action in order to alter the target and prevent the mode-of-action that induces susceptibility is more intuitive and likely to have practical applications that could enhance disease resistance if deployed in the field.

Fusarium **genomics**

Genome sequences are available for most of the FSSC clade II species, with the exception of *F. crassistipitatum* (Huang et al., 2016). The *F. virguliforme* genome is quite fragmented with over 3,000 contigs (Srivastava et al., 2014), compared to the high-quality genomes for its relatives *F. graminearum*, *F. oxysporum*, *F. fujikuroi*, and *F. verticillioides*, which all have chromosome-level assemblies (Cuomo et al., 2007; Jeong et al., 2013; King et al., 2015; Ma et al., 2010). However, the *F. virguliforme* genome is quite complete relative to the

other FSSC clade II species, which have > 15,000 contigs each (Huang et al., 2016). To date, neither *F. virguliforme* or *F. brasiliense* genomes have been annotated for gene content, though multiple RNA-seq and microarray datasets are available (Chang et al., 2016a; Marquez et al., 2019; Radwan et al., 2011; Sahu et al., 2017). However, these non-annotated genomes facilitated gene prediction and benchmarking using single copy orthologs (BUSCO) that suggest both existing genomes are relatively complete since at least 87% of the core single-copy orthologs found in *F. graminearum* were also found in the current *F. virguliforme* and *F. brasiliense* genomes. To learn more about the pathogenicity mechanisms employed by *F. virguliforme* and *F. brasiliense*, improvements to available genomes are needed.

Using chromosome level assemblies, researchers studying *F. oxysporum* pathogenicity have identified small mobile pathogenicity chromosomes associated with host range (Vlaardingerbroek et al., 2016a, 2016b). These chromosomes are rapidly evolving through the presence of many active transposons (Sperschneider et al., 2015). In addition, these chromosomes can be transferred from a virulent isolate to non-virulent isolate and confer virulence, expanding the host range of the previously non-virulent isolate (Ma et al., 2010; van Dam et al., 2017). A formal karyotype has never been done for *F. virguliforme*, though whole-genome alignments with *F. graminearum* and pulsed-field gel electrophoresis of *F. virguliforme* DNA extractions have tried to determine the number of chromosomes present in *F. virguliforme* (Mansouri 2012; Shultz et al., 2007). In Michigan, *F. virguliforme* and *F. brasiliense* isolation frequencies indicate a host preference, where *F. virguliforme* preferentially colonizes soybean and *F. brasiliense* preferentially colonizes dry bean. Therefore, a chromosome-level understanding of these pathogens may reveal a similar trend of mobile pathogenicity

chromosomes that can boost pathogenicity of each species on each host, or help explain the wide host range of *F. virguliforme* (Kolander et al., 2012).

High quality genomes for these pathogens can facilitate the development of molecular diagnostic tools and also reveal a lot about the biology of pathogens, including genetic potential for fungicide resistance, mating potential, and pathogenicity chromosomes. Two studies have used available FSSC clade II sequences to develop highly specific and sensitive qPCR assays for *F. virguliforme* and *F. brasiliense* (Roth et al., 2019c; J. Wang et al., 2015). One study has shown differential responses among FSSC clade II species to fluopyram, the only fungicide currently efficacious for these pathogens, which was caused by a single nonsynonymous mutation in the *SdhB* gene (Sang et al., 2018). Identifying genes associated with fungicide resistance may guide engineering of new fungicide compounds that have improved function against these pathogens. Curiously, PCR tests investigating mating type loci in *F. virguliforme* revealed only one mating type, while both mating types have been identified in *F. brasiliense* isolates (Hughes et al., 2014). These mating type loci within the genomes of each species suggests that only asexual reproduction is possible for *F. virguliforme*, while both sexual and asexual reproduction may be occurring within *F. brasiliense* isolates. In *F. oxysporum*, genome sequencing efforts have identified dispensable chromosomes highly associated with pathogenicity on specific hosts (Vlaardingerbroek et al., 2016b; van Dam et al., 2017). Genomic studies have already helped design diagnostic tools for *F. virguliforme* and *F. brasiliense*, and additional improvements to current genomes may reveal more about their biology and reproduction, identifying potential avenues to restrict movement and revealing genetic potential for fungicide resistance.

Conclusions

Soybean SDS pathogens *F. virguliforme* and *F. brasiliense* continue to spread globally and are difficult to manage with a single approach. The development of more management approaches for integration with current strategies is needed, as is a greater understanding of the genetics, genomics, and biology of these pathogens. In Chapter 2 of this work, I describe an SDS risk prediction model that uses *F. virguliforme* abundance data to predict SDS development at a field level. I envision a tool being used by growers to guide their decisions for soybean germplasm selection or fungicide seed treatments, particularly in regions of a field with high risk. Many growers already use soil-based maps to guide planting population density, and a similar concept could be used automatically adjust variety or seed treatments in high-risk SDS regions of a field. A similar SDS risk prediction model could be made for *F. brasiliense* using the qPCR assay developed in this work, described in Chapter 3. This qPCR assay will also be helpful to diagnostic labs throughout the U.S. to monitor the spread of *F. brasiliense*.

A greater understanding of pathogen biology and SDS development is also needed to enhance SDS management. Though genetic studies have been performed in *F. virguliforme*, none have been performed in *F. brasiliense*. The protoplasting and genetic transformation protocol described in Chapter 4 provides significant details for performing classical genetic experiments in these two organisms. Using this protocol to develop fluorescent strains of *F. virguliforme* and *F. brasiliense* allowed me to investigate the biological interaction between these fungi and the SCN in Chapter 5, using a new approach that has not previously been reported – fluorescent strains coupled with advanced microscopy. The evidence from this study suggests that *F. virguliforme* is not vectored into roots by SCN, but instead can colonize

nematodes as a saprophyte. It remains to be seen whether the presence of SCN inside the same soybean root as *F. virguliforme* induces the expression of fungal effectors.

In the final two Chapters, I describe the development of high-quality long-read genomes for *F. virguliforme* and *F. brasiliense*. As described in Chapter 6, these genomes assembled into less than 150 contiguous sequences and provide an opportunity to study genome-wide structural variation. These genomes will be a valuable resource for discovering new effector genes that can be studied with classical genetic approaches. Some of these genetic approaches were used to study the mechanisms of FvTox1 and FvNIS1, reported in Chapter 7. The evidence suggests that FvNIS1 has a conserved mechanism to induce cell death in tobacco and soybean, while FvTox1 may interact with a soybean-specific target.

CHAPTER 2: Predicting Soybean Yield and Sudden Death Syndrome Development using At-planting Risk Factors

By

Mitchell G. Roth, Z. A. Noel, J. Wang, F. Warner, A. M. Byrne, and M. I. Chilvers

This chapter has been accepted for publication to the journal *Phytopathology* pending minor revisions.

Author Contributions:

MGR, JW, and MIC designed the experiment, MGR, JW, FW, and AMB collected data, MGR and ZAN analyzed data and generated figures, MGR, ZAN, and MIC wrote the manuscript.

Abstract

In the U.S., sudden death syndrome (SDS) of soybean is caused by the fungal pathogen *Fusarium virguliforme* and is responsible for significant yield losses each year. Understanding the risk of SDS development and subsequent yield loss could provide growers with valuable information for proper management of this challenging disease. Current management strategies for *F. virguliforme* use partially resistant varieties, fungicide seed treatments, and extended crop rotations with diverse crops. The aim of this study was to develop models to predict SDS severity and soybean yield loss using at-planting risk factors to integrate with current SDS management strategies. In 2014 and 2015, field studies were conducted in adjacent fields in Decatur, MI, which were intensively monitored for *F. virguliforme* and nematode quantities at-planting, plant health throughout the growing season, end-of-season SDS severity, and yield using an unbiased grid sampling scheme. In both years, *F. virguliforme* and soybean cyst nematode (SCN) quantities were unevenly distributed throughout the field. The distribution of *F. virguliforme* at-planting had a significant correlation with end-of-season SDS severity in 2015, and a significant correlation to yield in 2014 ($P < 0.05$). SCN distributions at-planting were significantly correlated with end-of-season SDS severity and yield in 2015 ($P < 0.05$). Prediction models developed through multiple linear regression showed that *F. virguliforme* abundance ($P < 0.001$), SCN egg quantity ($P < 0.001$), and year ($P < 0.01$) explained the most variation in end-of-season SDS ($R^2 = 0.32$), while end-of-season SDS ($P < 0.001$) and end-of-season root dry weight ($P < 0.001$) explained the most variation in soybean yield ($R^2 = 0.53$). Further, multivariate analyses support a synergistic relationship between *F. virguliforme* and SCN, enhancing the severity of foliar SDS. These models indicate that it is possible to predict patches of SDS severity using at-planting risk factors. Verifying these models and incorporating

additional data types may help improve SDS management and forecast soybean markets in response to severe SDS threats.

Introduction

Soybean (*Glycine max* [L.] Merr.) is one of the most cultivated and top grossing crops in the U.S. but is prone to yield losses caused by many pathogens (Allen et al., 2017; Koenning and Wrather 2010). In North America, the fungal pathogen *Fusarium virguliforme* O'Donnell & T. Aoki causes soybean sudden death syndrome (SDS). *Fusarium virguliforme* has no known sexual reproductive stage (Hughes et al., 2014) but can produce asexual microconidia, macroconidia, and overwintering chlamydospores (Aoki et al., 2003). These spores can germinate into mycelia in the soil, which release cell wall degrading enzymes after coming into contact with soybean roots (Chang et al., 2016b) and develop an appressorium (Navi and Yang 2008) to facilitate infection. Soybean roots of any age can be infected (Gongora-Canul and Leandro 2011; Hartman et al., 2015). Initial symptoms develop as root discoloration and root rot, but eventually foliar symptoms develop as interveinal chlorosis, necrosis, and premature defoliation, leading to yield loss (Hartman et al., 2015). However, *F. virguliforme* remains in the root tissues throughout foliar disease development and has never been isolated from above ground tissues (Roy et al., 1989). SDS commonly appears in heterogeneous patches, or "hot spots", within a field and differentially affects yield throughout a single field (Hartman et al., 2015). Evidence suggests that foliar SDS symptoms are the result of *F. virguliforme* penetration to the vascular tissues (Islam et al., 2017a; 2017b; Navi and Yang 2008), where various secondary metabolites and protein toxins are secreted into the xylem and translocated to the

foliar tissues (Abeysekara and Bhattacharyya, 2014; Brar et al., 2011; Chang et al., 2016a; Pudake et al., 2013).

Heterodera glycines Ichinohe, the soybean cyst nematode (SCN), is commonly found in fields throughout the U.S., and also causes significant yield loss in soybean (Allen et al., 2017; Koenning and Wrather, 2010). The infectious SCN juveniles (J2) pierce soybean roots with a stylet and burrow to the vascular tissue where they induce the formation of syncytia, specialized host-derived feeding structures that enable nematodes to mature and complete their life cycle (Endo, 1986; Hussey and Grundler, 1998; Ithal et al., 2007a). Multiple plant-parasitic nematodes have been implicated in disease complexes with plant pathogenic fungi and oomycetes, including SCN with *F. virguliforme* in soybean (Back et al., 2002; Rupe, 1989; Rupe et al., 1993). Independently, both *F. virguliforme* and SCN can penetrate to the vascular tissue, but it is unknown if the two pathogens interact before reaching the vascular tissues, or if *F. virguliforme* preferentially colonizes wounds caused by SCN or other nematodes. Previous studies have shown that *F. virguliforme* can colonize SCN eggs and cysts (Donald et al., 1993; McLean and Lawrence, 1995). Field studies have found that foliar SDS severity is worse when soybeans are inoculated with both pathogens compared to *F. virguliforme* alone (Brzostowski et al., 2014; McLean and Lawrence 1993; Scherm et al., 1998; Westphal et al., 2014; Xing and Westphal, 2013). Another recent study showed that managing SCN through partially resistant cultivars also reduced SDS severity (Kandel et al., 2017). Together, these studies indicate a unique relationship between *F. virguliforme* and SCN that results in severe SDS, with strong corollary evidence suggesting that the relationship is synergistic (Xing and Westphal, 2013). Since SCN cannot cause SDS independently, the relationship is not additive, and any relationship with *F. virguliforme* that enhances SDS severity could be classified as synergistic. However, other field

studies have failed to find evidence to support a synergistic relationship leading to increased SDS (Hershman et al., 1990; Marburger et al., 2014; Rupe et al., 1993). A factorial greenhouse experiment revealed that these pathogens caused a more significant reduction in root mass together, compared to either pathogen alone, but there was no increase in foliar SDS due to the presence of SCN (Gao et al., 2006).

Current management strategies for SDS use partially resistant varieties, seed treatments with fungicides (Kandel et al., 2018), crop rotation (Leandro et al., 2018), and soil tillage practices (Hartman et al., 2015). However, each strategy has drawbacks. Crop rotations may fail because *F. virguliforme* can successfully colonize other crop and weed species without causing visual symptoms, allowing inoculum to build up (Kolander et al., 2012). Extended crop rotations with diverse crops can be costly depending on crop markets and is not widely adopted by growers. Soil tillage may fail because *F. virguliforme* can overwinter in soybean and corn residue (Navi and Yang 2016). Seed treatments containing the fungicide fluopyram (BASF, Ludwigshafen, Germany) have shown efficacy *in vitro* and *in planta* (Gaspar et al., 2017; Kandel et al., 2016; Sang et al., 2018; Wang et al., 2016). However, few other fungicides show significant reduction of *F. virguliforme* inside plant roots (Weems et al., 2015), and reliance on a single mode of action fungicide is undesirable due to its potential to select for fungicide resistance. Identification of QTLs has led to improved genetic resistance to SDS; however, resistance is quantitative and complex since separate QTLs control resistance to root and foliar symptoms (Chang et al., 2018; de Farias Neto et al., 2007; Kazi et al., 2008; Lightfoot 2015; Luckew et al., 2013; Tan et al 2019; Wen et al., 2014). Data suggests that suppressing foliar SDS symptoms significantly improves yield (Luo et al., 2000) and some breeding efforts focus solely on foliar SDS symptoms (Wen et al., 2014). However, cultivars with no foliar symptoms may

still be heavily colonized by *F. virguliforme* (Wang et al.,, 2018). The impact of root rot on yield is difficult to estimate, and the impact of root rot caused by *F. virguliforme* in soybean is currently unknown. Additionally, some SDS resistance QTLs overlap with known SCN resistance QTLs, complicating the role of each in specific resistance to SDS or SCN (Meksem et al., 1999; Srour et al., 2012).

Another SDS management strategy that has yet to be widely implemented is risk prediction. Risk prediction has been used for other soybean diseases, such as Asian soybean rust and Sclerotinia stem rot (Del Ponte et al., 2006; Mila et al., 2004; Willbur et al., 2018a; 2018b), as well as SDS at the regional level (Scherm et al., 1996; 1998; Scherm and Yang 1999). These previous studies modelled SDS development using environmental data such as soil temperature, soil water potential (Scherm and Yang 1996), cold stress response, and geographic location (Scherm and Yang 1999). While environment plays a key role in disease development, the presence of the pathogen may not be evenly distributed across a field. These climate-driven regional models indicated a highly unfavorable environment for SDS development in Minnesota, South Dakota, and Nebraska (Scherm and Yang 1999) even though *F. virguliforme* has been identified there and is consistently ranked in the top 5 most damaging soybean diseases in the Northern U.S. (Allen et al., 2017). Incorporating pathogen abundance data into SDS predictive models at the field level is essential for improved prediction since *F. virguliforme* is present and causing SDS in locations predicted to have an unfavorable environment for SDS.

In this study, we aimed to incorporate SCN and *F. virguliforme* abundance data into SDS predictive models at the field level. We employed a high-intensity sampling method over two years to quantify SCN and *F. virguliforme* and examine their spatial distribution in a naturally infested field in Michigan. The goals of this study were to 1) determine the spatial distribution of

F. virguliforme and SCN in a field site naturally infested with both pathogens, 2) identify at-planting risk factors for modelling SDS severity and yield, and 3) explore synergistic effects of *F. virguliforme* and nematodes on SDS severity.

Materials and Methods

Field and sampling design

Two adjacent field sites in Decatur, MI with sandy loam soils were selected for field trials in 2014 and 2015. Both fields are naturally infested with both *F. virguliforme* and SCN and managed under a corn-soybean rotation with minimal-till conditions using a chisel plow. In both years, the field was the same size, measuring 9.1 m by 48.8 m. The fields were divided into 24 plots, each measuring 3.0 m by 6.1 m. Each plot contained four rows of soybeans with 0.8-m row spacing, planted at a density of approximately 9 seeds per 0.3 m. In 2014, untreated Asgrow AG2534 seeds were planted, and in 2015 Asgrow AG2535 (Monsanto, St. Louis, MO) containing the company's "complete" Acceleron treatment package were planted (Rossman et al., 2018). These seed choices represent common varieties and treatments available to Michigan growers. Both varieties are rated 7 out of 9 for SDS tolerance by the seed company, where 1 = excellent and 9 = poor. Soybeans were planted in early May of each year. Fields received natural rainfall with additional overhead irrigation, resulting in an average weekly water volume of 2.7 cm in 2014 and 3.0 cm in 2015. The plots were harvested with an Almaco combine equipped with a 1.5-m head, and yield was determined with the HarvestMaster system (Juniper Systems, Logan, UT). In 2014, the center two rows of each four-row plot were harvested providing 24 data points, while in 2015 all four rows were harvested, two rows at a time, providing 48 data points for yield.

A predetermined grid sampling scheme was used so that sampling locations were in the outside rows of the 24 plots, 1.5 m from the end of the row, for a total of 96 sampling areas. Sampling locations were marked with a stake to ensure future samples could be obtained from the same location throughout the season. Soil samples were collected in-furrow, within 3 days of planting and again after harvest. Soil was collected using a 2.45-cm diameter, 15.2-cm deep soil core. Six soil cores were collected per sampling location and homogenized in a plastic bag. Three soybean plants were collected at each sampling location at an early vegetative growth stage (V3) and a late reproductive growth (R5) stage (Fehr et al., 1971).

Fusarium virguliforme and nematode detection

Root samples were separated from foliar tissues, oven dried at 50°C for 48 h, and ground using a Christy Mill (Christy Turner Ltd, Ipswich, Suffolk, U.K.). DNA was extracted from 100 mg of ground root tissue using an automated phenol-chloroform technique performed on the AutoGen 850 Alpha system (AutoGen Inc, Holliston, MA), or the same phenol-chloroform protocol performed manually. DNA extractions from soil were performed in triplicate using 500 mg of homogenized soil with the FastDNA SPIN Kit for Soil (MP Biomedicals, Santa Ana, CA), and the DNA was quantified using a Nanodrop 1000 (Thermo Fisher Scientific, Waltham, MA). Two microliters of DNA, at concentrations ranging from 30 to 110 ng / µL, was used in qPCR reactions to determine the level of *F. virguliforme* using the primers, probes, and cycling conditions reported by Wang et al., (2015). The total DNA concentration of each extraction was used to normalize the results obtained by qPCR into a ratio of femtograms of *F. virguliforme* DNA detected per nanogram of total DNA. Two technical replicates of qPCR were performed on each DNA extract in a StepOnePlus thermal cycler (v2.3, Applied Biosystems). Quantifying *F.*

virguliforme from root samples was performed by taking the $Ct_{soy} - Ct_{Fv}$, where Ct_{soy} represents the cycle threshold for amplification of the soybean β-tubulin reference gene (Wang et al., 2018) and Ct_{Fv} represents the cycle threshold for amplification of the *F. virguliforme* qPCR target. In this way, samples with high levels of *F. virguliforme* (low Ct) have a high calculated value, which is intuitively interpreted as high levels of *F. virguliforme.*

Soil samples collected at planting and after harvest were also used for classifying and quantifying SCN, spiral nematodes (*Heliocotylenchus* spp.), lesion nematodes (*Pratylenchus* spp.), and dagger nematodes (*Xiphinema* spp.), based on morphology. One hundred milliliters of homogenized soil per sampling location was submitted to the Michigan State University Diagnostics Services (www.pestid.msu.edu) for nematode identification and quantification. Nematodes were isolated from soil using a modified soil centrifugation and floatation procedure (Jenkins 1964) and quantified under a dissecting microscope in a counting dish.

Tracking SDS development

Three plant samples were collected at each sampling point at growth stage V3 and R5, placed in a cooler, and transported back to Michigan State University. Foliar SDS incidence was calculated on each individual plant as the percent of leaves showing foliar symptoms, and the severity was assessed on symptomatic plants using a scale from 0-9 with increments of 0.5 developed at Southern Illinois University (Bond et al., *unpublished*). Ratings of 0 = no visible symptoms, 1 = 1-10% of leaf surface chlorotic and/or 1-5% necrotic, 2 = 10-20% chlorotic and/or 6-10% necrotic, 3 = 20-40% chlorotic and/or 11-20% necrotic, 4 = 40-60% chlorotic and/or 21-40% necrotic, 5 = greater than 60% chlorotic and/or greater than 40% necrotic, 6 = premature leaf drop up to 1/3 defoliation, 7 = premature leaf drop up to 2/3 defoliation, 8 =

premature leaf drop greater than 2/3 defoliation, 9 = premature plant death (Fig. 2-1). The 0.5 increment was applied when symptoms exceeded the requirements of one integer but did not meet the full requirements of the next integer, or when averaging symptomology across plants. The SDS severity and incidence measurements were converted to a normalized disease index (DX) score on a scale from 0-100 by multiplying the incidence times severity, then dividing by the maximum severity score of 9 (Njiti et al., 2001). The roots of the sampled plants were washed with water and rated for discoloration and rotten roots, on a percentage scale from 0-100. The mean of the three plants was used to represent the sampling location and used for subsequent correlation analyses. These roots were dried as described above, and dry weight was collected. These roots were then processed for DNA extraction and qPCR as described above.

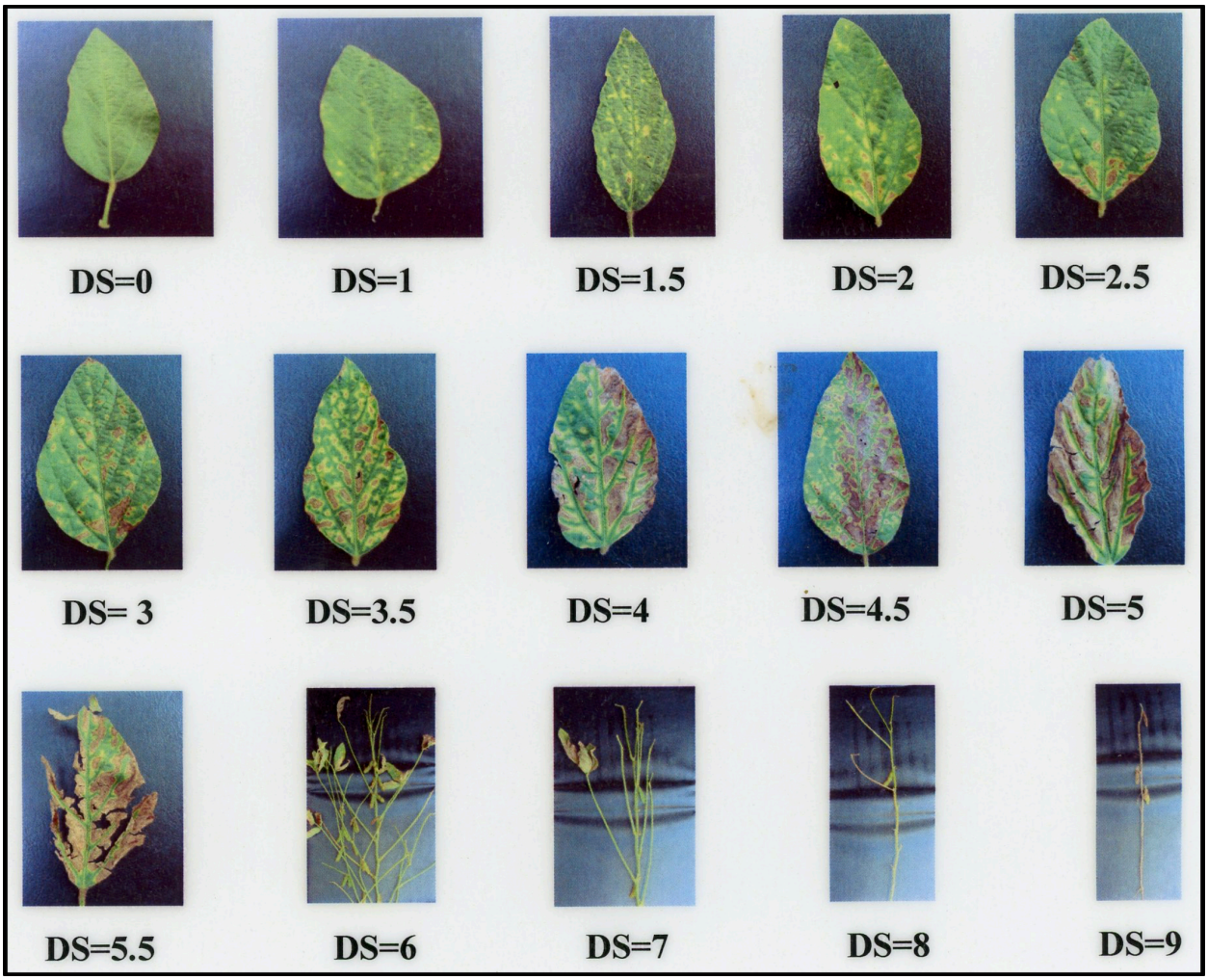

Figure 2-1. Soybean sudden death syndrome (SDS) disease severity rating scale used in this study. Based on Southern Illinois University, J. Bond et al,, *unpublished*; images courtesy of B. Serven, Michigan State University, *unpublished*. DS = disease severity.

Foliar SDS incidence and severity measurements were also collected in the field at growth stages R5 (Fehr et al., 1971). Foliar SDS incidence was observed as the percentage of plants in a given region showing foliar SDS, and severity was rated using the 0-9 scale detailed above. These incidence and severity ratings were also transformed into a DX score, and the R5 SDS DX represents the end-of-season SDS severity in all analyses. In 2014, SDS incidence and severity were collected on a plot-wide basis, providing 24 data points. However, significant variation was observed within each plot in 2014, where some areas of severe SDS were averaged

with areas of low SDS, which decreased spatial resolution of SDS in the field. Therefore, in 2015 foliar SDS severity and incidence ratings were measured only on approximately 25 plants that were in the same row as, and within 1 m of, each sampling location. This provided 96 data points, decreased within-plot variability, and increased spatial resolution of SDS in the field.

Data analysis

The 2014 and 2015 data sets were analyzed separately for Lloyd's index of patchiness (LIP), spatial interpolation, and Pearson's correlations. The 2014 and 2015 data were combined prior to 3D modeling, principal coordinates analysis (PCoA), and two-way stepwise multiple linear regression. All data was analyzed in R version 3.2.0 (R Core Team 2015, Vienna, Austria). Data and R scripts for these analyses can be found online at github.com/rothmi12/SDS-Risk-Assessment.

The qPCR data obtained from soil samples were normalized to their respective total sample DNA concentration obtained to account for differences in DNA extraction efficiency per soil sample. This ratio represents the femtograms of *F. virguliforme* DNA detected per nanogram of total DNA extracted. This ratio normalizes the data to account for differences in DNA extraction efficiency per soil sample. The ratio of *F. virguliforme* DNA was used in all interpolation, correlation, linear regression, and pathway analyses. However, for LIP and PCoA, raw DNA quantities from qPCR (in femtograms) from soil samples were used to meet the assumption of count data for these analyses. Using density or proportional data instead of count data can cause incorrect calculations in these analyses (Bez, 2000).

Contour plots were developed by using the 'Krig' and 'surface' functions within the 'fields' R package (Nychka et al., 2017). Briefly, each data point for each variable was assigned

an X and Y coordinate (in meters) based on their location within the field. A stationary covariance model was applied to the data to generate predictions of values from all areas, sampled and not sampled. The predicted data had a significant correlation to the true values in all cases (adjusted $R^2 > 0.86$, $P < 0.001$), suggesting the kriging models accurately display values in non-sampled regions.

Pearson's correlation analyses were done using the 'stats' R package (R Core Team). Briefly, all variables were combined into a single matrix, where each row represented the same sampling area described above. Then, each variable was independently correlated to all other variables and assigned a *P*-value and plotted for visualization of all pairwise correlations. *P*-values were adjusted using a false discovery rate (FDR) correction with the 'p.adjust' function from the 'stats' package to reduce the chance of obtaining false-positive significant correlations associated with multiple testing (Noble, 2009). Only correlations between risk factors and end-of-season SDS or yield are presented (Table 2-1).

A 3D scatter plot was made using the 'plot3D' R package (Soetaert, 2017). A PCoA was performed using only the at-planting *F. virguliforme* quantity and at-planting nematode quantities to investigate potential synergism in the development of SDS. PCoA was performed by calculating a dissimilarity matrix of Bray-Curtis distances using the 'vegan' R package (Oksanen et al., 2018), which is commonly used for analyzing species abundance data (Bray and Curtis, 1957; Faith et al., 1987). The 'cmdscale' function of the 'stats' R package was then used to run the PCoA. Principle coordinate scores of the first two dimensions, which correspond to the dimensions with the highest variance, were plotted using the R package 'ggbiplot' (Vu, 2011), and points were colored by the R5 SDS DX.

Two-way stepwise multiple linear regression was implemented to develop models of best fit using the 'MASS' R package (Venables and Ripley, 2002), with cross validation performed using the 'caret' R package (Kuhn, 2018). All models initially included all variables collected prior to the response variable so that each model had predictive capacity. For example, variables used in the initial model to predict R5 SDS included at-planting risk factors and V3 plant variables, but not R5 plant variables. All models were evaluated using the Bayesian Information Criterion (BIC), which penalizes models for the number of factors included in the model to prevent over-fitting the observed data. Each variable was dropped from each model and re-assessed via BIC. If the model was not significantly worse, the variable was left out of the model, another variable was dropped, and the model was re-assessed via BIC. If the model was significantly worse without the variable, the variable was placed back into the model, a different variable was dropped, and the model was re-assessed via BIC. This iterative process was repeated until the best model was identified and no more variables could be dropped without significantly affecting the model. Finally, each of the best models was trained with a randomly selected subset of the data, representing 75% of the data. The models were subjected to a ten-fold cross validation, then used to make predictions on the remaining 25% of the data. The training and prediction was repeated 1,000 times, randomly selecting the training and testing data each time. After each training, the predicted values were correlated to the observed data, and an R^2 value was obtained for the cross validation. Model accuracy was determined by the R^2 of the cross validations, also called Q^2 (Alexander, Tropsha, and Winkler 2015). The best models were formatted into a confirmatory factor analysis model for pathway analysis with the 'lavaan' (Rosseel, 2012) and 'semPlot' packages (Epskamp, 2017) in R. The pathway analysis was re-created by hand using Cytoscape v3.7.1 (Shannon et al., 2003).

Results

Distribution of F. virguliforme and H. glycines in the soil

The field trials were in two different but adjacent fields in 2014 and 2015. Patches of severe SDS and yield loss were seen in the fields in both years. Many of the soil risk factors had a LIP greater than 1 (Table 2-1) indicating that the variance of these variables exceeds the mean, which can be interpreted as significant aggregation (Bez, 2000; Lloyd, 1967). Subsequently, the physical locations of this aggregation were determined via kriging. In 2014 and 2015, areas of elevated at-planting *F. virguliforme* and SCN eggs visually overlapped with areas that developed more severe SDS and had reduced soybean yield (Fig. 2-2).

	LIP		R5 SDS Disease Index		Yield	
Variable	**2014**	**2015**	**2014**	**2015**	**2014**	**2015**
At-planting						
F. virguliforme quantity[a]	**1.08**	**1.10**	0.41	**0.51**	**-0.64**	-0.3
SCN cysts	**1.31**	**1.26**	0.21	**0.5**	-0.32	**-0.45**
SCN eggs	**1.36**	**1.44**	0.23	**0.52**	-0.3	**-0.48**
SCN juveniles	**1.58**	**1.46**	0.18	**0.52**	-0.34	**-0.46**
Spiral nematodes	**1.74**	**1.73**	-0.24	0.03	0	0.03
Lesion nematodes	n.d.	4.78	n.d.	0.01	n.d.	0
Dagger nematodes	n.d.	30.37	n.d.	0.08	n.d.	0.22
Mid-season						
V3 root *F. virguliforme* quantity[b]	0.87	**1.10**	0.44	-0.19	**-0.58**	0.22
V3 root dry weight	-0.51	-0.60	-0.33	-0.01	0.11	0.13
V3 root rot	**1.24**	**1.22**	0.21	**0.28**	-0.21	**-0.5**
V3 foliar SDS of collected plants	**1.16**	**9.99**	0.09	**0.24**	-0.05	-0.22
R5 root *F. virguliforme* quantity[b]	0.86	0.86	-0.29	0.17	0.28	-0.03
R5 root dry weight	0.85	0.89	**-0.54**	**-0.49**	0.27	**0.72**
R5 root rot	**1.18**	**1.69**	0.26	**0.52**	-0.27	**-0.65**
R5 foliar SDS of collected plants	0.90	**1.11**	**0.72**	**0.6**	**-0.72**	**-0.52**
R5 foliar SDS disease index in field	**1.52**	**1.99**	NA	NA	**-0.7**	**-0.66**
Yield	**1.03**	**1.02**	**-0.7**	**-0.66**	NA	NA

Table 2-1. Lloyd's index of patchiness (LIP) and correlation coefficients (*r*) to end-of-season SDS disease index (DX) and yield for variables collected throughout the growing season. Bolded LIP values are > 1 indicating significant aggregation. Bolded R values indicate FDR corrected $P < 0.05$. SCN = soybean cyst nematode, V3 = soybean vegetative growth stage V3, R5 = soybean reproductive growth stage R5, n.d. = not detected in that year, NA indicates uninformative autocorrelations that = 1.

[a]For LIP, femtograms of *F. virguliforme* DNA detected. For correlations with R5 SDS DX and yield, femtograms of *F. virguliforme* DNA per nanogram of total DNA extracted

[b]Calculated as $Ct_{soy} - Ct_{Fv}$, as described in the materials and methods section

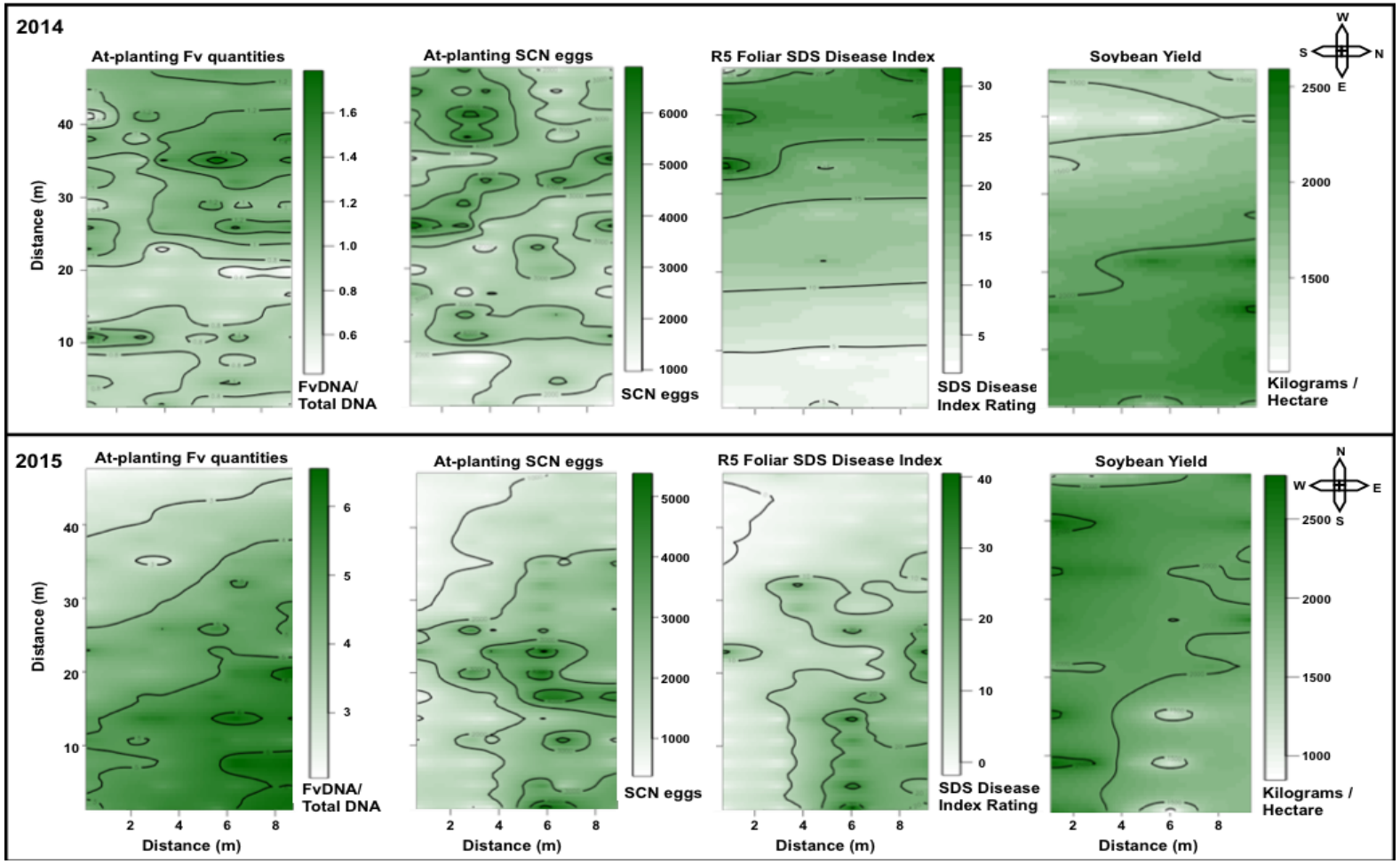

Figure 2-2. Contour plots determined via kriging of the grid-sampled data representing *Fusarium virguliforme* (Fv) DNA quantities, soybean cyst nematode egg quantities, soybean growth stage R5 foliar SDS disease index ratings, and soybean yield. (**A**) Data from 2014 (**B**) Data from 2015. *Fusarium virguliforme* quantities are shown as a proportion of *F. virguliforme* DNA detected (femtograms) from total DNA extracted (nanograms). SCN eggs are shown as the quantity of eggs detected. R5 foliar SDS disease index is determined on a scale from 0-100. Yield is shown in kilograms per hectare. In all plots, white represents low values, and green represents high values. Compass rose indicates cardinal direction of the plot in each year. SDS = sudden death syndrome, Fv = *Fusarium virguliforme,* SCN = soybean cyst nematode, R5 = soybean reproductive growth stage R5.

Pearson's Correlations to end-of-season SDS DX and Yield

Pearson's correlation analysis was used to determine if the at-planting and mid-season variables were significantly correlated to end-of-season SDS and yield (Table 2-1). Nine variables had a significant correlation to end-of-season (R5) SDS DX or yield in at least one year ($P < 0.05$, Table 2-1). However, only root dry weight at R5 and SDS DX of collected R5 plants had a significant correlation to R5 SDS DX in both years. Similarly, only SDS DX of collected R5 plants had a significant correlation to yield in both years. Yield and R5 SDS DX had a significant negative correlation in both years ($P < 0.05$, Table 2-1).

The at-planting *F. virguliforme* quantities had a positive correlation with end-of-season SDS DX in both years, though it was significant only in 2015 ($P < 0.05$, Table 2-1). Additionally, at-planting *F. virguliforme* quantities had a negative correlation with yield in both years, though it was significant only in 2014 ($P < 0.05$, Table 2-1). At-planting SCN cysts, eggs, and juveniles all had positive correlations with end-of-season SDS DX and negative correlations with yield in both years but were only significant in 2015. Mid-season plant variables like V3 root rot and R5 root dry weight had some significant correlations to end-of-season SDS DX and yield, as expected (Table 2-1).

Modeling Yield Loss and SDS Severity

The best model to predict soybean yield, determined by two-way stepwise multiple linear regression and assessment via the BIC, consisted of only two factors; R5 SDS DX and R5 root dry weight (Table 2-2). The best model to predict R5 SDS DX consisted of three factors; year, at-planting *F. virguliforme* quantity, and at-planting SCN eggs (Table 2-2). As R5 root dry weight was a significant factor in the yield model, we further determined that it is significantly

impacted by two factors; V3 root rot and at-planting SCN cysts (Table 2-2). For each of these three models, interaction terms between the explanatory variables were added to the model and re-assessed. Two of the models had marginally improved R^2 values, but none of them had improved *P*-values (data not shown). In addition, multicollinearity of independent factors within the final models were examined using variance inflation factors (VIF), and all were < 2.5. Since multicollinearity does not inhibit interpretation of model predictions and VIF values were < 10, multicollinearity was not regarded as a significant concern (Kutner et al., 2005; O'Brien 2007).

Response variable	Explanatory variables	Parameter estimate	Parameter standard error	*P*	Adjusted R^2	Overall *P*	Average R of Predicted vs Actual	Q^2
Yield	R5 SDS DX	-0.351	0.563	< 0.001	0.5310	< 0.001	0.5740	0.349
	R5 root dry weight[a]	1.951	0.068	< 0.001				
R5 SDS Disease Index	Year	-9.460	3.085	0.003	0.3162	< 0.001	0.4607	0.224
	At-planting Fv qPCR[b]	2.506	5.935	< 0.001				
	At-planting SCN eggs	0.003	0.001	< 0.001				
R5 root dry weight[a]	V3 root rot[c]	-0.029	0.009	0.005	0.2300	< 0.001	0.5175	0.274
	At-planting SCN cysts	-0.026	0.009	0.001				

Table 2-2. Prediction models and cross validations for yield, soybean sudden death syndrome (SDS) disease index (DX), and root dry weight models. Q^2 represents the average R^2 statistic of 1000 replications of a 10-fold cross validation of each model. Fv = *Fusarium virguliforme*, SCN = soybean cyst nematode, V3 = soybean vegetative growth stage V3, R5 = soybean reproductive growth stage R5.
[a]Dry weight in grams
[b]Femtograms of *F. virguliforme* DNA per nanogram of total DNA extracted
[c]In percentage of root system rotten

The R^2 values of the model cross validations (Q^2) was lower than the original model R^2 value, with the exception of the R5 root dry weight model (Table 2-2). These models were visualized in a pathway analysis, which shows the relative contribution of each risk factor on

each dependent variable, along with covariant relationships with other risk factors (Fig. 2-3). Pathway analysis showed that the risk factors included in the yield, R5 SDS DX, and R5 root dry weight models have positive covariance, particularly between at-planting *F. virguliforme* and SCN egg and cyst quantities, which together increase R5 SDS DX and decrease R5 root dry weight, which both affect yield (Fig. 2-3).

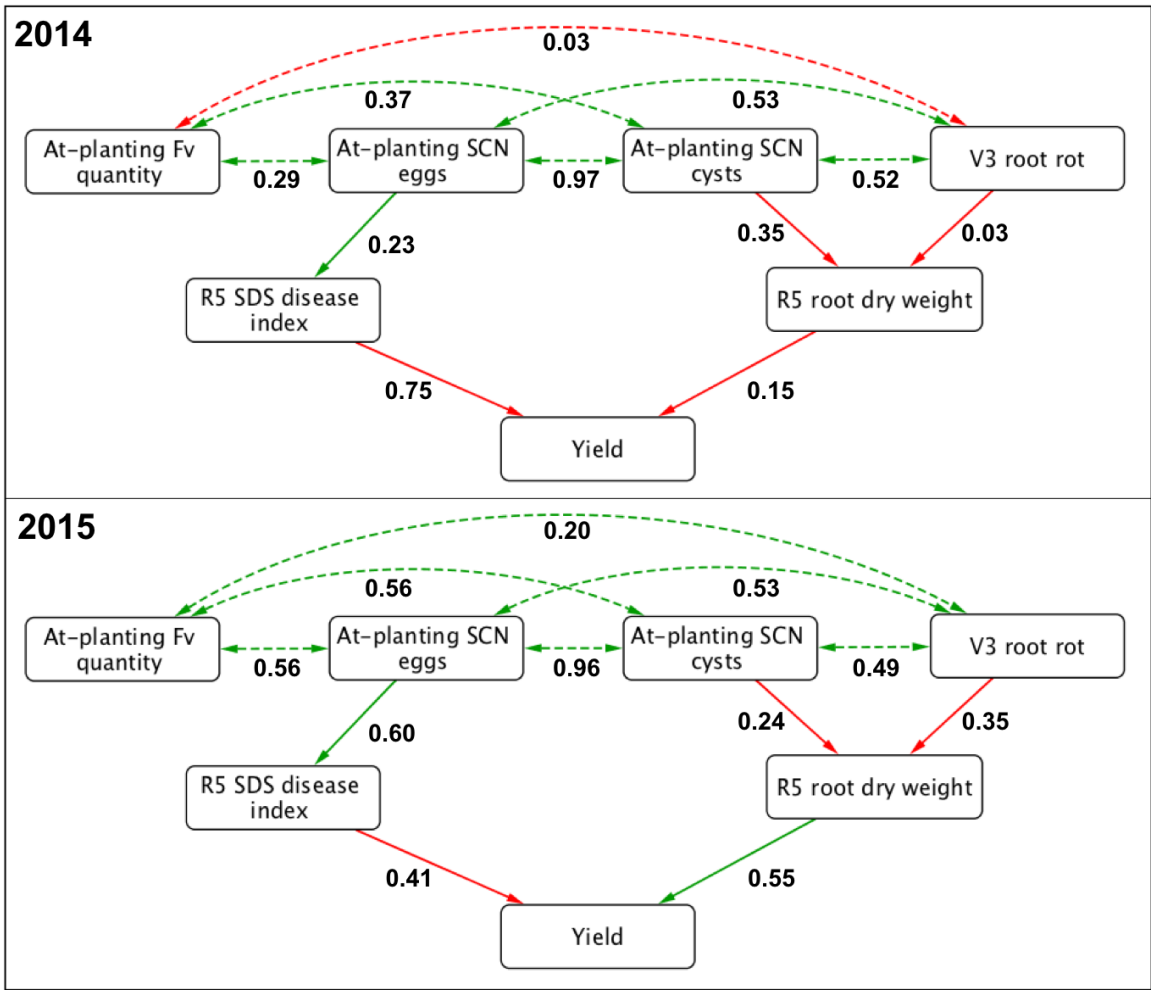

Figure 2-3. Pathway analysis from at-planting risk factors to R5 plant health variables, to yield. (**A**) Data from 2014. (**B**) Data from 2015. Numbers below arrows represent standardized parameter estimates, or beta estimates, which represent the change in standard deviations of the response variable per 1 standard deviation in the predictive variable. Green dashed lines represent positive covariant relationships, green solid lines inicate positive causal relationships, red solid lines indicate negative relationships. SDS = sudden death syndrome, Fv = *Fusarium virguliforme,* SCN = soybean cyst nematode, V3, R5 = soybean vegetative growth stage V3 or R5, respectively.

Multivariate Analysis of F. virguliforme and Nematode Distributions

There was a positive correlation between at-planting *F. virguliforme* and at-planting SCN quantities in both years, but was significant only in 2015 (2014: cysts $r = 0.38$, eggs $r = 0.29$, juveniles $r = 0.30$; 2015: cysts $r = 0.38$, eggs $r = 0.39$, juveniles $r = 0.38$, all $P < 0.001$). Using a 3D plot of at-planting *F. virguliforme*, at-planting SCN juveniles, and end-of-season SDS DX, we found that at low, non-zero *F. virguliforme* levels, the severity of SDS increases as SCN increases (Fig. 2-4 A). Similarly, with high at-planting *F. virguliforme* quantities, the severity of SDS also increases as the number of SCN eggs increases (Fig. 2-4 A). Using PCoA, we investigated additional nematode species and found that the first two dimensions explained 54.0% and 45.2% of the variation, respectively (Fig. 2-4 B). Both at-planting *F. virguliforme* quantities and at-planting SCN juveniles had significant correlations with these dimensions (x and y axes) ($P < 0.001$), and the impact of year is also apparent. While both at-planting *F. virguliforme* quantity and at-planting SCN juveniles had significant positive correlation with the second dimension (y axis), they had significant correlations in opposite directions with the first dimension (x axis) (Fig. 2-4 B, vectors). None of the other nematode species explained a significant amount of variation observed in the data.

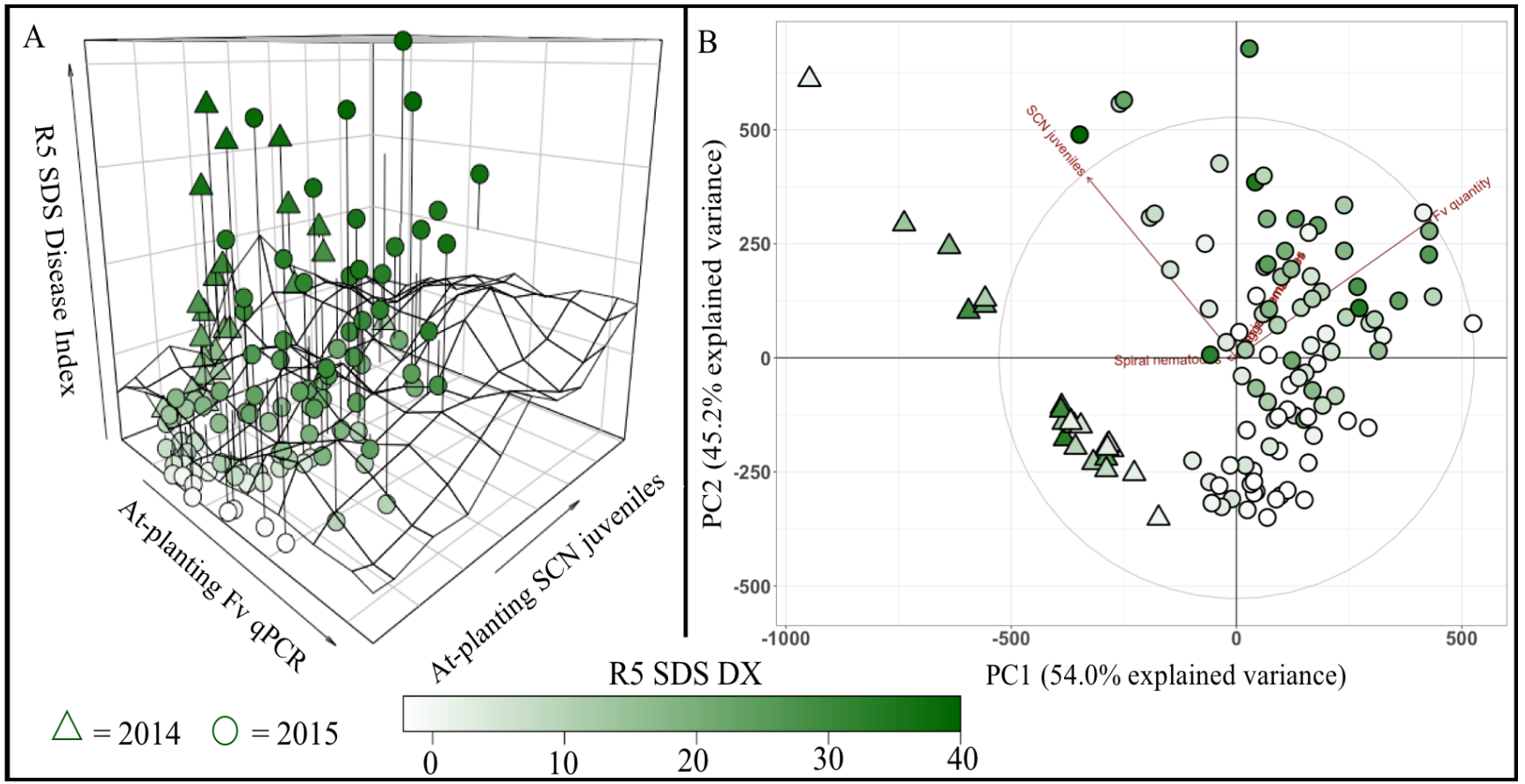

Figure 2-4. Multivariate analyses of sudden death syndrome (SDS) in terms of *Fusarium virguliforme* and nematode pressure. (**A**) 3D plot depicting the quantities of at-planting *F. virguliforme* (femtograms of *F. virguliforme* per nanogram of extracted), SCN juveniles, and ratings of SDS foliar symptoms at soybean growth stage R5. The grid represents the 3D trend in data, as a line of best fit would represent in a traditional 2D plot. (**B**) Principal coordinates analysis (PCoA) of at-planting *F. virguliforme* and multiple nematode species quantities. The circle represents the total calculated distance for the two dimensions represented in the plot. Length of vector arrows show the contribution of each variable to the variation observed in the two dimensions represented. All data points are colored by SDS disease index at stage R5.

Discussion

Soybean SDS is commonly observed in patches with strong severity. Here, we show that many soil variables are significantly aggregated within fields, including the causal agent of SDS, *F. virguliforme* (Table 2-1). These patches of high *F. virguliforme* abundance physically overlapped with future patches of severe SDS and yield loss (Fig. 2-2). Since the data are spatially aggregated (Table 2-1), the correlations between *F. virguliforme* and SDS and yield may be driven by their geospatial location rather than their biological functions, but their overlapping distribution and etiology of *F. virguliforme* suggests a biological explanation. Other studies have also observed that higher *F. virguliforme* populations increase foliar SDS (Freed et al., 2017; Roy et al., 1997).

SDS caused by *F. virguliforme* is difficult to manage, particularly due to a lack of effective in-season strategies. Therefore, knowing the risk of SDS development ahead of planting can influence decision making about purchasing partially resistant varieties and whether or not to use a seed treatment. The present study supports previous findings that *F. virguliforme* inoculum has the largest contribution to SDS development and that SCN has a minor contribution to SDS development (Scherm et al., 1998). By quantifying pathogen abundance at-planting, valuable risk information can be gained and implemented into a risk prediction model for SDS development. The risk prediction models developed here show promise pending further validation in different environments. Our initial cross-validations resulted in Q^2-values, which can be difficult to interpret (Alexander, Tropsha, and Winkler 2015; Golbraikh and Tropsha, 2002). All of the model Q^2 values in this study were positive, indicating that the models have good potential, as poorly performing models yield negative Q^2 values (Alexander, Tropsha, and Winkler 2015). However, the Q^2 values were not > 0.5, and fail to meet the criteria for 'highly

accurate' models (Alexander, Tropsha, and Winkler 2015; Golbraikh and Tropsha, 2002). Therefore, we encourage that these models be applied cautiously and adapted to incorporate even more data, such as soil temperature, soil moisture (Scherm and Yang 1996), photosynthesis (Bajwa et al., 2017; Kuhlgert et al., 2016), and microbiome data (Srour et al., 2017). Combining these types of biotic and environmental risk factors will likely enhance SDS risk prediction further.

Fusarium virguliforme is a soil-borne pathogen that infects soybean roots and remains there throughout foliar SDS development. Detailed mechanisms of foliar SDS development are complicated and largely unknown. Previous studies have shown that there is no consistent correlation between root *F. virguliforme* quantity and the amount of root rot or foliar SDS observed (Wang et al., 2018). In this study, we also observed inconsistent correlations between root *F. virguliforme* quantities and disease symptoms. *Fusarium virguliforme* quantities in V3 roots had opposite trends with R5 SDS DX in 2014 and 2015. Similarly, it had opposite trends with yield in 2014 and 2015 (Table 2-1). Finally, *Fusarium virguliforme* quantities in R5 showed the exact opposite trends with R5 SDS DX and yield as *Fusarium virguliforme* quantities in V3 roots (Table 2-1). In contrast to root qPCR quantities, the abundance of *F. virguliforme* in the soil at planting consistently had positive correlations to R5 SDS DX and yield (Table 2-1). These results support previous findings that observed that the amount of *F. virguliforme* inside of the root does not necessarily indicate current or future disease severity (Wang et al., 2018).

Previous studies have shown that soybean vascular colonization by *F. virguliforme* is critical for severe foliar symptom development (Islam et al., 2017a; 2017b; Navi and Yang, 2008), and the *F. virguliforme* qPCR assay used in this study does not provide localization information when used on entire roots. The combination of high *F. virguliforme* quantity in the

root with low foliar symptoms, or vice versa, might be explained by the location of colonization within the root. It has also been suggested that some *F. virguliforme* isolates may be good at colonizing root tissues but poor at secreting toxins, while others may be poor root colonizers but efficient toxin producers (Li et al., 2009). Regardless, the abundance of *F. virguliforme* in the soil is valuable risk information, and pathogen quantities in post-harvest soil should be examined to determine if these data are representative of pathogen quantities in the soil the following spring. If so, risk information could be obtained even earlier, allowing growers to know their risk of developing SDS prior to placing their variety and seed treatment orders.

It is well established that both SDS and SCN can cause significant yield loss in soybeans independently (Hartman et al., 2015; Koenning and Wrather, 2010), but many reports have also indicated a synergism between SCN and *F. virguliforme* that results in more severe foliar SDS in the field (Back et al., 2002; Brzostowski et al., 2014; McLean and Lawrence, 1993; Scherm et al., 1998; Westphal et al., 2014; Xing and Westphal, 2013). The multivariate analyses in this study indicate that the presence of both pathogens affects the severity of SDS development (Fig. 2-4). Interestingly, the PCoA also shows that the two pathogens have strong correlations in opposite directions along the x-axis (Fig. 2-4 B). This suggests that there is competition between the two pathogens for nutrients within the root, either directly or indirectly. In instances where SCN are highly abundant, *F. virguliforme* may not be able to thrive and co-exist with SCN because of competition for nutrients. Similarly, in instances where *F. virguliforme* is highly abundant, SCN may not be able to thrive and co-exist with *F. virguliforme*. Overall, more SCN juveniles were observed in 2014 than in 2015 (data not shown), but this is likely because the studies were done in adjacent fields. Still, it was surprising that the SCN quantities had a significant correlation to R5 SDS DX and yield in 2015, not 2014. This observation could be due

to the increased sampling effort and higher resolution of data collected in 2015. Taken together, our data support the hypothesis that *F. virguliforme* is primarily responsible for SDS development, and that the additional presence of SCN can increase the risk of developing severe SDS in a density dependent manner.

It has been suggested that SCN or other nematodes may cause wounds and forge a path to the vascular tissue, making it easier for *F. virguliforme* to enter the roots (Diaz Arias 2012). Our analyses found that SCN had a significant association with SDS development, but other nematodes did not (Fig. 2-4 B). Soybean responds to SCN infections by altering expression of pathogenesis related genes and WRKY and MYB transcription factors (Ithal et al., 2007a). Infectious SCN juveniles also upregulate cell wall loosening enzymes, suppress JA in syncytia, and increase peroxidase expression to remove reactive oxygen species (Ithal et al., 2007b). These physiological responses to SCN could make soybean more susceptible to infections by *F. virguliforme*, as a reduction of JA within plants benefits necrotrophic fungi (Antico et al., 2012). It is also possible that a juvenile SCN infecting the same root as *F. virguliforme* may create an environmental change that stimulates more phytotoxin production. In fact, the pathway analysis indicates that *F. virguliforme* increases foliar SDS through interactions with SCN (Fig. 2-3). The exact mechanism by which SCN increases the amount of foliar SDS caused by *F. virguliforme* is still unknown.

Soybean yield and disease severity are simple to measure, but difficult to predict because numerous environmental, edaphic, and biotic factors can affect them. Data from other locations should be processed through these models to further test the accuracy of each model and also determine if different models are better suited to other locations. However, the work here provides a basic framework for incorporating biotic information into risk prediction models for

an economically important disease of soybean. This work is an important step towards facilitating improved SDS management and also provides insights into potential soybean yield losses which can affect soybean markets.

Acknowledgements

The authors would like to thank Dr. D. Kramer and Dr. D. TerAvest for helpful discussions, Dr. H.-X. Chang, Dr. J. Willbur, and J.L. Jacobs for critical review of this manuscript, J.L. Jacobs for root rot disease severity ratings, and Dr. C. and Mrs. A. Druskovich for use of fields in Decatur, MI. This study was supported by the Michigan Soybean Promotion Committee, Bayer CropSciences, the Michigan State University Plant Science Fellowship, the Everett “Tex” Beneke Fund, and the Syngenta Agricultural Scholarship.

CHAPTER 3: Diagnostic qPCR Assay to Detect *Fusarium brasiliense*, a Causal Agent of Soybean Sudden Death Syndrome and Root Rot of Dry Bean

By

Mitchell G. Roth, K. A. Oudman, A. Griffin, J. L. Jacobs, H. Sang, and M. I. Chilvers

This chapter submitted to the journal *Plant Disease* and was accepted with minor revisions.

Author Contributions:

MGR, JLJ, and MIC formalized the objectives of the project. MGR designed primers, probes, and reaction conditions. MGR, KAO, AG, and HS used and validated the method. MGR analyzed data and generated figures. MGR and MIC wrote the manuscript.

Abstract

Species within clade II of the *Fusarium solani* species complex (FSSC) are significant pathogens of dry bean (*Phaseolus vulgaris*) and soybean (*Glycine max*), causing root rot and/or sudden death syndrome (SDS). These species are morphologically difficult to distinguish, and often require molecular tools for proper diagnosis to a species level. Here, a TaqMan probe-based qPCR assay was developed to distinguish *Fusarium brasiliense* from other closely related species within clade II of the FSSC. The assay displays high specificity against close relatives and high sensitivity, with a detection limit of 100 femtograms. This assay was able to detect *F. brasiliense* from purified mycelia, from infected dry bean roots, and from soil samples throughout Michigan. When multiplexed with an existing qPCR assay specific to *F. virguliforme*, accurate quantification of both *F. brasiliense* and *F. virguliforme* was obtained, which can facilitate accurate diagnoses and identify co-infections with a single reaction. The assay is compatible with multiple qPCR thermal cycling platforms and will be helpful in providing accurate detection of *F. brasiliense*. Management of root rot and SDS pathogens in clade II of the FSSC is challenging and must be done proactively, as no mid-season management strategies currently exist. However, accurate detection can facilitate management decisions for subsequent growing seasons to successfully manage these pathogens.

Introduction

The *Fusarium solani* species complex (FSSC) is composed of three major clades, designated I, II, and III (Chitrampalam and Nelson 2016; O'Donnell 2000). *Fusarium* species within clade II are soil-borne plant pathogens that cause root rot of soybean (*Glycine max*) and dry bean (*Phaseolus vulgaris*) (Aoki et al., 2014; Chitrampalam and Nelson 2016). Macroscopic

and microscopic morphological features of the species within clade II are very challenging to differentiate, as all produce similar pigments, and conidia lengths and widths overlap (Aoki et al., 2003). Of the eight species within this clade, six are also capable of causing sudden death syndrome (SDS) on soybean (Aoki et al., 2003, 2005; 2012a; 2012b; Tewoldemedhin et al., 2016). In South America, the SDS-causing pathogens include *F. virguliforme* O'Donnell & T. Aoki*, F. brasiliense* T. Aoki & O'Donnell*, F. tucumaniae,* and *F crassistipitatum*, while in North America SDS is caused by *F. virguliforme* and the recently identified *F. brasiliense* (Wang et al., 2018b). *F. virguliforme*, *F. brasiliense*, and a third undescribed *Fusarium* sp. cause soybean SDS in South Africa (Tewoldemedhin et al., 2014, 2016). The sixth SDS-causing species, *F. azukicola*, has only been isolated from adzuki bean (*Vigna angularis*), but when inoculated on soybeans it caused foliar SDS symptoms (Aoki et al., 2012b).

Soybean SDS is an annual threat in both the U.S. and Brazil (Aoki et al., 2003; O'Donnell et al., 2010). These countries dominate soybean production in North and South America, respectively, both producing an estimated 120 million metric tons of soybeans in 2017-2018 (World Agricultural Supply and Demand Estimates, 2018). Managing these SDS-causing FSSC clade II species is challenging, as few fungicides demonstrate efficacy (Kandel et al., 2018; Sang et al., 2018; Wang et al., 2017), genetic resistance is partial (Chang et al., 2018), and crop rotation practices take up to 3 or 4 years of non-host crops to lower SDS pressure (Leandro et al., 2018). However, some SDS-causing species like *F. tucumaniae* show increased sensitivity to certain chemistries (Sang et al., 2018), so it is important to know the species present in order to recommend proper management.

Monitoring the spread of fungal pathogens is also important to determine if management strategies are effective. Fungal pathogens can be spread through the transfer of infected

materials, shared use of contaminated field equipment, and through wind-blown spores. The mechanism of *F. virguliforme* spread remains unknown, though the sexual stage has never been observed and only one mating type has been detected (Hughes et al., 2014), so spread through the discharge of sexual ascospores appears unlikely. A single mating type for *F. brasiliense* was identified in South Africa (Tewoldemedhin et al., 2016), but both mating types have been found in South America (Hughes et al., 2014) and Michigan isolates (Oudman et al, *in prep*). In addition, *F. brasiliense* isolates with different mating types were identified in the same field (Oudman et al, *in prep*). This indicates that conventional fungal sexual reproduction is probable in *F. brasiliense*, providing an opportunity for the pathogen to produce perithecia and spread through the discharge of sexual ascospores into the air. Only one isolate of *F. brasiliense* had been identified in the U.S. prior to 2014 from an unknown host in California (Aoki et al., 2005), so it is unlikely that it has spread from California to Michigan without being detected in agricultural states in between. Population genetic studies of *F. virguliforme* suggest that it originated in South America and spread to North America (Wang 2016). It may be possible that *F. brasiliense* also originated in South America and spread to the U.S. through unknown mechanisms, but a native Michigan population of *F. brasiliense* cannot be ruled out.

As both soybeans and dry beans are hosts for *Fusarium* root rot pathogens, accurate identification of these species in these fields is critical to prevent significant inoculum increases, severe yield losses, and potential spread to neighboring fields. Accurate identification of *F. brasiliense* and monitoring its spread throughout the U.S. will allow growers to implement the few successful management strategies available. Additionally, with consumer trends increasing the demand of non-genetically modified foods, many dry bean growers are beginning to rotate non-genetically modified soybeans with dry beans (B. Glass, *personal communication*),

potentially leading to even more significant inoculum increases. Our primary objective was to develop a highly specific and sensitive quantitative polymerase chain reaction (qPCR) assay to detect *F. brasiliense*. The second objective was to validate the performance of this qPCR assay in detecting *F. brasiliense* from purified mycelia, infected plant roots, and soil. Third, we examined the compatibility of this assay with a *F. virguliforme* qPCR assay for multiplexing purposes, which provides fast and efficient diagnosis of closely related species or the presence of co-infections.

Materials and Methods

Assay Design

The intergenic spacer (IGS) region of the ribosomal RNA gene has been used to distinguish species within the FSSC (Wang et al., 2011), including SDS- and brown root rot-causing fusaria (O'Donnell et al., 2010), and was used as the target locus for this assay as in other qPCR assays (Chilvers et al., 2007; Okubara et al., 2013; Wang et al., 2015). IGS sequences from species within clade II of the FSSC were obtained from National Center for Biotechnology Information (NCBI); *F. azukicola* GenBank number JQ670149*, F. brasiliense* GenBank numbers KF706657 and FJ919512*, F. cuneirostrum* GenBank numbers FJ919511 and FJ919548*, F. crassistipitatum* GenBank numbers FJ919521 and FJ919554*, F. phaseoli* GenBank numbers FJ919498, FJ919510*,* and FJ919500*, F. tucumaniae* GenBank numbers FJ919507 and FJ919515*,* and *F. virguliforme* GenBank numbers FJ919499 and FJ919557. Sequences were aligned in MEGA7 (Kumar et al., 2016) using the MUSCLE algorithm (Edgar 2004).

Primer/Probe Name	Sequence (5'-3')	Length (bp)	Tm (°C)[a]	Reference
Fb_F2	AGGTCAGATTTGGTATAGGGTAGGTGAGA	29	67.4	This study
Fb_R2	CGGACCATCCGTCTGGGAATTT	22	66.3	This study
Fb_Prb1	5HEX-TGGGATGCCCT+AATTTTT+ACGG-3IABkFQ	22	64.7	This study
F6-3	GTAAGTGAGATTTAGTCTAGGGTAGGTGAC	30	57.8	Wang et al., 2014
R6	GGGACCACCTACCCTACACCTACT	24	59.6	Wang et al., 2014
FvPrb-3	6FAM-TTTGGTCTAGGGTAGGCCG-MGBNFQ	19	70.0	Wang et al., 2014

Table 3-1. Primers and probes used in this study. Tm = melting temperature, bp = base pairs
[a] Calculated with the OligoAnalyzer tool from IDT, using the default "qPCR" parameter settings.

A TaqMan probe using two locked nucleic acids was designed to capitalize on the presence of two single nucleotide polymorphisms (SNPs) specific to *F. brasiliense* within eight base pairs of each other (Fig. 3-1). Primer and probe sequences are reported in Table 3-1. Each qPCR reaction was performed with two technical replicates, and contained 10 µL of 2X TaqMan Universal real-time PCR master mix (1X final concentration, Applied Biosystems), 250 nM Fb_Prb1, 500 nM Fb_F1 primer, 500 nM Fb_F2 primer, 400 ng BSA, 2 µL DNA template, and molecular grade water up to a total reaction volume of 20 µL. All assays were performed on the StepOnePlus v2.3 (Applied Biosystems) and were set up in clear MicroAmp 96-well plates (Thermo-Fisher Scientific, Waltham, MA), except for multiplexed assays. Multiplexed reactions were performed with two technical replicates, each containing 10 µL of 2X TaqMan Universal real-time PCR master mix (Applied Biosystems), 250 nM Fb_Prb1, 500 nM Fb_F1 primer, 500 nM Fb_F2 primer, 100 nM FvPrb3, 500 nM F6-3, 500 nM R6, 400 ng BSA, 2 µL of each DNA template, and molecular grade water up to a total reaction volume of 20 µL.

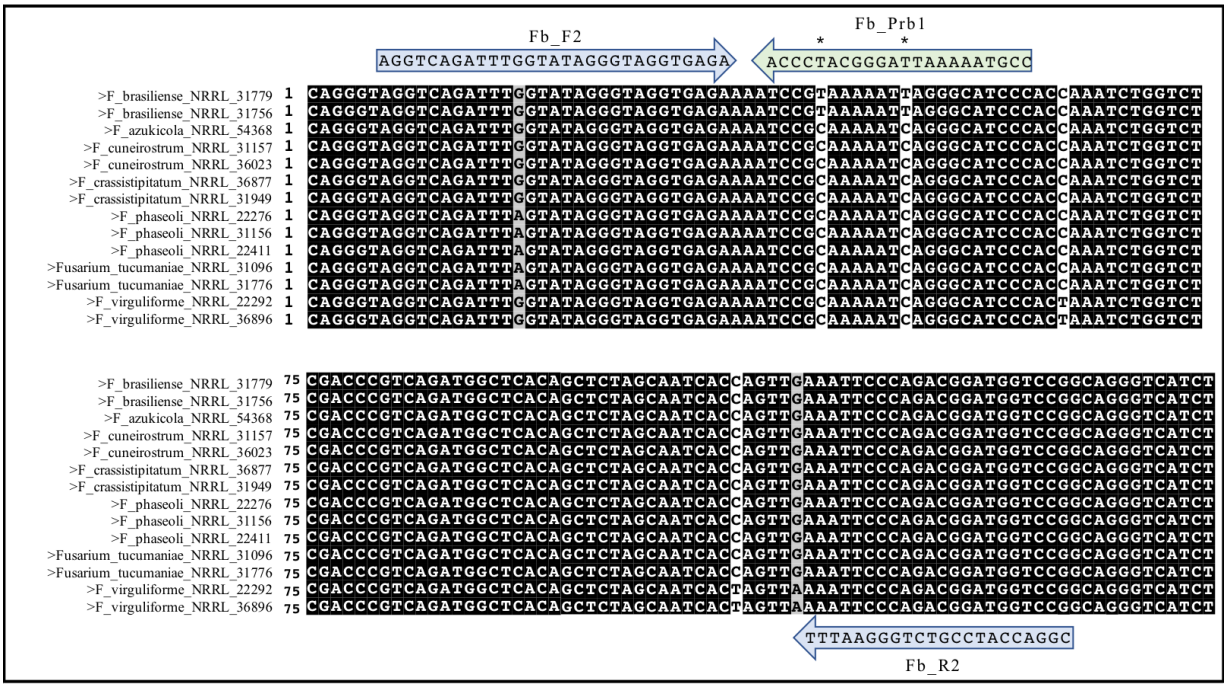

Figure 3-1. Sequence alignment of 149 base pairs of the intergenic spacer (IGS) of species within clade II of the *Fusarium solani* species complex. Primers (blue) and probe (green) sequences are displayed as arrows at their annealing location within the IGS. Asterisks represent locked nucleic acids designed in the qPCR probe.

qPCR Assay Specificity

Fusarium isolates used for testing the assay specificity were either collected from counties throughout Michigan or requested from the USDA ARS Culture Collection (NRRL) (Table 3-2). Isolates collected from Michigan were obtained from root tissues of infected soybean or dry bean plants. Briefly, plants displaying stunting or foliar SDS symptoms from fields throughout Michigan were uprooted and transported to the lab where soil was thoroughly washed off roots. Root sections displaying severe discoloration and rot were soaked in 5% bleach solution (0.4% NaOCl) for 4 minutes, rinsed thoroughly in sterile deionized water for 4 minutes, blotted dry with sterile paper towel, and plated on WMS agar (2% agar, 15µg/mL metalaxyl, 300µg/mL streptomycin) to select for fungal growth. Plates were incubated for seven days at room temperature and observed under a dissecting microscope (Leica Microsystems,

Buffalo Grove, IL, USA) for the formation of sporodochia. Using an insect pin, macroconidia from a sporodochium were transferred and spread on fresh WMS agar and allowed to grow for 24 hours. Finally, a single germinating macroconidium was aseptically transferred onto full strength potato dextrose agar (Neogen, Lansing, MI). Isolates were stored at room temperature on synthetic nutrient agar slants (1 g/L KH_2PO_4, 1 g/L KNO_3, 0.5 g/L $MgSO_4$, 0.5 g/L KCl, 0.2 g/L glucose, 0.2 g/L sucrose, 2% agar) in scintillation vials (Research Products International, Mount Prospect, IL, USA) for long-term storage.

Macroconidia from pure cultures were inoculated into potato dextrose broth and allowed to grow at room temperature for 48 hours with shaking at 100 rpm. DNA was extracted with two similar methods. For testing specificity at a standard 5ng per reaction, mycelia were filtered from broth with two layers of Miracloth (Millipore Sigma, St. Louis, MO, USA) and rinsed with 200 mL of sterile deionized water. The fresh, rinsed mycelia were immediately transferred to a sterile, pre-chilled mortar and ground with a pestle in the presence of liquid nitrogen. After approximately 1 minute of tissue disruption, the ground mycelia were immediately transferred into microcentrifuge tubes containing a DNA extraction buffer (200 mM Tris-HCl, 1 M NaCl, 25 mM EDTA, 25 mM sodium dodecyl sulfate, 100 µg RNaseA) and incubated for 30 minutes at room temperature, with gentle inversions every 5 minutes. Proteinase K (200 µg) was added to each sample and incubated at room temperature for 20 minutes, with gentle inversions every 5 minutes. The samples were chilled on ice for 5 minutes, followed by an addition of 0.2 volumes of ice-cold 5 M potassium acetate, another 5-minute incubation, and then centrifuged at 5000 x g for 12 minutes at 4°C. The supernatant was transferred to fresh tubes, and an equal volume of 25:24:1 phenol:chloroform:isoamyl alcohol (Millipore Sigma) was added, mixed gently by inversion, and centrifuged. The phenol:chloroform step was repeated, followed by an additional

step using chloroform only. The DNA was precipitated by adding 0.1 volumes 5 M NaCl, 1 volume isopropanol, incubated on ice for 10 minutes, and pelleted at 10,000 x g in a refrigerated centrifuge at 4°C. The pelleted DNA was washed twice with freshly prepared 80% ethanol and resuspended in 10 mM Tris buffer pH 8.0 overnight. The quality of the DNA was determined by measuring the 260/280 nm and 260/230 nm readings using a Nanodrop 1000 (Thermo-Fisher Scientific), and quantity was determined using the Qubit dsDNA BR Assay Kit (Thermo-Fisher Scientific). An aliquot of DNA from each isolate was diluted to 2.5 ng/µL, with 2 µL used in qPCR assays for specificity testing (Fig. 3-2). For testing specificity of other isolates at various starting DNA concentrations (Table 3-2), mycelia were harvested with sterilized wooden stirrers (STR Supplies Inc., British Colombia, Canada) into sterile 1.5 mL tubes. The tube was plugged with a sterile cotton ball, and mycelia were lyophilized for 48 hours. Approximately 20 mg of lyophilized mycelia were ground with 3-5 2 mm glass beads and subjected to the same extraction protocol as described above.

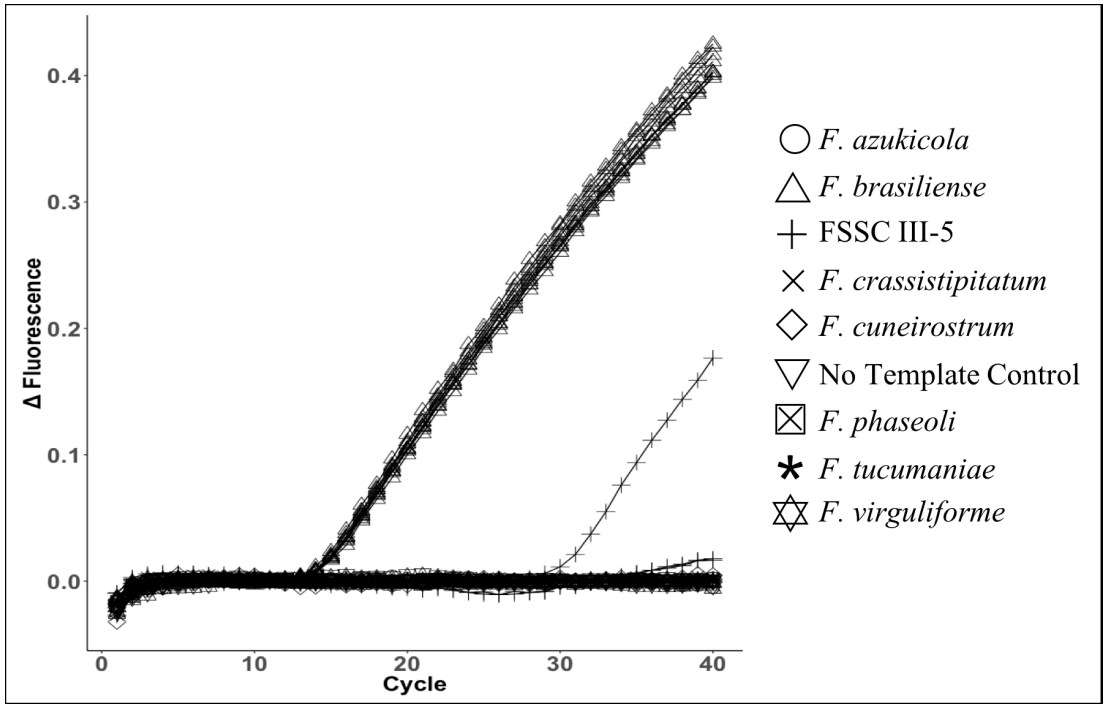

Figure 3-2.

Figure 3-2 (cont'd). Amplification results of 5 ng DNA of select isolates across different species within the *Fusarium solani* species complex. Isolates represented are *F. azukicola* isolates NRRL 54361 and 54362, *F. brasiliense* isolates F-14-42, F-15-158, F-16-137, NRRL 34938, MI-Mtc-C1, FSSC III-5 isolates MI-Mtc-B10 and F-15-118, *F. crassistipitatum* isolate NRRL 31949, no-template (water) control, *F. cuneirostrum* F-14-52, *F. phaseoli* isolates MI-Mtc-A12 and NRRL 22411, *F. tucumaniae* isolates NRRL 43334 and 31777, and *F. virguliforme* isolates DB P28 R13 and Vb-2a.

Table 3-2.

Isolate[a]	Species[b]	Host	Location isolated	Assay Result	Ct with 5 ng starting DNA
54361	*F. azukicola*	*Vigna angularis*	Obihiro, Hokkaido, Japan	–	n.d.
54362	*F. azukicola*	*V. angularis*	Obihiro, Hokkaido, Japan	–	n.d.
34938	*F. brasiliense*	Unknown	Vila Maria, Rio Grande do Sul, Brazil	+	14.92
22678	*F. brasiliense*	*Phaseolus vulgaris*	California, USA	+	
MI-Mtc-C1	*F. brasiliense*	*Glycine max*	Montcalm County, MI, USA	+	14.21
MI-Mtc-A13	*F. brasiliense*	*G. max*	Montcalm County, MI, USA	+	14.43
F-14-12	*F. brasiliense*	*P. vulgaris*	Ingham County, MI, USA	+	
F-14-42	*F. brasiliense*	*P. vulgaris*	Montcalm County, MI, USA	+	14.71
F-14-44	*F. brasiliense*	*P. vulgaris*	Montcalm County, MI, USA	+	
F-15-33	*F. brasiliense*	*P. vulgaris*	Montcalm County, MI, USA	+	
F-15-101	*F. brasiliense*	*P. vulgaris*	Huron County, MI, USA	+	
F-15-102	*F. brasiliense*	*P. vulgaris*	Huron County, MI, USA	+	
F-15-144	*F. brasiliense*	*P. vulgaris*	Montcalm County, MI, USA	+	
F-15-158	*F. brasiliense*	*P. vulgaris*	Saginaw County, MI, USA	+	14.47
F-15-162	*F. brasiliense*	*P. vulgaris*	Saginaw County, MI, USA	+	
F-15-174	*F. brasiliense*	*P. vulgaris*	Gratiot County, MI, USA	+	
F-15-192	*F. brasiliense*	*P. vulgaris*	Michigan, USA	+	
F-16-21	*F. brasiliense*	*G. max*	Montcalm County, MI, USA	+	
F-16-59	*F. brasiliense*	*G. max*	Montcalm County, MI, USA	+	13.94
F-16-118	*F. brasiliense*	*P. vulgaris*	Saginaw County, MI	+	
F-16-119	*F. brasiliense*	*P. vulgaris*	Saginaw County, MI	+	
F-16-124	*F. brasiliense*	*P. vulgaris*	Saginaw County, MI	+	
F-16-125	*F. brasiliense*	*P. vulgaris*	Saginaw County, MI	+	
F-16-127	*F. brasiliense*	*P. vulgaris*	Saginaw County, MI	+	
F-16-128	*F. brasiliense*	*P. vulgaris*	Saginaw County, MI	+	
F-16-131	*F. brasiliense*	*P. vulgaris*	Saginaw County, MI	+	
F-16-136	*F. brasiliense*	*P. vulgaris*	Saginaw County, MI	+	
F-16-137	*F. brasiliense*	*P. vulgaris*	Saginaw County, MI, USA	+	14.52
31949	*F. crassistipitatum*	*G. max*	Cristalina, Goias, Brazil	–	n.d.

Table 3-2 (cont'd)

46170	*F. crassistipitatum*	*G. max*	Las Lajitas, Salta, Argentina	–	
46175	*F. crassistipitatum*	*G. max*	Las Lajitas, Salta, Argentina	–	
F-14-52	*F. cuneirostrum*	*P. vulgaris*	Montcalm County, MI, USA	–	n.d.
Fsp3	*F. cuneirostrum*	*P. vulgaris*	Uganda, Africa	–	
F5	*F. oxysporum*	*Solanum tuberosum*	Michigan, USA	–	
F-16-16	*F. phaseoli*	*G. max*	Montcalm County, MI, USA	–	
MI-Mtc-A12	*F. phaseoli*	*G. max*	Montcalm County, MI, USA	–	n.d.
22158	*F. phaseoli*	*P. vulgaris*	Rockville, MD, USA	–	
22276	*F. phaseoli*	*P. vulgaris*	Rockville, MD, USA	–	
MI-Mtc-A4	*F. phaseoli*	*G. max*	Montcalm County, MI, USA	–	
22411	*F. phaseoli*	*P. vulgaris*	California, USA	–	n.d.
36549	*F. proliferatum*	*Gladiolus sp.*	The Netherlands	–	
MI-Mtc-C3FS (Wht)	FSSC clade III-11	*G. max*	Montcalm County, MI, USA	–	
MI-Mtc-A2FS	FSSC clade III-11	*G. max*	Montcalm County, MI, USA	+	21.13
F-15-118	FSSC clade III-5	*P. vulgaris*	Montcalm County, MI, USA	–	n.d.
MI-Mtc-C17FS	FSSC clade III-5	*G. max*	Montcalm County, MI, USA	–	
MI-Mtc-B16FS	FSSC clade III-5	*G. max*	Montcalm County, MI, USA	–	
MI-Mtc-B10	FSSC clade III-5	*G. max*	Montcalm County, MI, USA	+	30.43
31777	*F. tucumaniae*	*G. max*	Vila Maria, Rio Grande do Sul, Brazil	–	n.d.
43334	*F. tucumaniae*	*G. max*	Armstrong, Sante Fe, Argentina	–	n.d.
31096	*F. tucumaniae*	Unknown	Argentina	–	
DB P28 R13	*F. virguliforme*	*P. vulgaris*	Van Buren County, MI, USA	–	n.d.
Vb-2a	*F. virguliforme*	*G. max*	Van Buren County, MI, USA	–	n.d.
F-14-77	*F. virguliforme*	*G. max*	Ingham County, MI, USA	–	
DB P27 R13	*F. virguliforme*	*P. vulgaris*	Van Buren County, MI, USA	–	
DB P30 R5	*F. virguliforme*	*P. vulgaris*	Van Buren County, MI, USA	–	
22292 (Mont-1)	*F. virguliforme*	*G. max*	Illinois, USA	–	
36897	*F. virguliforme*	*G. max*	Argentina	–	
54291	*F. virguliforme*	*G. max*	Argentina	–	
VB-1	*F. virguliforme*	*G. max*	Van Buren County, MI, USA	–	
	Rhizoctonia solani (AG2-2)	*G. max*		–	
	Rhizoctonia solani (AG4)	*G. max*		–	

Table 3-2 (cont'd)

Phialophora gregata (genotype A)	*G. max*	–
Phialophora gregata (genotype B)	*G. max*	–
Macrophomina phaseolina	*G. max*	–
Sclerotinia sclerotiorum	*G. max*	–

Table 3-2 (cont'd). Panel of isolates used to determine specificity of *F. brasiliense* qPCR assay. + indicates positive amplification, while – indicates no amplification. n.d. = not determined.
[a]Isolate IDs with only numbers were obtained from the USDA ARS Culture Collection (NRRL). All other isolates were obtained by J. Jacobs and Dr. Martin Chilvers.
[b]FSSC = *Fusarium solani* species complex. Clade III designation indicates phylogenetic placement within the FSSC, where III-5 and III-11 represent unnamed species within the FSSC clade III.

qPCR Assay Sensitivity

Extracted DNA from four *F. brasiliense* isolates were used to test the sensitivity of the assay using serial DNA dilutions. Concentrations tested were 10-fold dilutions beginning with 1,000,000 femtograms (1 nanogram) of *F. brasiliense* DNA to 10 femtograms (Fig. 3-3 A). The Ct values for each concentration were averaged across isolates, since rDNA copy number can vary among strains of the same species (Balajee et al., 2009; Wang et al., 2015). The qPCR efficiency was calculated by finding the line of best fit on a plot with the logarithm of the DNA concentrations and their respective Ct value (Fig. 3-3B, Table 3-3). The limit of detection was determined using samples showing > 95% amplification at the lowest DNA concentration tested, as previously described (Bustin et al., 2009).

Isolate[a]	DNA Concentration[b]	Ct[c]	Mean Ct	Standard Error
F-14-42	1000000	17.20	17.22	0.099
F-15-158	1000000	16.82		
F-16-137	1000000	17.37		
NRRL 34938	1000000	17.50		
F-14-42	100000	20.50	20.49	0.075
F-15-158	100000	20.22		
F-16-137	100000	20.57		
NRRL 34938	100000	20.69		
F-14-42	10000	24.08	24.08	0.097
F-15-158	10000	23.72		
F-16-137	10000	24.33		
NRRL 34938	10000	24.17		
F-14-42	1000	27.65	27.66	0.079
F-15-158	1000	27.35		
F-16-137	1000	27.92		
NRRL 34938	1000	27.72		
F-14-42	100	30.96	31.18	0.139
F-15-158	100	30.86		
F-16-137	100	31.28		
NRRL 34938	100	31.62		
F-14-42	10	35.26	34.93	0.249
F-15-158	10	33.93		
F-16-137	10	35.36		
NRRL 34938	10	35.16		

Table 3-3. Serial dilutions for four *F. brasiliense* isolates used to determine assay sensitivity.
[a]Isolate 34938 was obtained from the USDA ARS Culture Collection (NRRL). All other isolates were obtained by J. Jacobs and Dr. Martin Chilvers.
[b]Concentration in femtograms of DNA per reaction
[c]Ct = cycle threshold, or cycle at which fluorescent signal crossed the detection threshold.

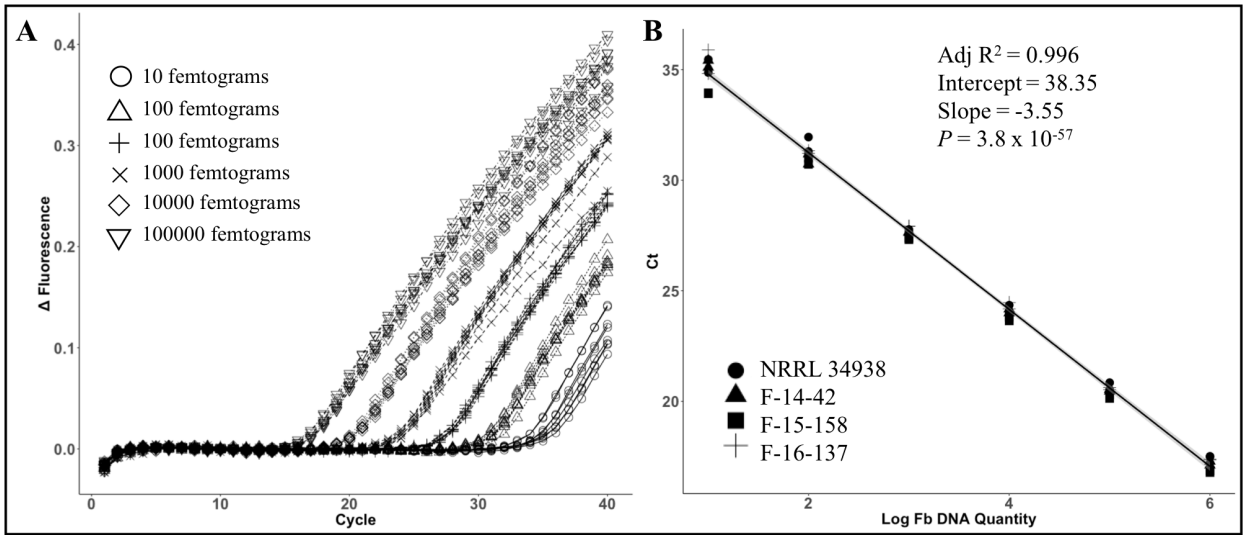

Figure 3-3. Detection of serial dilutions of 4 *F. brasiliense* isolates. The qPCR assay sensitivity reached 10 fg (**A**). These isolates consistently amplified at all concentrations tested, with an average of 99.6% efficiency (**B**). Fb = *Fusarium brasiliense*

Assay Validation

A field site in Ingham County, MI was planted with a randomized complete block design containing two dry bean cultivars (Zenith and Red Hawk), three treatments (non-inoculated, *F. brasiliense* inoculated, and *F. oxysporum* inoculated), with 4 plot replicates per cultivar x treatment combination. Each plot was 20 ft (6.1 m) long with 4 rows of plants with 76 cm (30 inch) row spacing. The plots were planted on 8 June 2018 at 69,696 seeds/acre for Red Hawk and 78,408 seeds/acre for Zenith using a cone planter. Inoculum was produced on autoclaved sorghum grains, as described in Wang et al., 2018a. Inoculum was packaged into envelopes directly with seeds, and the entire contents were poured into the cone planter, sowing the seeds and inoculum in-furrow at an average rate of 7.1 mL of inoculum per linear foot. Three plants from each plot were sampled on 12 September 2018. The foliar tissues were removed from the roots in the field, and the roots were thoroughly washed clean of soil and allowed to dry at 55°C for 2 days. The dried roots from each sample were placed in a 50 mL plastic container (OPS Diagnostics, Lebanon, NJ, USA) with 2, 1 cm diameter steel balls and ground into a powder

using a GenoGinder 2010 (SPEX Sample Prep, Metuchen, NJ, USA) at 1500 rpm for 5 minutes. DNA was extracted from these roots using the same phenol:chloroform procedure described above. Total DNA was quantified using a Nanodrop 1000 (Thermo-Fisher Scientific).

To validate the assay with soil samples, bulk soil was collected from ten soybean fields throughout Michigan during the spring and summer of 2018, using a 3 cm diameter, 15 cm deep soil core. Soil was placed into a 3.8 L (1-gallon) plastic bag, homogenized, subsampled into 0.45 kg (5 lb) paper bags, and dried at 55°C for 2 days. Approximately 500 mg of dried soil was used for DNA extraction using a FastDNA Spin Kit for Soil (MP Bio, Solon, OH). Two technical DNA extraction replicates were performed, and a third technical replicate was extracted after being spiked with approximately 5000 *F. brasiliense* conidia. An estimated number of conidia in non-spiked soil samples that showed positive qPCR results was obtained by performing the following calculation: 5000 spores * z = x spores * y, where 5000 is the number of spores spiked into each soil sample, z is the Ct of the spiked sample, and y is the Ct of the non-spiked sample. Non-spiked samples that amplified at a Ct > 31 cannot be reliably quantified because they are below the limit of detection. Therefore, an estimated number of conidia was not calculated for these samples (Table 3-4).

To test the multiplexing capacity and transferability of this assay onto other platforms, serial dilutions of *F. virguliforme* DNA and *F. brasiliense* DNA were amplified in a single reaction containing primers F6-3, R6, and probe FvPrb-3 (Wang et al., 2015) along with primers and probe developed in this study (Table 3-1). Reactions were set up in LightCycler 480 96-well plates (Roche Diagnostics, Mannheim, Germany) and performed on a CFX96 Real-Time PCR Detection System v3.1 (BioRad Laboratories, Hercules, CA). Multiplexed reactions were set up as described above.

Location in MI	Type	Ct[a]	Quantity DNA detected[b]	Spores / 500 mg soil[c]
Clinton County	Unknown	–	–	–
	Spiked	21.26	57083	5000
Hillsdale County	Unknown	–	–	–
	Spiked	18.10	346132	5000
Lenawee County	Unknown	36.92	7	n.d.
	Spiked	20.14	108360	5000
Montcalm County	Unknown	32.03	137	n.d.
	Spiked	18.90	226150	5000
Ingham County	Unknown	34.13	39	n.d.
	Spiked	17.29	547582	5000
Saginaw County	Unknown	30.83	246	2804*
	Spiked	18.01	363252	5000
Sanilac County	Unknown	29.51	529	3052*
	Spiked	17.41	512226	5000
St. Joseph County	Unknown	32.95	74	n.d.
	Spiked	19.72	137118	5000
Van Buren County, Field 1	Unknown	–	–	–
	Spiked	19.90	123579	5000
Van Buren County, Field 2	Unknown	–	–	–
	Spiked	21.97	70167	5000

Table 3-4. Amplification of *F. brasiliense* from soils across Michigan. Values with an asterisk (*) are estimates, calculated as indicated in the materials and methods. Dashes indicate no detection, and n.d. indicates not determined since detection was below the limit of detection.
[a]Ct = cycle threshold, or cycle at which fluorescent signal crossed the detection threshold.
[b]Quantity in femtograms
[c]Estimated by taking solving for x, using the equation: 5000 spores * z = x spores * y, where 5000 is the number of spores spiked into each soil sample, z is the Ct of the spiked sample, and y is the Ct of the non-spiked sample.

Results

Assay Design

A 149 base pair segment in the IGS was identified containing *F. brasiliense* specific SNPs, and the primers and probe were designed in this region (Fig. 3-1). The forward primer encompasses one SNP shared by *F. brasiliense*, *F. cuneirostrum, F. crassistipitatum,* and *F. virguliforme*, but excludes *F. phaseoli* and *F. tucumaniae*. The reverse primer is conserved among all species used in the IGS alignment. The probe encompasses two SNPs unique and

specific to *F. brasiliense*, containing two thymines instead of two cytosines. The probe associated with these residues was designed with locked nucleic acid bases to enhance specific binding at these sites (Fig. 3-1, asterisks). The primers and probe are not predicted to form any significant homo- or heterodimers ($\Delta G > -9$), and performs at an ideal anneal and extension temperature of 60°C.

qPCR Assay Specificity

Genomic DNA isolated from purified mycelia was used to evaluate specificity across closely related species within clade II of the FSSC (Table 3-2). The only isolates detected were *F. brasiliense* and some members of FSSC clade III (Chitrampalam and Nelson 2016) (Fig. 3-2, Table 3-2). However, when tested with a standard 5 ng of starting DNA, *F. brasiliense* isolates consistently had Ct values within 1 Ct of each other (13.94 - 14.92, Table 3-2). In contrast, FSSC clade III isolates with positive reactions had higher Ct values. These results indicate that the assay designed here can distinguish *F. brasiliense* from closely related clade II species and other common soil-borne pathogenic fungi (Table 3-2). However, there may be some cross-reactivity with clade III species. With pure cultures, *F. brasiliense* can readily be distinguished from clade III species based on growth rate and morphology (Fig. 3-4).

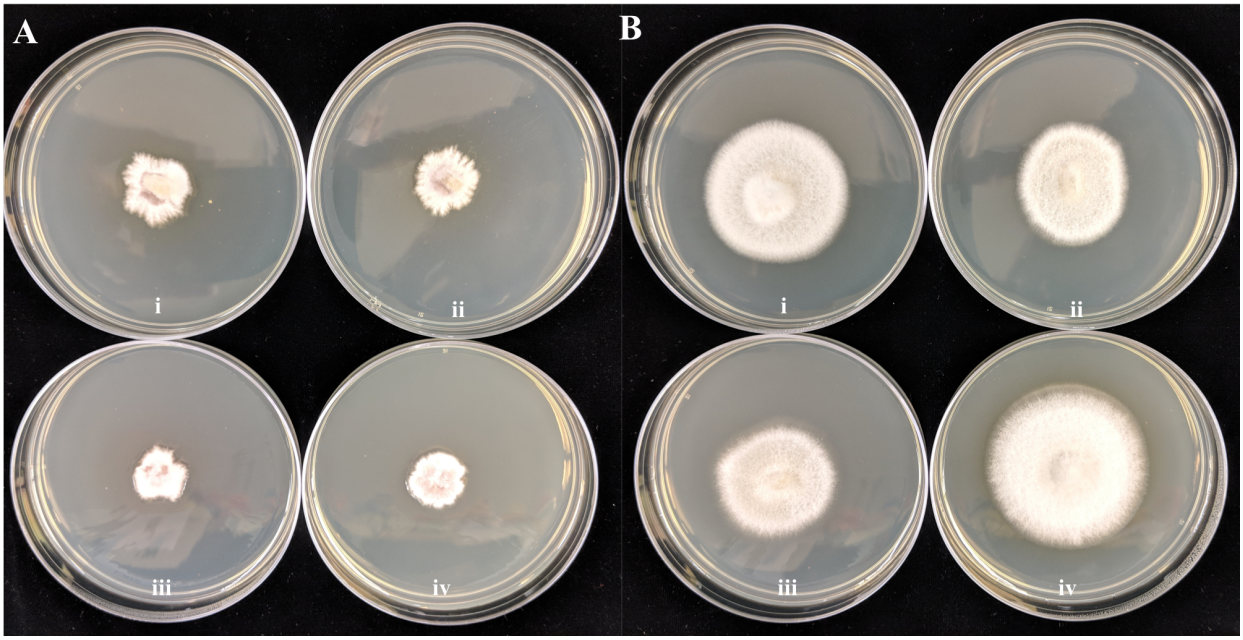

Figure 3-4. Representative isolates of (A) *F. brasiliense* and (B) *Fusarium solani* complex clade III isolates plated on potato dextrose agar, 7 days post inoculation. *F. brasiliense* isolates represented are (i) MI-Mtc-C1, (ii) MI-Mtc-A13, (iii) F-16-137, and (iv) F-15-158. *F. solani* clade III isolates represented are (i) MI-Mtc-C17, (ii) MI-Mtc-B16, (iii) MI-Mtc-B10 (iv) MI-Mtc-A2.

qPCR Assay Sensitivity

The *F. brasiliense* qPCR assay targeting the IGS region provided high sensitivity, reproducibly amplifying target DNA from multiple isolates at concentrations as low as 10 femtograms of target DNA (Fig. 3-3). Although all four isolates amplified with just 10 femtograms of starting DNA, the standard error of detection was also highest at this concentration. Therefore, the limit of detection (Bustin et al., 2009) was conservatively determined to be 100 fg, or a Ct $\geq$ 31 (Table 3-3). Although target DNA can be amplified at lower concentrations, quantities determined below this cycle threshold may not be reliable.

Assay Validation

To determine the applicability of this assay to field trials, roots from artificially inoculated dry beans were harvested and subjected to DNA extraction and tested with the *F. brasiliense* qPCR assay developed here. *F. brasiliense* was detected consistently in dry bean plots inoculated with *F. brasiliense* (average Ct = 29.6), but not in samples from non-inoculated plots or plots inoculated with *F. oxysporum* (average Ct = 36.3) (Fig. 3-5).

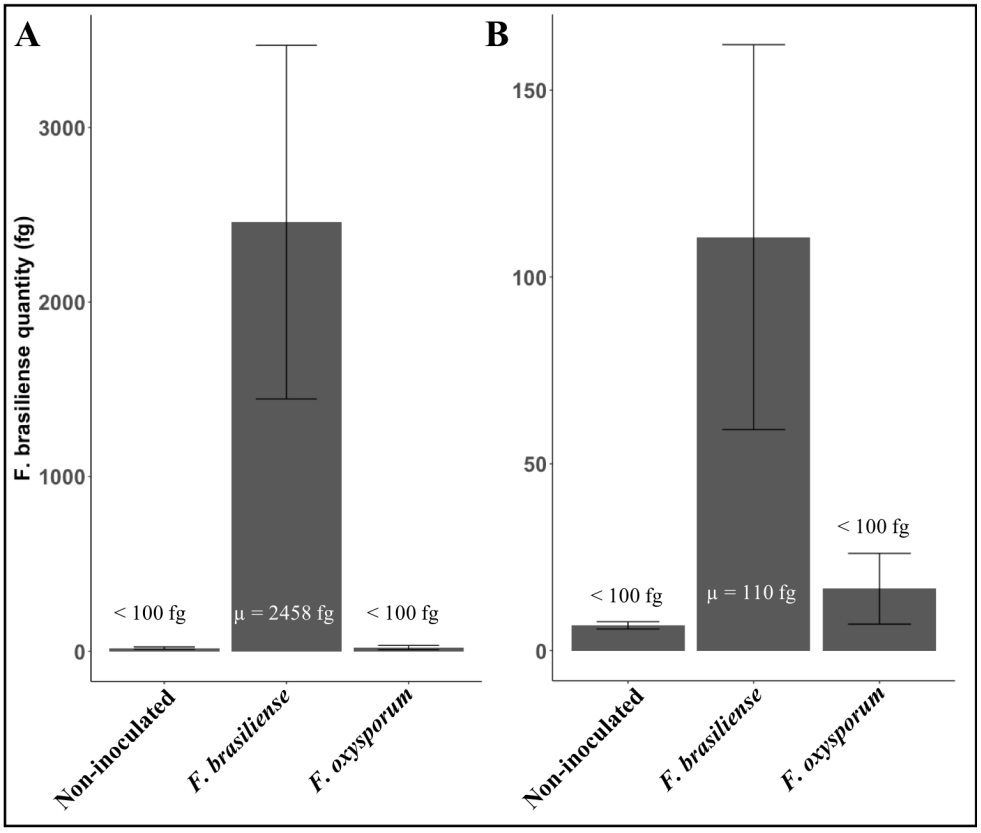

Figure 3-5. **Detection of *F. brasiliense* within root tissues of dry bean cultivar (A) Zenith or (B) Red Hawk.** Values listed over bars indicate the average femtograms of *F. brasiliense* DNA detected within roots of 12 plants per treatment. Non-inoculated and *F. oxysporum* inoculated samples were not detected above the limit of detection of 100 fg.

Soil samples obtained from ten counties throughout Michigan were screened for the presence of *F. brasiliense*. All soil samples spiked with *F. brasiliense* conidia were successfully detected with Ct values ranging from 17.29 to 21.97 indicating relatively pure DNA samples

lacking PCR inhibitors (Table 3-4). Additionally, *F. brasiliense* was detected in non-spiked soil samples from six counties, although only two were confidently above the limit of detection of 100 fg (Table 3-4). Using a known quantity of spores in the spiked samples, an estimated 2804 and 3051 spores were present in Saginaw and Sanilac Counties, respectively, per 500 mg of soil.

The primers and probes for the *F. brasiliense* assay and a *F. virguliforme* assay (Wang et al., 2015) were used simultaneously in a multiplexed reaction (Table 3-1). Amplification for each assay was only observed when target DNA was present, indicating no cross-reactivity between the assays (Table 3-5). Combinations of serial dilutions of *F. brasiliense* and *F. virguliforme* DNA were successfully amplified in pooled reactions, and an accurate quantification of each target was obtained (Table 3-5).

F. virguliforme **DNA added[a]**	***F. brasiliense*** **DNA added[a]**	***F. virguliforme*** **Ct[b]**	***F. brasiliense*** **Ct[c]**
1,000,000	0	17.35	–
100,000	0	20.95	–
10,000	0	24.46	–
1,000	0	28.10	–
100	0	31.53	–
0	1,000,000	–	17.57
0	100,000	–	21.02
0	10,000	–	24.17
0	1,000	–	26.60
0	100	–	31.80
1,000,000	1,000,000	17.49	18.86
10,000	1,000,000	24.74	17.26
10,000	100,000	24.52	20.73
100	100,000	33.34	20.87
1,000	10,000	28.02	23.61
100	1,000	31.82	27.00
0	0	–	–

Table 3-5. Amplification of serial dilutions of *F. brasiliense* and/or *F. virguliforme* DNA. Assays display specificity towards target species and can be distinguished and quantified in a multiplexed system. Dashes represent no detection.
[a]Quantity in femtograms
[b]Ct = cycle threshold, or cycle at which fluorescence crossed the threshold for *F. virguliforme*.
[c]Ct = cycle threshold, or cycle at which fluorescent signal crossed the detection threshold for *F. brasiliense*.

Discussion

Clade II species in the FSSC are economically important pathogens capable of causing root rot and/or soybean SDS, and significant yield losses. They are very similar morphologically with a slow growth rate and are taxonomically distinguished by conidia measurements and number of septa (Aoki et al., 2014). However, since a pure culture is required to obtain conidia, and conidia measurements of these species overlap (Aoki et al., 2003), it can be very difficult to obtain accurate identifications in a timely manner, if at all, using morphology alone. DNA extractions and qPCR assays can be performed in a single day, expediting accurate diagnoses. High quality qPCR assays have high sensitivity, capable of detecting very low quantities of target DNA. Designing an assay around a multi-copy target like the IGS region can increase sensitivity. Previous assays designed around the IGS region have provided sensitivity to as low as 100 femtograms of target DNA (Rojas et al., 2017; Wang et al., 2015). The assay developed here validates two SNPs specific to *F. brasiliense* compared to other species within the FSSC clade II (Fig. 3-1, Table 3-2). The assay performs at a high efficiency of 99.6%, and consistently detected 10 fg of target DNA when obtained from pure culture and has a confident limit of detection of 100 fg (Fig. 3-3, Table 3-3).

Interestingly, some FSSC clade III isolates showed amplification, while others did not. The use of the name *F. solani* has been discouraged by taxonomists (Aoki et al., 2014), so isolates not confidently identified to a species level were listed with their phylogenetic clades. For instance, clade III-5 and clade III-11 isolates in this study represent unnamed species that fall within the FSSC clade III, though FSSC clade III-5 is sometimes considered the true *F. solani* (Coleman, 2016). Amplification was not specific to clade III-5 or clade III-11 isolates, suggesting some IGS sequence diversity among these unnamed species. Sanger sequencing of

the 149-base pair IGS region amplified with this qPCR assay showed that clade III-11 isolate MI-Mtc-C3FS (Wht) and clade III-5 isolates F-15-118 and MI-Mtc-C17FS share SNPs with other non-*F. brasiliense* species, confirming their negative reactions. Sanger sequencing of this region for clade III-11 isolate MI-Mtc-A2FS and clade III-5 isolate MI-Mtc-B10 IGS showed SNPs shared with *F. brasiliense*, thus explaining the positive reactions. Phylogenetic analyses of *F. solani* clade III isolates commonly use the other molecular markers such as *TEF1*, ITS rDNA, and *RPB2* (Chitrampalam and Nelson, 2016, Wang et al., 2018b), perhaps due to the difficulty of sequencing and assembling the repetitive IGS region. However, this assay provides specificity to *F. brasiliense* within *F. solani* clade II, and qPCR positive FSSC clade III strains can be distinguished from *F. brasiliense* though morphology (Fig. 3-4). However, the identity of all isolates should be confirmed through PCR and Sanger sequencing of multiple loci (Wang et al., 2018b).

This assay can provide an initial screen for *F. brasiliense* in soil and root samples even if pure fungal cultures are not being obtained. The assay is not likely to produce false-positive results by cross-amplification of FSSC clade III species because some of these species do not cross react even at high concentrations, and others that do cross-react do so with much lower efficiency, producing significantly higher Ct values (Table 3-2, Fig. 3-2). For instance, with five nanograms of purified fungal DNA, cross-reactive FSSC clade III species showed higher Ct values by at least 6 cycles (Table 3-2). Therefore, obtaining a sufficient concentration of FSSC clade III DNA from root or soil samples for cross-reactivity is unlikely. In contrast, all *F. brasiliense* isolates from international locations were consistently detected with high accuracy and efficiency. Therefore, obtaining a sufficient concentration of *F. brasiliense* from root or soil samples for successful amplification and detection is possible, as shown in Table 3-4 and Figure

3-5. Initial screens using this qPCR assay can help guide when and where to begin isolation attempts for pure cultures, and also help generate an understanding of the global distribution of *F. brasiliense*. For example, the *F. brasiliense* assay yielded Ct values < 31 from soil samples from Saginaw and Sanilac, counties, where *F. brasiliense* has already been successfully isolated from plant roots (Oudman et al., *in prep*). The assay also gave Ct values > 31, but < 36 with DNA from soil samples from Montcalm and Ingham counties, where *F. brasiliense* has also been successfully isolated (Oudman et al., *in prep*). Finally, the assay gave Ct values > 31, but < 36, from Lenawee and St. Joseph soils, where *F. brasiliense* has not yet been identified. Therefore, the assay provides evidence that warrants further investigation and isolation attempts for *F. brasiliense* from these counties.

Soybean and dry bean are valuable crops in Michigan worth a combined $1.08 billion in 2017 (USDA-NASS, 2017). Fusarium root rot and SDS consistently rank in the top 10 most destructive soybean diseases in northern states, including Michigan (Allen et al., 2017). To date, genetic resistance to Fusarium root rot is partial, and only few fungicides are effective against it (Sang et al., 2018; Wang et al., 2017). Therefore, accurate detection and integrating successful management practices like using seed treatments (Kandel et al., 2018), crop rotations (Leandro et al., 2018), tillage practices, and planting partially resistant cultivars are key to preventing yield loss. Further understanding of a possible host preference is also needed in order to inform management strategies, as *F. brasiliense* is more commonly found in areas of dry bean production while *F. virguliforme* is more commonly found in areas of soybean production in Michigan (Oudman et al., *in prep*). Preliminary experiments examining host preference have shown that both *F. brasiliense* and *F. virguliforme* cause disease on both soybean and dry bean, and that disease severity or root colonization is not significantly different from one another in a

growth chamber setting (Roth and Chilvers, *unpublished*). Symptomatic roots infected by *F. brasiliense* and *F. virguliforme* are indistinguishable from one another, and co-infections may also be possible. Therefore, the ability to multiplex the *F. brasiliense* and *F. virguliforme* assays can also save time and effort in accurate diagnoses.

Partial genetic resistance will continue to be an important part of integrated management for Fusarium root rot pathogens. Though more research has been done with resistance to *Fusarium* spp. in soybean, resistance is complicated and partial (Chang et al., 2018). Dry beans (*Phaseolus vulgaris*) originated from Mesoamerica (Bitocchi et al., 2012), but were traded through Central America and experienced a bottle neck while reaching South America. Therefore, gene pools in current bean breeding lines originate from Mesoamerica or the northern Andean region of South America (Bellucci et al., 2014; Miklas et al., 2006; Singh 2001; Singh and Schwartz 2010). Dry bean varieties from Mesoamerican gene pools, like cultivar Zenith, are smaller in size and typically have higher resistance to root rot diseases (Román-Avilés and Kelly, 2005; Schneider et al., 2001). Another Mesoamerican variety, Zorro, was shown to have more resistance to *F. virguliforme* than the Andean variety Red Hawk, a large-seeded red kidney bean cultivar (Dry Bean Research Report, 2017). Interestingly, more *F. brasiliense* was detected in inoculated Zenith roots than Red Hawk roots in this study. However, root colonization and disease severity are not always strongly correlated, particularly among the clade II FSSC species (Wang et al., 2018a). A formal study should be conducted to determine the inherent resistance levels of multiple varieties from the two different gene pools to *F. brasiliense*.

Acknowledgements

The authors would like to thank Z.A. Noel, M. Breunig, V. Ortiz, and A.G. McCoy for helpful discussions and manuscript revisions. This work was funded in part by the Michigan Soybean Promotion Committee, Michigan Dry Bean Commission, Michigan Department of Agriculture and Rural Development, Bayer CropSciences, the Syngenta Agricultural Scholarship, and Project GREEEN.

CHAPTER 4: A Protoplast Generation and Transformation Method for Soybean Sudden Death Syndrome Causal Agents *Fusarium virguliforme* and *F. brasiliense*

By

Mitchell G. Roth and Martin I. Chilvers

This chapter was accepted for publication pending minor revisions in the journal *Fungal Biology and Biotechnology*, an open-access journal.

Author Contributions:

MGR and MIC developed the ideas to generate this protocol. MGR designed primers and plasmids, performed the experiments, and acquired all images. MGR and MIC wrote and revised the manuscript, approving of the final draft.

Abstract

Soybean production around the globe faces significant annual yield losses due to pests and diseases. One of the most significant causes of soybean yield loss annually in the U.S. is sudden death syndrome (SDS), caused by soil-borne fungi in the *Fusarium solani* species complex. Two of these species, *F. virguliforme* and *F. brasiliense*, have been discovered in the U.S. However, genetic mechanisms that these pathogens employ to induce root rot and SDS are largely unknown. Previous methods describing *F. virguliforme* protoplast generation and transformation have been used to study gene function, but these methods lack important details and controls. In addition, no reports of protoplast generation and genetic transformation have been made for *F. brasiliense*. We developed a new protocol for developing fungal protoplasts in these species and test the protoplasts for the ability to take up foreign DNA. We show that wild-type strains of *F. virguliforme* and *F. brasiliense* are sensitive to the antibiotics hygromycin and nourseothricin, but mutants transformed with resistance genes displayed resistance to these antibiotics. In addition, integration of a reporter gene demonstrates that the foreign DNA is expressed and results in a functional protein, providing fluorescence to both pathogens. This protocol provides significant details for reproducibly producing protoplasts and transforming *F. virguliforme* and *F. brasiliense*. The protocol can be used to develop high quality protoplasts for further investigations into genetic mechanisms of growth and pathogenicity of *F. virguliforme* and *F. brasiliense*. Fluorescent strains developed in this study can be used to investigate temporal colonization and potential host preferences of these species.

Introduction

Soybean sudden death syndrome (SDS) is an economically important disease across soybean growing regions around the world (Allen et al., 2017; Aoki et al., 2005; Tewoldemedhin et al., 2014, 2017). Causal agents of soybean SDS are soil-borne ascomycete fungi in clade II of the *Fusarium solani* species complex (Aoki et al., 2014; Chitrampalam and Nelson 2016). Two of the SDS-causing species, *F. virguliforme* and *F. brasiliense*, have been discovered in the U.S. (Roy et al., 1997; Wang et al., 2018). Although transformation of *F. virguliforme* has been demonstrated (Mansouri et al., 2009), it has not been for *F. brasiliense*. Due to the recent discovery of *F. brasiliense* on common bean (*Phaseolus vulgaris*) and soybean (*Glycine max*) roots in the U.S. (Jacobs et al., 2018; Wang et al., 2018) and the significance of soybean SDS caused by these pathogens, it is desirable to have a detailed protocol for efficient genetic manipulation that is applicable to both pathogens. Improved understanding of the genetic underpinnings of SDS development could lead to improved management for these two pathogens.

Both *F. virguliforme* and *F. brasiliense* infect root tissues, with evidence suggesting that both appressoria and cell wall degrading enzymes are involved (Chang et al., 2016b; Navi and Yang, 2008). However, the genetic mechanisms of SDS development are largely unknown. Two effector proteins have been identified and characterized from *F. virguliforme*, which seem to play a role in SDS development (Brar et al., 2011; Chang et al., 2016a; Pudake et al., 2013). These two effector genes can also be found in isolates of *F. brasiliense* via BLAST searches, but the mechanism by which these effector proteins induce SDS remain unknown in both species. Breeding efforts have improved soybean tolerance to foliar symptom development, but no completely resistant lines exist to date (Hartman et al., 2015). Successful management of these

pathogens can be achieved through long-term crop rotations and with seed treatments containing the fungicide fluopyram (Kandel et al., 2018; Leandro et al., 2018), but long-term crop rotations are not widely adopted by growers, and different members of the *Fusarium solani* species complex have shown different sensitivities to fluopyram (Sang et al., 2018). Therefore, improved genetic resistance is desired, but requires a deeper understanding of the genetic mechanisms of SDS development caused by each pathogen. Genome sequences are available for both of these pathogens, but experimental identification and characterization of effector genes through genetic manipulation needs to be done in order to gain a better understanding of how these pathogens induce soybean SDS.

One of the major challenges in genetic transformation of fungi is the development of high-quality protoplasts. Each fungus has unique cell wall properties, which can require different sets of expensive cell wall degrading enzymes to successfully remove the cell wall (Peberdy 1979). Once the cell wall is digested to reveal the membrane bound protoplast, it is prone to lysing or shriveling due to osmotic stress (Peberdy 1979). One protocol for protoplasting and transformation of *F. virguliforme* has been reported and used to generate a fluorescent strain (Mansouri et al., 2009), with additional studies using it to knock out candidate effector genes (Chang et al., 2016a; Pudake et al., 2013) and genes involved in fungal development (Islam et al., 2017b, 2017a). However, no such protocols exist for *F. brasiliense*. Difficulties obtaining *F. brasiliense* and *F. virguliforme* protoplasts using the existing protocol led us to investigate other methods. The objective of this study was to develop an efficient protoplasting and transformation method suitable for genetic manipulation in both *F. brasiliense* and *F. virguliforme* for future hypothesis testing of gene function.

Materials and Methods

Sensitivity to selectable antibiotics

To determine an appropriate concentration to select for growth of successful transformants, an initial screen using amended agar plates was conducted. The wild type strain of *F. virguliforme* chosen was Mont-1 (NRRL 22292), which was isolated from soybean in Illinois, and the wild type strain of *F. brasiliense* chosen was F-16-137, which was isolated from dry bean in Michigan. Full strength potato dextrose agar (PDA) (Neogen Corporation, Lansing, MI) was amended with 0, 25, 50, 100, or 150 µg / mL of hygromycin B (Millipore-Sigma, Burlington, MA) or nourseothricin (Research Products International, Mt. Prospect, IL). A single 0.5 mm PDA plug from 14-day old cultures of *F. virguliforme* isolate Mont-1 (NRRL 22292) or *F. brasiliense* isolate F-16-137 were added to each amended plate. After 14 days, fungal growth was visually assessed to determine an appropriate concentration that provides 100% growth inhibition. Based on a visual assessment, 100 µg / mL of each antibiotic was sufficient to prevent fungal growth of both isolates.

Development of transformation constructs

To provide evidence of genetic transformation, we constructed DNA vectors containing a resistance gene to a selectable antibiotic and a gene that provides a fluorescent phenotype under ultraviolet light. Both transformation vectors were constructed with Gibson assembly (Gibson et al., 2009) of four DNA fragments; a bacterial origin of replication, a bacterial selection marker, a fungal selection marker, and a fluorescent protein marker. A high copy origin of replication and a kanamycin resistance gene were cloned from a plasmid designed for the overexpression of MinC in cyanobacteria (MacCready et al., 2017), which we refer to as pJM2016. For *F.*

virguliforme, the selectable marker was the hygromycin phosphotransferase gene (*hph*) under the control of the *Aspergillus nidulans* TrpC promoter and terminator derived from pCB1004 (Carroll et al., 1994) and the fluorescent protein marker was enhanced green fluorescent protein (eGFP) under the control of the *A. nidulans* gpd promoter and TrpC terminator, derived from pDS23-eGFP (M. Nowrousian, *unpublished*). For *F. brasiliense*, the selectable marker was the nourseothricin acetyltransferase gene (*nat*) under the control of the *A. nidulans* TrpC promoter derived from pDS23-eGFP and the fluorescent protein marker was the red fluorescent protein mCherry, derived from pCMB-TMEr (Ivanov and Harrison, 2014) under the control of the *A. nidulans* gpd promoter and TrpC terminator. All primers used to amplify these regions prior to Gibson assembly are listed in Table 4-1. Assembled plasmids were named FvGFP2 and pmCherry_NAT, respectively, and propagated in *E. coli* strain DH5α plated on LB amended with 50 μg / mL kanamycin. Plasmids were isolated using the GeneJET Plasmid Miniprep kit (Thermo Fisher Scientific, Waltham, MA) and linearized with either SacI-HF or EcoRI-HF (New England Biolabs, Ipswich, MA) prior to transformation, according to the manufacturer protocol. The plasmid pmCherry_NAT is designed such that the selectable marker can be replaced by restriction digest with EcoRI and NheI, and the fluorescent marker gene can be replaced by restriction digest with NheI and SacI. A double digest of these plasmids can separate the transformation construct from the bacterial DNA sequences, which can be purified via gel extraction. However, gel extraction decreases DNA yield and transformation efficiency (data not shown). Plasmid maps are presented in Figure 4-1.

Primer name	Sequence (5'-3')	Template	PCR Product Length	Purpose
Nat_F_NheI	GACGACAGCTAGCATCGATCTGACGATACTTTCTAG AGAATAGGAACTTCGG	pDS23-eGFP	1333 bp	Amplify *nat* gene
Nat_R_EcoRI	AGTTCTGGTGAATTCTCACCAGTGTAACTGATATTGA AGGAGCATTTTTTGG			
HindIII-mChF	GTGTGAAGCTTATGGTGAGCAAGGGCGAG	pCMB-TMeR	708 bp	Cloning mCherry into pDS23-eGFP
NotI-mChR	TTCTTGCGGCCGCCTACTTGTACAGCTCGTCCATGCC			
GPD_F_PstI	GACGACACTGCAGATCGATCTGACGGTACAGTGACC GGTGACTCTTTCTGG	pDS23-eGFP	2410 / 2427 bp	Amplifying GPD promoter + eGFP + TrpC terminator
GPD_F_SacI	ATGCTCGATGAGTTTTTCTAAGAGCTCTGTACAGTGA CCGGTGACT	pDS23-eGFP with eGFP replaced by mCherry	2410 bp	Amplifying GPD promoter + mCherry + TrpC terminator
TrpC_R_NheI	AGATCGATGCTAGCTGTCGTCGACTTCGAGTGGAGA TGTGGAGTG	Both versions of pDS23 (eGFP or mCherry)	2427 bp	Amplifying GPD promoter + eGFP or mCherry + TrpC terminator
OriF_EcoRI	TGGTGAGAATTCACCAGAACTGTCAAGATCAAAGGA TCTTCTTGAGATCCTT	pJM2016	655 bp	Amplify high copy number OriC
Ori-F2	TGGCTTTCCCCGCGTTGCTGGCGTT			
KanF3	GCCAGCAACGCGGGGAAAGCCACGTTGTGTCTC	pJM2016	941 bp	Amplify kanamycin resistance gene
Kan-R	TTAGAAAAACTCATCGAGCATCAAATGAAACTGCA			

Table 4-1. Primer pairs designed and used in this study for cloning and assembly into plasmids.

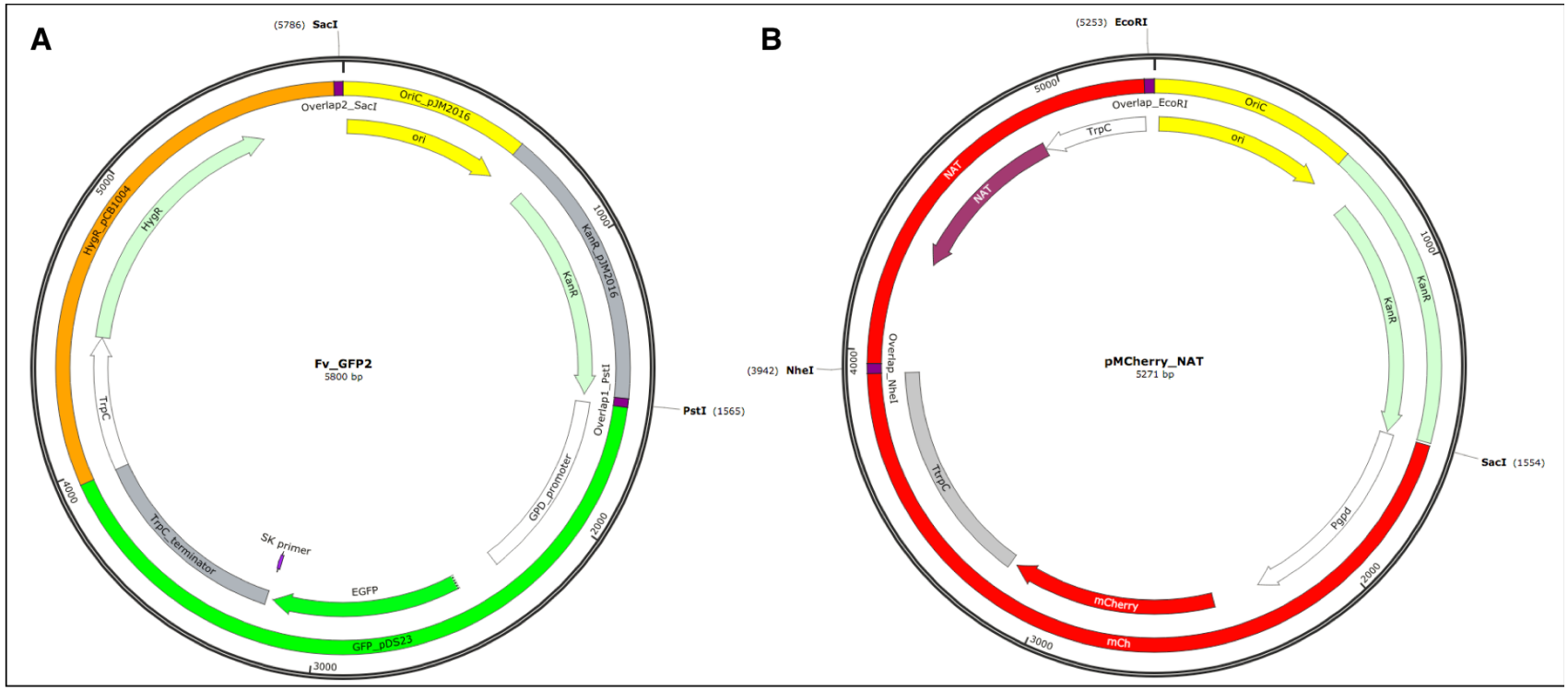

Figure 4-1. Plasmid maps used to generate transgenic *Fusarium* strains. (**A**) Plasmid used to transform *F. virguliforme*, providing resistance to hygromycin and creating a GFP fluorescent phenotype. (**B**) Plasmid used to transform *F. brasiliense*, providing resistance to nourseothricin and creating an RFP fluorescent phenotype.

Protoplasting

A hybrid method of two existing protocols was used for developing protoplasts of *F. virguliforme* and *F. brasiliense* (Hallen-Adams et al., 2011; Mansouri et al., 2009). A two to three-week-old PDA plate containing mature *Fusarium* sporodochia was flooded with 5 mL sterile water and scraped gently with a sterile spreader to dislodge spores. Approximately 4 mL of the water could be recovered from the plate and was filtered through two layers of sterile cheesecloth into a 15 mL conical tube to purify conidia away from mycelia. One hundred microliters of conidia were used to inoculate 50 mL sterilized potato dextrose broth (PDB, Neogen) in a 250 mL flask. The flasks were incubated for 36-48 hours at room temperature, with shaking at 125 rpm, to facilitate conidia germination.

Mycelia were collected aseptically using a sterile funnel and Miracloth (Millipore-Sigma), removing the spent PDB. Mycelia were transferred back into the empty 250 mL flask with a sterile spatula, and 30 mL of protoplasting solution was added immediately. The protoplasting solution was prepared one hour prior to protoplasting, composed of 1.2 M KCl, 750 mg driselase (Millipore-Sigma), 1.5 mg chitinase from *Streptomyces griseus* (Millipore-Sigma), and 150 mg lysing enzymes from *Trichoderma harzianum* (Millipore-Sigma). The protoplasting solution was stirred for at least 30 minutes prior to use and filtered through a 0.45 µm filter just before adding to the mycelia. Once immersed in the protoplasting solution, the mycelia were incubated at 30°C for 3-5 hours with shaking at 75 rpm. A 10 µL aliquot of the protoplasting reaction was taken every 30 to 60 minutes to determine the level of protoplasts. After 3-5 hours, the majority of the mycelia was visually determined to be digested and many protoplasts were easily identified with a microscope. The protoplasting reaction was filtered through a 30 µm Nylon mesh filter (Millipore-Sigma), with protoplasts passing through into a 50

mL conical tube. The protoplasts were centrifuged at 3,200 x g for 5 minutes at 4°C, then gently resuspended in 10 mL of chilled STC buffer (1.2 M D-sorbitol, 10 mM $CaCl_2$, 10 mM Tris-HCl, pH 7.5) using a wide orifice pipet tip (Mettler-Toledo Rainin, Oakland, CA). The centrifuge and resuspension steps were repeated twice, with the last resuspension using 1mL of STC buffer. A subsample of the protoplasts was diluted 1:100 and quantified using a hemocytometer to determine the initial quantity. The protoplasts were diluted to a final concentration of 10^7 per milliliter and transferred into aliquots of 400 µL. Dimethyl sulfoxide (DMSO) was added to a final concentration of 7%, and the protoplasts were stored immediately at -80°C.

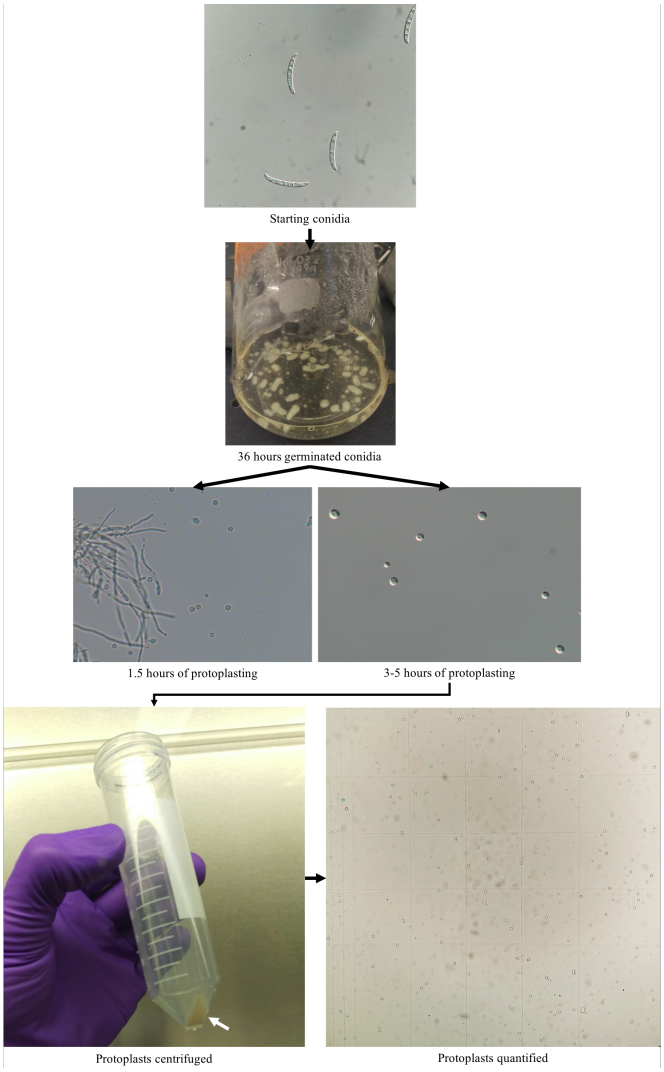

Figure 4-2. Overview of the protoplasting method.

Transformation

Protoplasts were removed from -80°C, thawed on ice, and centrifuged at 3000 x g for 4 minutes at 4°C. The supernatant was carefully pipetted out to remove DMSO, and the protoplasts were resuspended in 400 µL chilled STC buffer. The centrifugation and resuspension steps were repeated twice, with the final resuspension using 200 µL STC buffer. With the protoplasts on ice, 5 µg of linearized transformation vector was added, followed by 50 µL of 30% PEG-8000 solution (10 mM Tris-HCl, 50 mM $CaCl_2$, 30% poly-ethylene glycol w/v), so that PEG comprised 20% of the transformation reaction volume. *Fusarium virguliforme* was transformed with 5 µg of a linear construct containing *hph* and eGFP, while *F. brasiliense* was transformed with 5 µg of a linear construct containing *nat* and mCherry (Fig. 4-1). The reactions were gently inverted 3 times, then incubated on ice for one hour. Using a wide orifice pipet tip, each reaction was transferred into a sterile 15 mL tube containing 2 mL 30% PEG-8000 and incubated for 15 minutes. Four milliliters of room-temperature STC buffer was added and gently inverted three times to mix. The reaction was then poured into 250 mL sterile, molten regeneration medium at 42°C (67.75 g sucrose, 0.25 g yeast extract, 0.25 g N-Z amine, 1.86 g agar). The agar was swirled gently to mix, then poured as thin a layer into 20, 100 x 15 mm Petri plates (VWR International, Radnor, PA). After 24 hours of incubation at room temperature, another layer of regeneration medium amended with either 100 µg / mL hygromycin B or 100 µg / mL nourseothricin was overlaid onto the germinating protoplasts. One plate was overlaid with non-amended regeneration medium as a control to determine viability of protoplasts after the transformation and plating procedures.

Screening for stable transformants

Putative transformants that grew through the layer of regeneration medium amended with antibiotics were transferred to PDA amended with antibiotics. After 10-14 days of growth, a single spore of the putative transformant was isolated and re-transferred to a new PDA plate amended with antibiotics. After 10-14 days of germination from this single spore, hyphae were scraped off the surface of the plate using a sterile inoculation loop and transferred onto a small pad of 2% agarose on a microscope slide, and viewed under a compound fluorescent microscope (Leica Microsystems, Buffalo Grove, IL). Stable transformants and wild type strains were viewed under bright field and fluorescent channels. To determine fluorescence of *F. virguliforme*, a GFP/FITC filter was used, and for *F. brasiliense* a TexasRed filter was used (Leica Microsystems).

Results

Fusarium virguliforme is sensitive to hygromycin (Chang et al., 2016a; Islam et al., 2017b; Mansouri et al., 2009; Pudake et al., 2013; Sang et al., 2018), but sensitivity to hygromycin has not been reported for *F. brasiliense*. Medium amended with 100 µg / mL hygromycin prevents growth in two wild type strains of *F. virguliforme* and *F. brasiliense* (Fig. 4-3). Another common antibiotic used for genetic selection is nourseothricin, which has been used in *F. graminearum* and *F. fujikuroi* transformations, but not *F. virguliforme* or *F. brasiliense* (Menke et al., 2013; Wiemann et al., 2009, 2010). Medium amended with 100 µg / mL nourseothricin prevents growth in both wild type strains of *F. virguliforme* and *F. brasiliense* (Fig. 4-3). However, genetic mutants containing the antibiotic resistance genes *hph* or *nat* are able to grow on amended medium with hygromycin and nourseothricin, respectively.

Representative growth of these mutants on amended medium is presented after 14 days (Fig. 4-3).

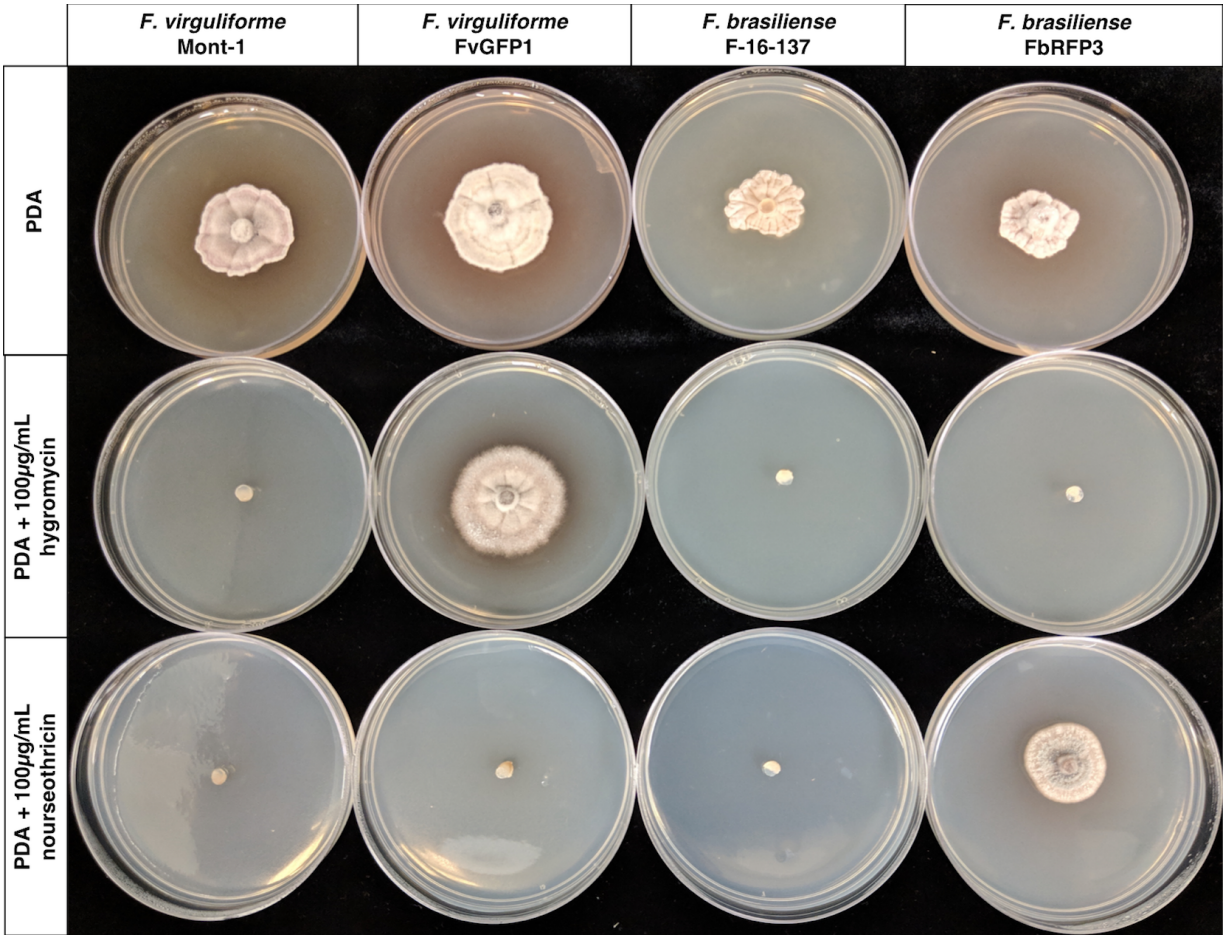

Figure 4-3. Wild type *F. virguliforme* and *F. brasiliense* strains are sensitive to hygromycin (100 µg / mL) and nourseothricin (100 µg / mL). Transgenic strains of *F. virguliforme* with the addition of the *hph* gene are resistant to hygromycin, while transgenic strains of *F. brasiliense* with the addition of the *nat* gene are resistant to nourseothricin.

Following the protocol described here and outlined in Fig. 4-2, high quality protoplasts of *F. virguliforme* were produced. The protocol was also successfully applied to *F. brasiliense*. These protoplasts were stored frozen at -80°C for up to two years and still showed viability throughout the transformation process (Fig. 4-4). Introducing the transformation vector to viable protoplasts resulted in successful transformation of some individual protoplasts, which allowed growth on medium amended with a high concentration of the selectable antibiotic (Fig. 4-4).

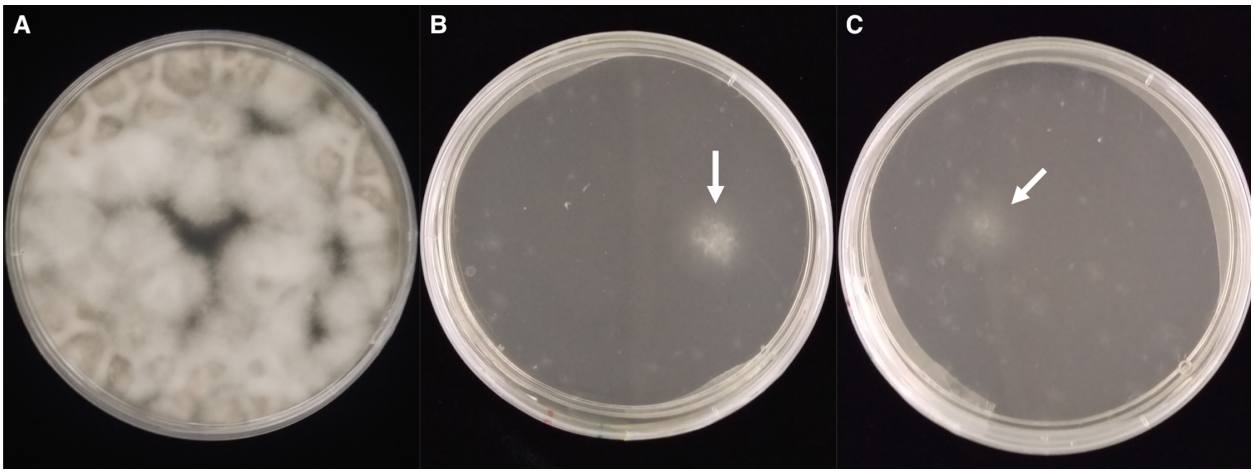

Figure 4-4. Representative protoplasts seven days post-transformation. Protoplasts were overlaid with non-amended regeneration medium (**A**), regeneration medium amended with hygromycin (**B**), or nourseothricin (**C**). Arrows represent putative transformants that have grown through the entire layer of amended medium.

Beginning with 10^7 protoplasts per transformation, up to 76 putative transformants were obtained in a single reaction (data not shown). Stable transformants were obtained and screened for fluorescence. Neither wild type strain of *F. virguliforme* or *F. brasiliense* demonstrated green or red autofluorescence (Fig. 4-5). However, many stable transformants displayed fluorescent phenotypes, and representative isolates are presented (Fig. 4-5). Phenotypic differentiation of *F. virguliforme* and *F. brasiliense* requires many spore measurements, which can be very challenging since spore lengths and widths overlap (Aoki et al., 2005). However, a mixed culture of spores of the transgenic strains developed here are easily distinguished based on fluorescence of individual spores (Fig. 4-6).

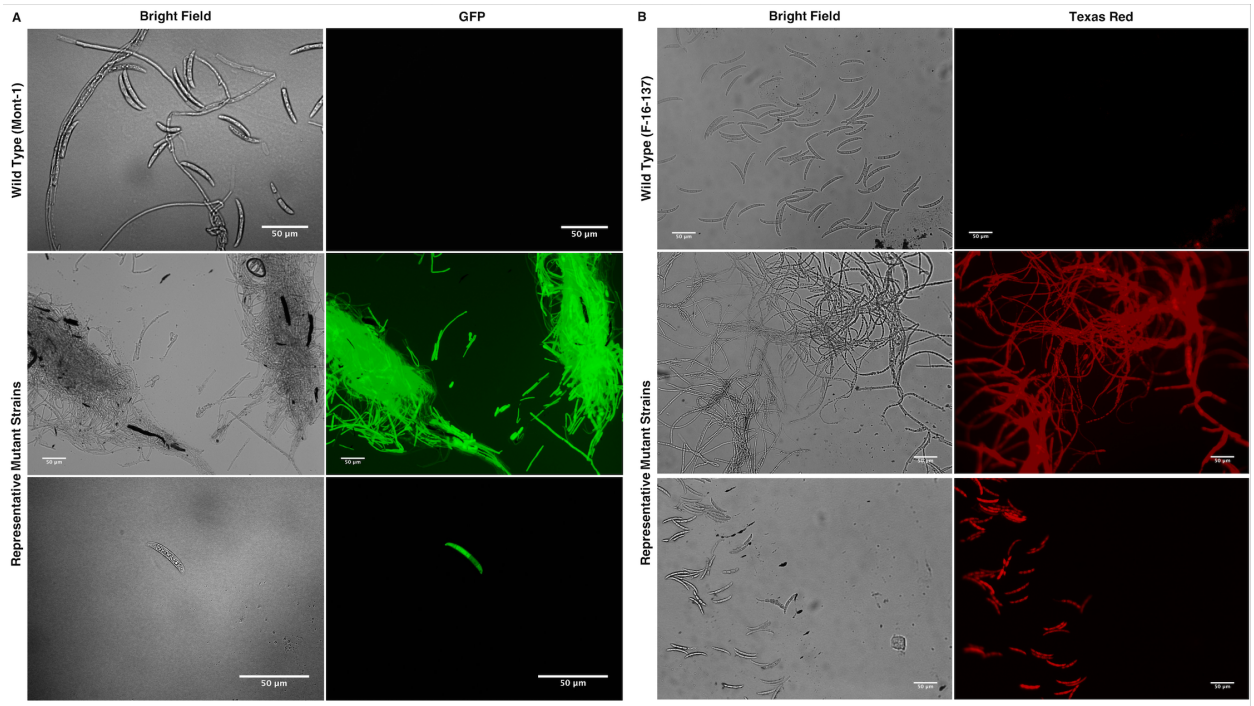

Figure 4-5. Microscopic features of wild type and representative mutant strains of *F. virguliforme* (A) and *F. brasiliense* (B). No autofluorescence was detected from the wild-type strains, but was detected in representative mutant strains transformed with a fluorescent reporter gene. All scale bars represent 50 µm.

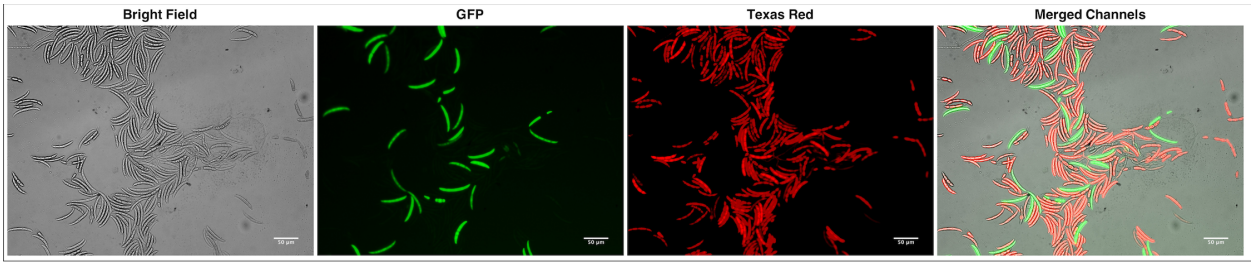

Figure 4-6. Mixed culture of *Fusarium* spores, distinguished by fluorescent reporter gene expression. *Fusarium virguliforme* fluoresces green and *F. brasiliense* fluoresces red under appropriate excitation spectra for eGFP and mCherry, respectively. All scale bars represent 50 µm.

Discussion

Generating protoplasts of *F. virguliforme* has been successful in other labs using a previously published protocol studies, but was unsuccessful in our hands (Chang et al., 2016a; Islam et al., 2017b, 2017a; Mansouri et al., 2009; Pudake et al., 2013). Protoplast generation was

successful following the protocol developed for *F. graminearum*, but the transformation method reported therein was unsuccessful for transforming *F. virguliforme* and *F. brasiliense* (Hallen-Adams et al., 2011). The transformation protocol for *F. virguliforme*, as written (Mansouri et al., 2009), also failed to produce successful transformants for us. Therefore, we integrated components from both of these published protocols, resulting in the protocol described here. Implementing this transformation protocol with high quality protoplasts allowed for the generation of stable transformants of both *F. virguliforme* and *F. brasiliense* (Fig. 4-3). In addition, *Fusarium virguliforme* protoplasts developed with the method described here were successfully used in a targeted gene replacement study testing different fungal succinate dehydrogenase alleles (Sang et al., 2018).

The two previously published protoplasting protocols for *F. graminearum* and *F. virguliforme* differ in many aspects (Hallen-Adams et al., 2011; Mansouri et al., 2009). Differences include buffer types, enzyme compositions, and enzyme concentrations. While the *F. virguliforme* protocol uses a sodium phosphate buffer containing β-glucuronidase and a high concentration of lysing enzymes (25 mg / mL), the *F. graminearum* protocol uses a potassium chloride buffer with chitinase rather than β-glucuronidase, and a lower lysing enzyme concentration (5 mg / mL). Given that chitin and β-glucan are the major polysaccharides found in *Fusarium* spp., the addition of chitinase likely increased our protoplasting efficiency for *F. virguliforme* and *F. brasiliense* (Schoffelmeer et al., 1999). It is worth noting that 3-5 hours were required to gain sufficient protoplasts in *F. virguliforme* and *F. brasiliense* compared to the 2 hours reported for *F. graminearum* (Hallen-Adams et al., 2011). A detailed comparison between protoplasting buffers and enzyme compositions also concluded that potassium chloride was

optimal for protoplast generation in the fungal pathogen *F. verticillioides*, and the addition of chitinase helps generate protoplasts in other *Fusarium* species (Ramamoorthy et al., 2015).

Fusarium brasiliense is a close relative of *F. virguliforme*, both members of clade II in the *Fusarium solani* species complex (Aoki et al., 2005; Chitrampalam and Nelson 2016). However, different members of this species complex display different sensitivities to fluopyram, a common fungicide used to control these species (Sang et al., 2018). Understanding the genetic mechanisms of fungicide sensitivity or resistance can be elucidated by testing gene function through gene knockout and gene replacement studies using split marker gene replacement constructs (Catlett et al., 2003). The genetic mechanisms of SDS development are poorly characterized, and whether mechanisms of SDS development are shared between *F. virguliforme* and *F. brasiliense* are also unknown. Though we introduced foreign DNA into *F. brasiliense* via random insertion in this study, this protocol should also facilitate knock out experiments via gene replacement as it has in *F. virguliforme* protoplasts obtained with this method (Sang et al., 2018).

Both *F. virguliforme* and *F. brasiliense* are capable of infecting soybean and common bean (*Phaseolus vulgaris*) (Kolander et al., 2012; Jacobs et al., 2018; Wang et al., 2018), and isolation frequency data suggests that *F. brasiliense* may have a host preference for common bean (Wang et al., 2018). The development of transgenic *F. virguliforme* and *F. brasiliense* strains expressing different fluorescent markers may allow for studies investigating host preference through co-inoculations, as they can easily be distinguished under the microscope based on their reporter gene expression (Fig. 4-6). With this protocol and carefully designed experiments we can come to a greater genetic understanding of these pathogens which could lead to new and effective management strategies.

Conclusions

Fusarium virguliforme and *F. brasiliense* are both causal agents of soybean SDS and are amenable to genetic manipulation for studying gene function. Confirmation of genetic transformation in these species requires high quality protoplasts and appropriate controls. The protocol developed here provides methods for producing high quality protoplasts that builds upon previously reported protocols and should be valuable to the soybean SDS and common bean root rot research community. The fluorescent strains developed here can be used to investigate temporal colonization and co-infections of plant roots as well as the potential host preferences of these species. Using this protocol to probe gene function in these pathogens will be critical to understanding their pathology and advancing plant genetics to improve SDS management.

Acknowledgements

The authors would like to thank R. Shay, Z. Noel, Dr. H.-X. Chang, and Dr. H. Sang for critical review of this manuscript prior to submission. This work was funded in part by the Michigan Soybean Promotion Committee, the United Soybean Board and the North Central Soybean Research Program.

CHAPTER 5: The role of soil-borne nematodes in soybean sudden death syndrome caused by *Fusarium virguliforme*

By

Mitchell G. Roth

This work presented in this chapter is unpublished.

Abstract

Soybean cyst nematode (SCN) and *Fusarium virguliforme* are major threats to soybean production throughout the U.S. Management strategies for both pathogens are similar and include using genetically resistant varieties, diverse crop rotations, and seed treatments containing a nematicide or fungicide. *Fusarium virguliforme* causes soybean sudden death syndrome (SDS) by infecting root tissues, colonizing vascular tissues, and releasing protein effectors and toxins into soybean xylem, inducing foliar SDS symptoms. Though SCN cannot cause SDS, many studies have identified a strong positive correlation between SDS severity and SCN abundance, though the role of SCN in SDS development remains unknown. In this study, we explored the interactions between *F. virguliforme* and the model nematode *Caenorhabditis elegans* and the soybean cyst nematode *Heterodera glycines*. *Fusarium virguliforme* is able to colonize dead and immobilized nematodes, suggesting that *F. virguliforme* is an excellent saprophyte and may be able to use nematodes as a nutrient source, which could increase *F. virguliforme* inoculum. However, colonization of living mobile nematodes was not observed, indicating that *F. virguliforme* is not vectored into soybean roots by nematodes. The presence of SCN in co-infected soybean roots significantly increased the level of *FvTox1* expression relative to *F. virguliforme*-only inoculated plants. *FvNIS1* expression was not affected by the presence of SCN. Overall, these results suggest that successful SCN management may also lead to improved SDS management.

Introduction

Soybeans are a global commodity known for quality protein content and valuable oils, but also have many industrial uses such as the production of adhesives and paints (Singh 2010).

The USDA projects an estimated 4.5 billion bushels of soybeans were produced in the U.S. during 2018-2019 (USDA 2019). However, soybean production faces numerous annual challenges including those from pests and pathogens, which lead to reduction in yields In 2010-2014, loses of approximately 41.9 million bushels were observed throughout the U.S. and Ontario, Canada (Allen et al., 2017). Two significant threats to soybean production in the U.S. are the soybean cyst nematode, *Heterodera glycines* Ichinohe (SCN), and the ascomycete fungus *Fusarium virguliforme*, which causes sudden death syndrome (SDS) (Allen et al., 2017).

The SCN is an obligate roundworm parasite that requires a compatible host to complete its life cycle (Niblack et al., 2006). Mature SCN females (cysts) can contain 600 or more eggs and survive in the soil for 10 years or more (Niblack et al., 2006; Sipes et al., 1992). The eggs can be induced to hatch into infectious juveniles (J2) by root exudates of developing soybean roots (Riga et al., 2001). The J2 physically pierce roots with a stylet, and their saliva contains cell wall degrading enzymes, together allowing the nematode to gain entry to the root system (Wang et al., 1999). Inside the root system, the J2 evades the plant immune system and develops a syncytium, or feeding site, by releasing effector proteins from their esophageal glands (Mitchum et al., 2013; Noon et al., 2015). Feeding off the root, J2 nematodes molt two more times (J3, J4) before becoming mature adults, completing their reproductive cycle in three to four weeks under typical field conditions (Alston and Schmitt, 1988; Anand et al., 1995). Above-ground symptoms are not always obvious even when SCN is causing significant yield losses (Noel and Edwards, 1996; Wang et al., 2003; Young, 1996). Symptoms associated with SCN damage often develop as secondary problems like nutrient deficiencies (Niblack et al., 2006).

Fusarium virguliforme is the main causal agent of soybean SDS in the U.S. (Aoki et al., 2003; Hartman et al., 2015). The soil-borne fungus infects root tissues by developing appressoria

and releasing cell wall degrading enzymes (Chang et al., 2016b; Navi and Yang 2008). Heavy colonization of the roots can lead to significant root rot symptoms without foliar symptom development (Wang et al., 2018). Root rot caused by *F. virguliforme* is sufficient to significantly reduce yield, though foliar symptoms of SDS are thought to be the primary driver of yield loss (Luo et al., 2000; Wang et al., 2018). Foliar symptom development is thought to require colonization of the vascular tissues (Islam et al., 2017a, 2017b; Navi and Yang 2008). There, *F. virguliforme* can secrete effector proteins and toxins into the xylem and translocate to the leaves, leading to the foliar symptoms of interveinal chlorosis and necrosis (Abeysekara and Bhattacharyya 2014; Brar et al., 2011; Chang et al., 2016a; Navi and Yang, 2008). *F. virguliforme* remains in the roots throughout foliar symptom development, and develops overwintering chlamydospores that can survive in soybean and corn debris (Aoki et al., 2003; Navi and Yang, 2016; Roy et al., 1989).

Multiple disease complexes include plant pathogenic fungi and plant parasitic nematodes (Back et al., 2002), including *Verticillium dahliae* with *Pratylenchus* nematodes in potato early die (Martin et al., 1982; Rowe et al., 1985) and wilt disease of mint (Wheeler et al., 2019), *Rhizoctonia solani* and *Ditylenchus dipsaci* in sugar beet crown and root rot (Hillnhütter et al., 2011), and *Fusarium solani* and *Meloidogyne incognita* in root rot of lentil (Ahmed and Shahab 2018). Similarly, it has been suggested that SDS is a disease complex composed of *F. virguliforme* and SCN, where SCN increases SDS synergistically with *F. virguliforme* (Back et al., 2002; Roth et al., 2019a; Xing and Westphal, 2013). However, the exact role of the nematode in these disease complexes remain unknown. Some hypotheses include nematodes vectoring fungi into plants (Khan and Pathak 1993), nematodes creating wounds that are easier for fungi to colonize (Hillnhütter et al., 2011), and altering defense gene expression that benefits fungal

invasion (Biere and Goverse, 2016). In the case of SCN and *F. virguliforme*, evidence has suggested that *F. virguliforme* colonizes wounds caused by SCN (Diaz Arias 2012). However, soybeans undergo tremendous transcriptional reprogramming upon infection by SCN, including altered expression of WRKY and MYB transcription factors and pathogenesis related genes (Ithal et al., 2007a). SCN also upregulate cell wall loosening enzymes, suppress JA, and increase peroxidase expression (Ithal et al., 2007b). This suggests that the presence of SCN could significantly affect the ability for *F. virguliforme* to induce SDS. Despite the unknown role of SCN in SDS, many field studies have observed an increase in foliar SDS severity when SCN is also present (Brzostowski et al., 2018; McLean and Lawrence, 1995; Roth et al., 2019a; Westphal et al., 2014; Xing and Westphal, 2013), though others have not observed this effect (Hershman et al., 1990; Marburger et al., 2014; Rupe et al., 1993). The objectives of this study were to 1) determine the ability for *F. virguliforme* to colonize living vermiform nematodes, 2) examine the temporal colonization of immobile nematodes by *F. virguliforme*, and 3) quantify the expression of two *F. virguliforme* effector genes *in planta* in the presence and absence of SCN.

Materials and Methods

Fungal and nematode strains

Fusarium virguliforme strain NRRL 22292, also called "Mont-1", was obtained from the USDA Agricultural Research Service Culture Collection. Fluorescent strains were developed from Mont-1 by protoplast development and homologous recombination, as described in Roth et al., (2019b). The temperature sensitive mutant strain SS104 of *Caenorhabditis elegans* was obtained from the Caenorhabditis Genetics Center (CGC, University of Minnesota, St. Paul,

MN). *Heterodera glycines* were obtained from soil samples obtained from Decatur, MI using a modified soil centrifugation and floatation procedure (Jenkins 1964). The *H. glycines* type was determined to be 2.5.7 (Niblack et al., 2002; Tylka 2016), and nematodes were propagated in the greenhouse using the susceptible soybean line 'Williams 82' grown in a 2:1 soil:sand mix.

In vitro Fusarium-nematode interactions

Synchronous *C. elegans* cultures were obtained by harvesting adult nematodes from nematode growth media (NGM) plates (0.3% NaCl, 0.25% peptone, 1.7% agar, 1 mM $CaCl_2$, 1 mM $MgSO_4$, 25 mM KPO_4, and 5 mg/L cholesterol) containing a lawn of *E. coli* strain OP50. Briefly, five-day old NGM plates were flooded with 6 mL sterile water and the supernatant was re-collected into a 15 mL conical tube. The nematodes were concentrated by centrifuging at 1500 x *g* for 1 minute and decanting the supernatant. Sodium hydroxide and sodium hypochlorite were added to the nematodes at a final concentration of 500 mM and 1% respectively, and incubated for 4 minutes with frequent vortexing, killing all adult nematodes and leaving only eggs. The eggs were centrifuged at 1,500 x *g* for 1 minute and washed three times with 15 mL M9 buffer (22 mM KH_2PO_4, 1 mM $Na_2HPO_4 \bullet 7H_2O$, 85.5mM NaCl, 50 µg/ml kanamycin, 5 µg/ml cholesterol, 2mM $MgSO_4$). The eggs were allowed to hatch overnight in 10 mL M9 buffer with shaking at 75 rpm, transferred to NGM plates containing a lawn of OP50, and incubated at room temperature for 36-48 hours. When all nematodes reached the L4 stage, they were collected with 10 mL M9 buffer, washed once to remove OP50, and used in interaction experiments with *Fusarium*.

Fusarium isolates were cultured on half strength PDA (Neogen Corporation, Lansing, MI) for 10-14 days. Spores were collected by flooding the plate with 5 mL of M9 buffer and

quantified with a hemocytometer. Approximately 10^5 spores and 150 nematodes were used in each experiment. Spores and synchronized nematodes were mixed in 1 mL reactions consisting of 80% M9 buffer and 20% BHI broth and incubated at 25°C for four hours. While centrifuge and washing steps has been reported to remove spores from nematodes (Muhammed et al., 2012b), this technique failed to separate spores from nematodes in this study. Instead, the reactions were centrifuged at 1,500 x *g* for two minutes to pellet nematodes and spores. Nine-hundred microliters were carefully removed with a pipet and discarded. The final 100µL containing nematodes and spores were plated onto one side half of an NGM plate. The other half of the NGM plate contained a lawn of OP50 (Fig. 5-1 A). Living nematodes were drawn away from the spores and towards OP50, their food source. These plates were incubated at 25°C for three days, then all dead and living nematodes were quantified. A subset of nematodes on each half of the plate were picked and visually examined for fungal colonization using a fluorescent microscope (Leica Microsystems, Buffalo Grove, IL). All nematodes were transferred onto a 2% agar pad containing 1 µM tetramisole hydrochloride (Millipore-Sigma, Burlington, MA) to immobilize living nematodes. Z-stack imaging of nematodes was performed on a confocal laser scanning microscope (Olympus, Center Valley, PA).

Temporal colonization of nematodes by Fusarium

Nematodes or eggs were transferred onto a 2% agar pad containing 1µM tetramisole hydrochloride. The agar pad was surrounded by petroleum jelly to create a small chamber. M9 buffer was added to this chamber to keep the agar pad from dehydrating. Bright-field and fluorescent images were captured every 20 minutes for 56 hours using a fluorescent microscope containing a GFP/FITC filter connected to a DFC450 C camera (Leica Microsystems). Acquired

images were exported to FIJI for merging channels, adding scalebars, and generating moving images (Schindelin et al., 2012).

In vivo expression of Fusarium effectors in the presence of SCN

Heterodera glycines were collected from greenhouse soil containing 'Williams 82' soybean roots using a modified centrifugation floatation protocol (Jenkins 1964). Briefly, 4,000 cm^3 (1 gallon) of soil was homogenized in an 18.9 L (5 gallon) bucket, filled to the top with water. The water was filtered through a 710 µm filter twice to remove soil aggregates, then filtered through a 45 µm filter (Hogentogler & Co., Columbia, MD) to collect nematodes (Shurtleff and Averre III 2000). Nematodes were back-washed from the sieve into 50 mL conical tubes and centrifuged for 5 min at 1,150 x *g*. Water was decanted until 10 mL remained, then 25 mL of a sucrose solution (1,210 g / L, in water) was added and nematodes were centrifuged again for 1 min at 1,150 x *g*. Cyst and vermiform nematodes floated to the top and were decanted onto a 45 µm filter and washed thoroughly with water, then back-washed into a 250 mL beaker (Shurtleff and Averre III 2000). Fifty microliters of water containing nematodes were aliquoted onto a microscope slide and the number of J2 juvenile nematodes were quantified. The nematodes were diluted to approximately 75 J2 juveniles per milliliter, and two milliliters were used to inoculate soybean roots for a total inoculation with 150 J2.

Williams 82 soybean seeds were surface sterilized by soaking in 6% bleach (0.4% NaOCl) for 10 minutes, rinsing in DI water for 10 minutes, then air drying on sterile paper towels in a laminar flow hood. A single seed was sown into a 107 mL conetainer (Greenhouse Megastore, Danville, IL) filled with 2:1 soil:sand mix of SureMix (Michigan Grower Products Inc., Galesburg, MI, USA) and washed play sand. The soybeans were allowed to germinate for 7

days in a growth chamber at 25°C and 75% relative humidity under a 14-10 h light-dark cycle. The conetainers were set up in a randomized complete block design with eight plants in the first biological replicate and seven plants in the second. A 6-cm deep hole was made next to each soybean using 1 mL pipet tip and was filled with one of four treatments; 2 mL sterile water and a single 3.4 mm non-colonized PDA plug (mock inoculation), 2 mL sterile water and a single 5 mm PDA plug colonized with *F. virguliforme*, 2 mL of water containing J2 nematodes and a single 5 mm non-colonized PDA plug, or 2 mL water containing J2 nematodes and a single 5 mm PDA plug colonized with *F. virguliforme.* The inoculated soybeans were incubated in the growth chamber for four weeks and watered daily to maintain adequate moisture. All samples were harvested at four weeks post inoculation (five weeks post planting). Plant roots were washed to remove attached soil, separated from foliar tissues, and fresh shoot and root weights was collected. Shoots were discarded and roots were snap frozen in liquid nitrogen and stored at -20°C for one week.

The inoculated roots were ground in liquid nitrogen using a mortar and pestle, and the ground tissues were subjected to RNA extraction. Approximately 100 mg of root tissue was added to 1 mL TRIzol (Thermo Fisher Scientific, Waltham, MA) and 150 µL of lysing matrix D (MP Biomedicals, Solon, OH). The samples were brought to room temperature then ground again in a FastPrep machine (Thermo Fisher Scientific) for 30 seconds on speed setting 5. The rest of the RNA extraction was performed following the TRIzol manual. One microgram of total RNA from each sample was reverse transcribed to cDNA using a High Capacity cDNA Reverse Transcription Kit (Applied Biosystems, Foster City, CA) according to manufacturer protocol.

Quantities of *FvTox1* and *FvNIS1* expression were obtained by using SYBR Green qPCR assays with previously reported primers (Chang et al., 2016a). Gene expression levels were

calculated relative to the *F. virguliforme TEF1* reference gene by taking ($Ct_{EF1a} - Ct_{GOI}$) + 10, where Ct_{EF1a} is the Ct value for *EF1a* expression, Ct_{GOI} is the Ct value for a gene of interest, either FvTox1 or FvNIS1, and 10 being a unitless addition to remove negative values and make interpretation of gene expression levels intuitive. In samples where no amplification was detected, "NA" values were replaced with the maximum Ct value of 40 so calculations could be made.

Results

Fusarium virguliforme does not actively colonize vermiform nematodes

The ability for *F. virguliforme* to colonize active nematodes was examined using *C. elegans* as a model and previously published protocols for fungal-nematode interactions (Muhammed et al., 2012b, 2012a). Most nematodes were found feeding on *E. coli*, while only some were found outside the *E. coli* lawn (Fig. 5-1 A). All nematodes feeding on *E. coli* were healthy and living, as observed by their behavior and indicated by the auto-fluorescent gut granules (Pincus et al., 2016) (Fig. 5-1 B). In contrast, most nematodes outside the lawn of *E. coli* were dead, and GFP signal was detected in a filamentous pattern consistent with fungal growth rather than gut granules (Fig. 5-1 B). Some nematodes outside the lawn of *E. coli* were alive and exploring but had no visual indication of fungal colonization. Despite being incubated with wild type *F. virguliforme* spores, GFP-expressing spores, or no spores, most nematodes were living and non-colonized (Fig. 5-1 C). Similar results were observed with *F. brasiliense* isolates expressing mCherry (Fig. 5-2).

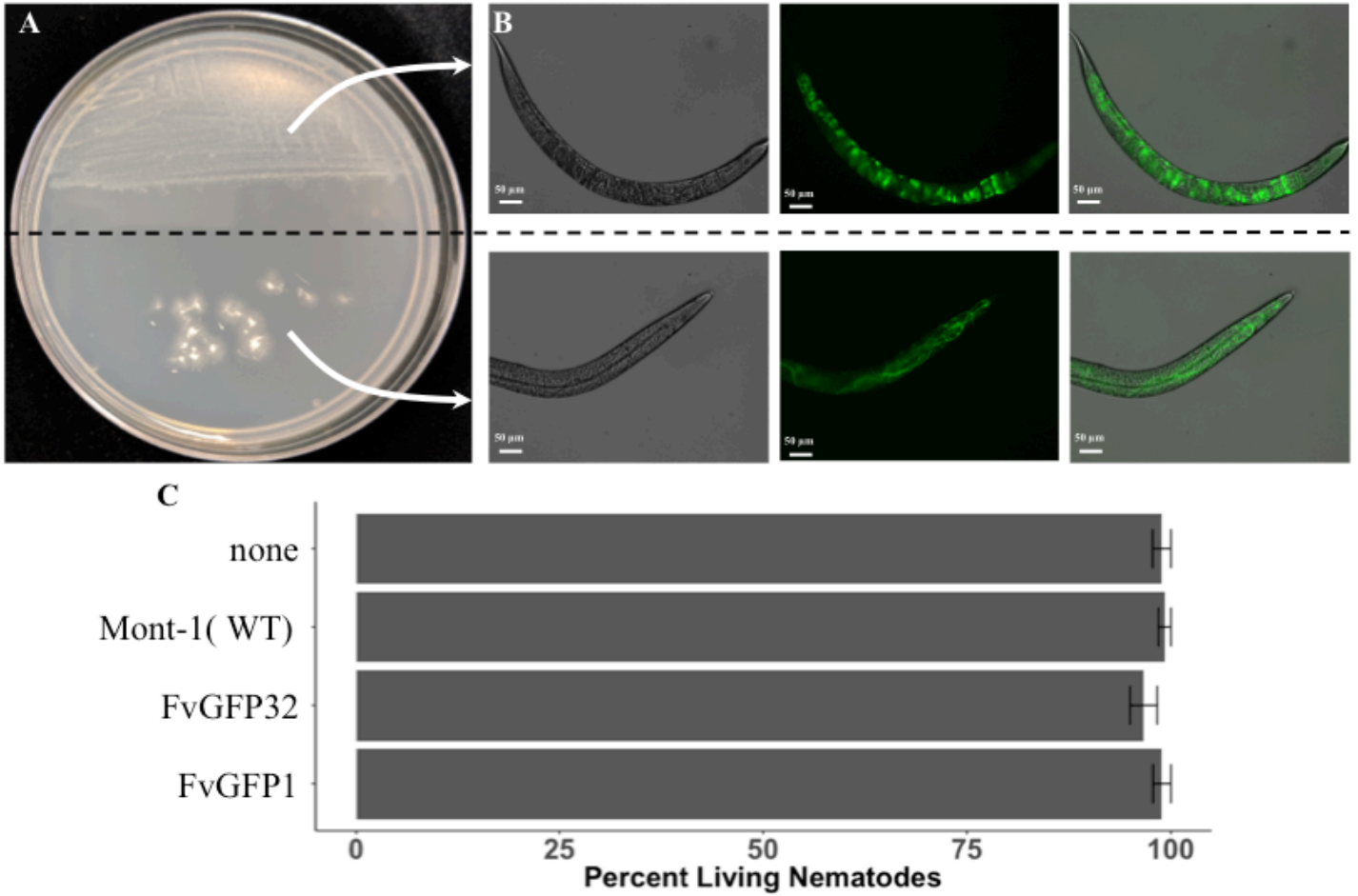

Figure 5-1. ***Fusarium virguliforme*** **interactions with** ***Caenorhabditis elegans*****.** After four hours of incubating fungal spores with L4 nematodes, experiments were plated onto half a plate containing a lawn of *E. coli* OP50 on the other half and incubated for three days (**A**). Nematodes from each half of the plate were transferred and viewed under bright field and GFP channels (**B**). Nematodes on the fungal half were dead, and nematodes on the bacterial half were alive, so the percent living nematodes were quantified per treatment (**C**).

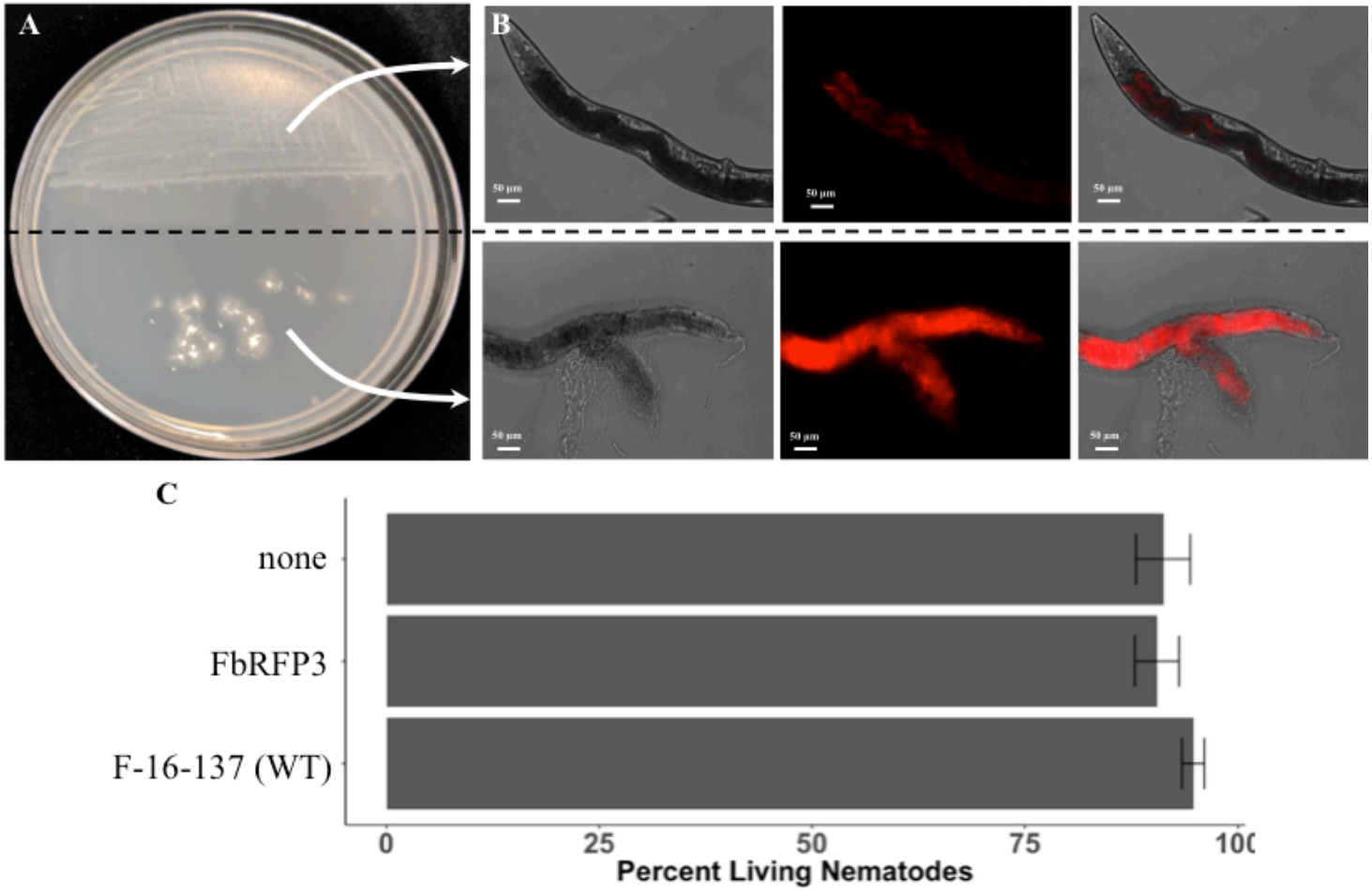

Figure 5-2. *Fusarium brasiliense* interactions with *Caenorhabditis elegans*. After four hours of incubating fungal spores with L4 nematodes, experiments were plated onto half a plate containing a lawn of *E. coli* OP50 on the other half and incubated for three days (**A**). Nematodes from each half of the plate were transferred and viewed under bright field and GFP channels (**B**). Nematodes on the fungal half were dead, and nematodes on the bacterial half were alive, so the percent living nematodes were quantified per treatment (**C**).

Fluorescent signals from dead nematodes were successfully separated to distinguish GFP fluorescence from transgenic *F. virguliforme* strains and autofluorescence from the nematode. These results show that dead nematodes were indeed colonized by *F. virguliforme* (Fig. 5-3). In colonized nematodes, Z-stack imaging revealed that colonization can occur inside the nematode, with most fluorescence being detected 16 µm from the nematode cuticle (Fig. 5-4).

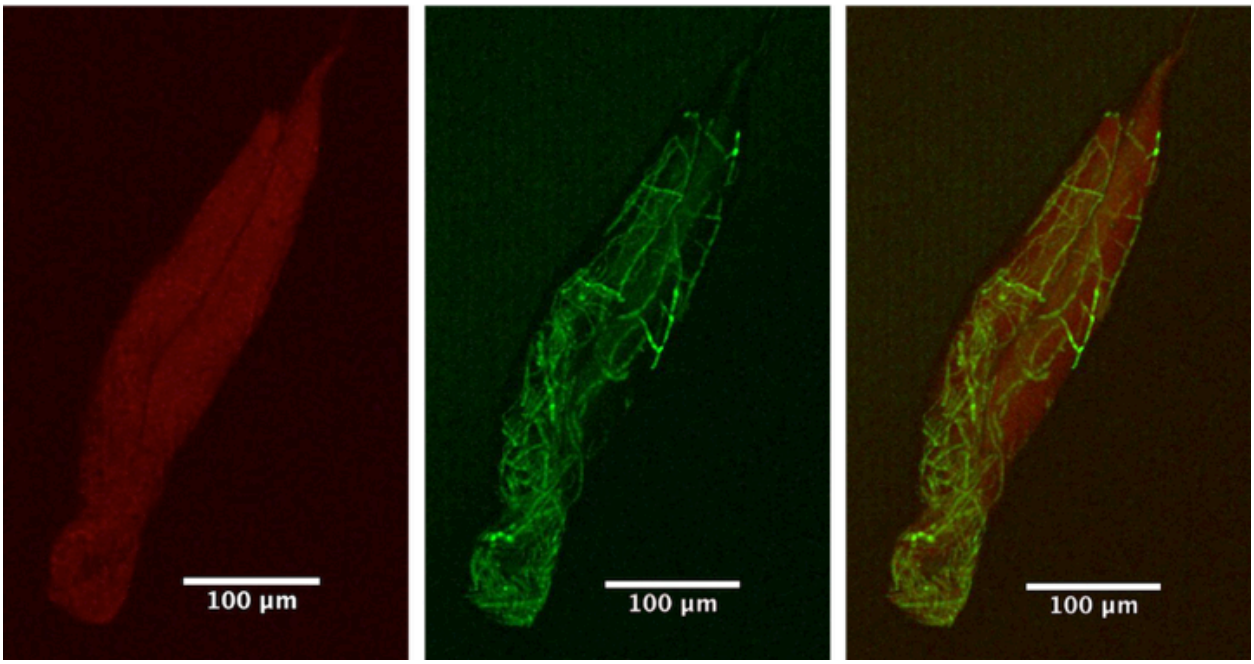

Figure 5-3. **Linear unmixing of green *C. elegans* autofluorescence and GFP fluorescence from transgenic *F. virguliforme* strains.** Autofluorescence from *C. elegans* was pseudo-colored red (left) while true GFP fluorescence was left as green (center), allowing visual discernment of the nematode body and fluorescent fungal hyphae (right).

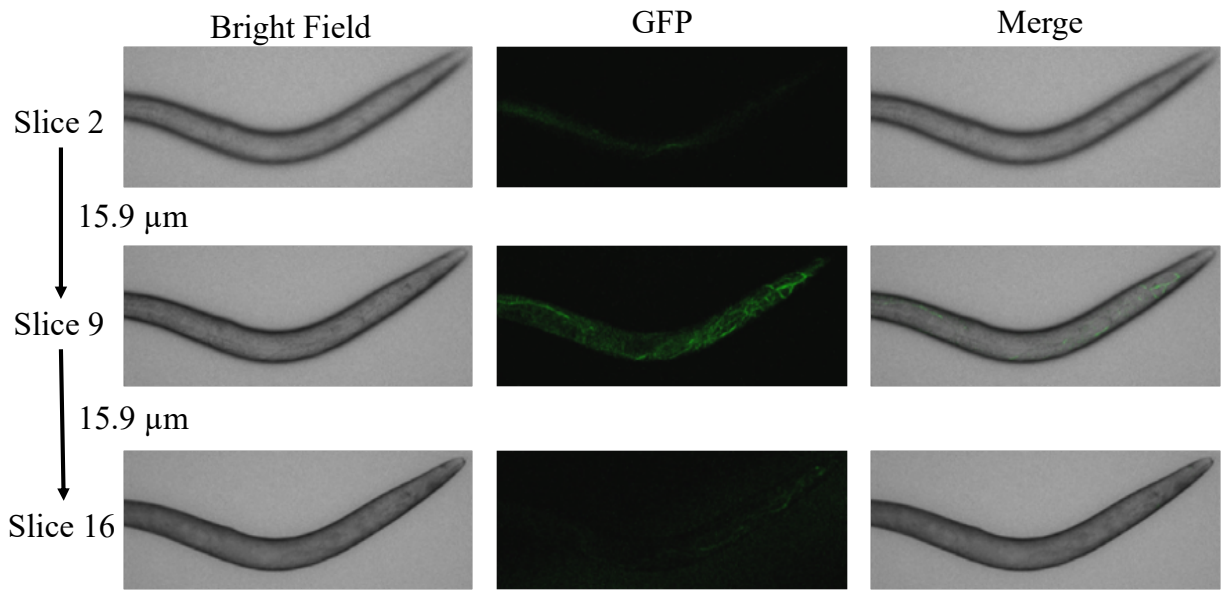

Figure 5-4. **Z-stack images (slices) of *C. elegans* colonized by a transgenic *F. virguliforme* strain expressing GFP.** Image (slice) 2 displays the dorsal surface of the nematode, image (slice) 9 displays the nematode internal body cavity colonized by *F. virguliforme*, and image (slice) 16 displays the ventral surface of the nematode. All slices shown are 15.9 µm apart in depth.

Fusarium virguliforme can colonize immobilized nematodes

Some *C. elegans* were found dead, outside of the *E. coli* lawn even when no fungal spores were added (Fig. 5-1 C, Fig. 5-2 C) suggesting that repeated pipetting of the nematodes may have caused some mortality. Therefore, *F. virguliforme* colonization of nematodes may be before nematode death (pre-mortem) or after (post-mortem). We investigated whether *F. virguliforme* can colonize immobilized, living nematodes. After 12 h, germination of *F. virguliforme* spores was observed, and by 48 h *F. virguliforme* spores were had penetrated the nematode cuticle, initiating a strong burst of autofluorescence from the nematode that indicates nematode death (Pincus et al., 2016) (Fig. 5-5).

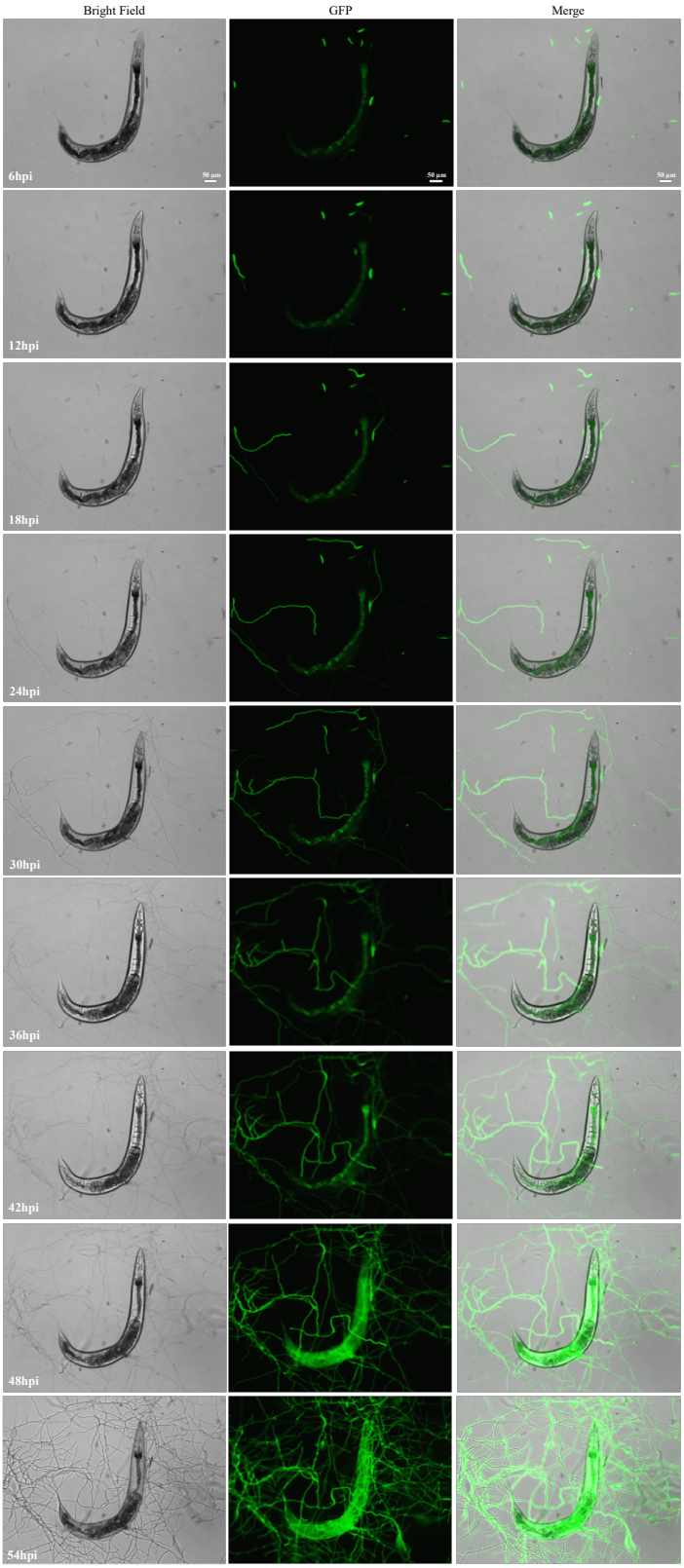

Figure 5-5. ***Fusarium virguliforme*** **colonization of an L4** ***C. elegans*** **nematode over time.** All images were taken at the same magnification, so the 50 µm scalebar at 6 hpi is representative for all images. hpi = hours post inoculation with transgenic *F. virguliforme* spores

SCN does not affect F. virguliforme effector expression

Biological replicate had a significant effect on root fresh weight, and therefore, were analyzed separately. In the first biological replicate, soybeans inoculated with *F. virguliforme* or both *F. virguliforme* and SCN had significantly lower root fresh weight compared to the mock-inoculated controls (Fig. 5-6 A). *FvTox1* and *FvNIS1* expression was detected in all treatments even though the primers were designed specifically for *F. virguliforme* genes, indicating some cross-reactivity. However, there was significantly higher *FvTox1* expression in soybean roots inoculated with *F. virguliforme* and SCN compared to *F. virguliforme* alone (Fig. 5-6 B). No significant differences in FvNIS1 expression were detected (Fig. 5-6 B).

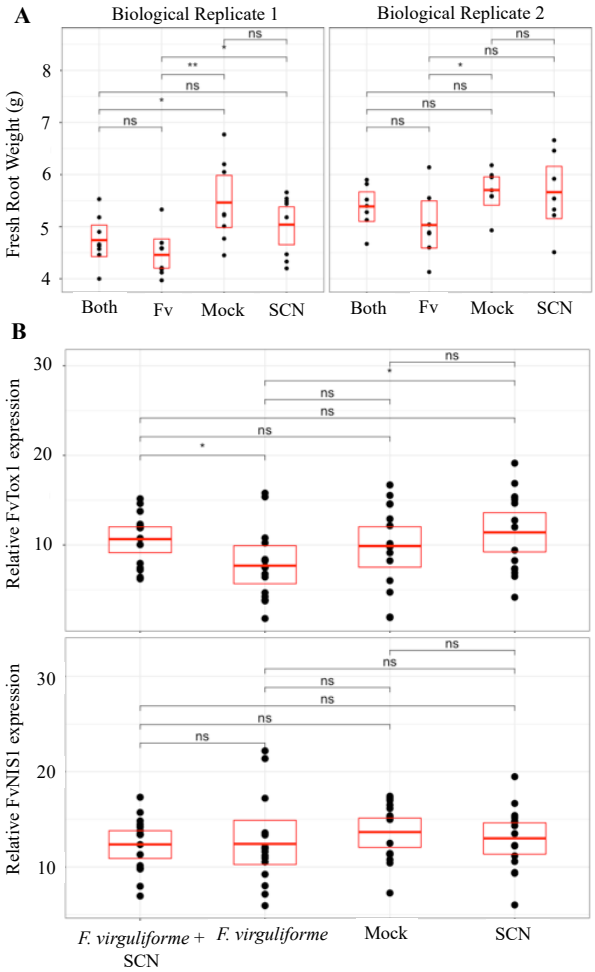

Figure 5-6.

Figure 5-6 (cont'd). Results of growth chamber factorial inoculation experiment. (**A**) Root dry weight of inoculated soybeans. (**B**) Expression levels of *F. virguliforme* effectors FvTox1 and FvNIS1, relative to the *F. virguliforme* housekeeping gene *TEF1*.

Discussion

Both SCN and *F. virguliforme* independently cause significant damage and yield loss in soybeans (Allen et al., 2017). Potential synergism between the two increases the risk of severe SDS symptoms and yield loss (Roth et al., 2019a; Xing and Westphal 2013). Though *F. virguliforme* is the sole cause of soybean SDS (Roy et al., 1989), it is interesting that Gao et al., (2006) observed some foliar necrosis in SCN-only inoculated plants. *Fusarium virguliforme* (formerly *F. solani* f. sp. *glycines*) has been isolated from SCN eggs and cysts (Donald et al., 1993; McLean and Lawrence 1995), and Gao et al., (2006) also indicated that *F. virguliforme* decreased SCN reproduction. These reports are suggestive of nematode vectoring *F. virguliforme*. However, our results support previous findings that *F. virguliforme* can colonize nematodes (Donald et al., 1993; McLean and Lawrence 1995), but is not actively vectored by nematodes (Fig. 5-1, Fig. 5-2).

Fungal colonization inside *C. elegans* adults was an interesting finding. Muhammed et al (2012b) reported a similar finding using clinical isolates of *F. solani* and suggested that this resulted from conidia germination inside *C. elegans*. For this to happen, fungal spores must get inside *C. elegans* prior to germination, likely by ingestion. However, *C. elegans* is reported to be a strict bacterial feeder, and SCN is reported to be a strict herbivore (Avery and You 2005; Davis and Tylka 2005). In contrast, the time-course infection presented in this work indicates that *F. virguliforme* can internally colonize *C. elegans* without the need to ingest spores (Fig. 5-5). Adult *C. elegans* are approximately 30-40 µm in diameter (Backholm et al., 2013), and *F. virguliforme* detection at 16 µm from the cuticle is within this range (Fig. 5-4). This colonization

of nematodes indicates the saprophytic abilities of *F. virguliforme*, which has been shown to colonize many other plant hosts outside of soybean (Kolander et al., 2012). Sufficient colonization of nematodes could lead to an increase in fungal inoculum, which has been shown to be significantly associated with increased SDS severity (Freed et al., 2017; Roth et al., 2019a; Roy et al., 1997).

Fungal development in culture is characterized macroscopically by outward radial growth of hyphae. Microscopically, radial growth is an over-simplification. The time-course experiment in this study shows that *F. virguliforme* spores germinate from their terminal (foot) cells and continue growing in seemingly random directions (Fig. 5-5). Since initial hyphae germinate and travel away from *C. elegans*, it is possible that fungal colonization of nematodes is a random event. However, once *F. virguliforme* successfully penetrated *C. elegans* (approximately 35-40 hours post inoculation), subsequent colonization of the nematode was rapid, killing the nematode (Fig. 5-4). Quorum sensing in fungi has been described, though is not a well-studied topic (Albuquerque and Casadevall 2012). In particular, some fungi have shown strong reactions to farnesol, an isoprenoid that inhibits mycelial development, including *F. graminearum* (Hornby et al., 2001; Albuquerque and Casadevall 2012; Semighini et al., 2008). Unlike arthropods and tardigrades, nematodes have retained their ability to synthesize farnesol (De Loof et al., 2015), which would suggest colonization of *C. elegans* by *F. virguliforme* would be inhibited. However, other fungal quorum sensing molecules have been identified, like tyrosol, which can induce fungal filamentation (Albuquerque and Casadevall 2012). It may be possible that *F. virguliforme* releases a quorum sensing molecule in the presence of nematodes, facilitating rapid colonization and utilization of the food source. A metabolomics study of colonized and non-colonized *C. elegans* may reveal potential quorum sensing molecules.

Root infections by SCN cause significant changes in soybean gene expression and is associated with increased SDS severity (Ithal et al., 2007a, 2007b; Roth et al., 2019a; Xing and Westphal 2013). However, *F. virguliforme* expression of two known effectors were not significantly affected by SCN in this study (Fig. 5-6 B). *Fusarium virguliforme* inoculations caused a significant reduction in root fresh weight in both biological replicates of this experiment, suggesting that soybeans were subjected to a sufficient level of inoculum (Fig. 5-6 A). However, expression of both *F. virguliforme* effectors were also detected frequently in Mock and SCN-only inoculated samples, suggesting a lack of specificity of primers designed by Chang et al., (2016a). Therefore, the presence of SCN may alter *F. virguliforme* gene expression and will need to be investigated further, with either 1) improved primer design or 2) higher inoculum levels to reduce false-positive detection of *F. virguliforme* gene expression.

Acknowledgements

The authors would like to thank Dr. M. Frame for confocal and spectral imaging assistance, and Z. Noel, J. Jacobs, A. McCoy, M. Breunig, V. Ortiz, H.-X. Chang, and H. Sang for helpful discussions on interpretation of results. This work was funded in part by the Michigan Soybean Promotion Committee, the United Soybean Board, the North Central Soybean Research Program, and the Syngenta Agricultural Scholarship.

CHAPTER 6: Investigating legume host preference among *Fusarium virguliforme* and *F. brasiliense* using factorial inoculations and whole-genome sequencing

By

Mitchell G. Roth, Jie Wang, Janette L. Jacobs, Kevin Childs, and Martin I. Chilvers

This work presented in this chapter is unpublished.

Author Contributions:

MGR, JW, and MIC conceptualized project goals, MGR, JW, and KC generated methods, MGR and JLJ worked with isolates to generate high molecular weight DNA, KC prepared all libraries and generated all sequences, MGR and JW analyzed all data, and MGR wrote the manuscript.

Abstract

Soybean sudden death syndrome is caused by multiple species within clade II of the *Fusarium solani* species complex (FSSC). Two of these species, *F. virguliforme* and *F. brasiliense*, are present in Michigan. The geographic distribution of *F. virguliforme* aligns with the soybean producing regions in Michigan, while the geographic distribution of *F. brasiliense* aligns with the dry bean producing regions of Michigan. Isolation frequencies of *F. virguliforme* from soybean and *F. brasiliense* from dry bean led us to hypothesize that these two pathogens adapted to their preferred hosts, where *F. virguliforme* colonizes soybeans better than dry beans, and *F. brasiliense* colonizes dry beans better than soybeans. We used a factorial inoculation experiment in a growth chamber and whole-genome sequencing to investigate a potential host preference. Both *F. virguliforme* and *F. brasiliense* caused significant root rot on soybean and dry bean compared to the non-inoculated control. However, neither pathogen caused a significant reduction in dry weights of roots nor shoots during the 3-week experiment. Additionally, neither pathogen showed significantly more root rot symptoms than the other, on either host. Whole genome sequencing using long-read Nanopore technologies improved the genome assembly continuity with longer N50 length and a smaller number of contigs. Indeed, the current assemblies are an improvement over currently available genomes assembled via short-read sequencing technology, but the sequencing error-rate of Nanopore resulted in decreased genome quality with respect to gene-predictions of single copy orthologs. Whole-genome alignments suggest that *F. virguliforme* might be more clonal than *F. brasiliense*. These alignments also fail to provide evidence of lineage-specific or host-specific pathogenicity chromosomes. Both *F. virguliforme* and *F. brasiliense* are significant pathogens of soybean and dry bean with little evidence of a host preference among these legume crops.

Introduction

Sudden death syndrome (SDS) is an economically important disease of soybean caused by some soil borne ascomycetes in clade II of the *Fusarium solani* species complex (Aoki et al., 2005; Coleman 2016). In South America, SDS is caused by four species; *F. virguliforme*, *F. tucumaniae*, *F. cuneirostrum*, and *F. brasiliense* (Aoki et al., 2005). In North America, *F. virguliforme* was identified in 1971 in Arkansas causing SDS (Roy et al., 1989), but *F. brasiliense* isolates have also recently been reported in Michigan, capable of causing soybean SDS and root rot of dry bean, *Phaseolus vulgaris* (Jacobs et al., 2018; Wang et al., 2018b).

Root rot and SDS caused by these species are difficult to manage, and there are no mid-season management strategies currently available to growers. The fungicide fluopyram has shown efficacy in controlling *F. virguliforme*, both *in vitro* and in the field as a seed treatment (Kandel et al., 2016, 2018; Sang et al., 2018; Wang et al., 2017). However, few other fungicides have shown efficacy in the field (Weems et al., 2015) and different SDS-causing species respond differently to fluopyram (Sang et al., 2018). Genetically resistant or tolerant lines are available, but resistance is partial and controlled by many quantitative trait loci (QTLs) that overlap with QTLs for other diseases (Chang et al., 2018; Meksem et al., 1999). Crop rotations with non-hosts can be effective, but *F. virguliforme* has a broad asymptomatic host range, so rotations of up to 3 or 4 years may be necessary to lower SDS pressure (Kolander et al., 2012; Leandro et al., 2018).

Fusarium virguliforme has spread from Arkansas throughout the U.S. via unknown mechanisms, but spreading through aerial dispersal of ascospores appears unlikely because only one mating type has been detected among global isolates (Hughes et al., 2014). In contrast, both mating types have been found in *F. brasiliense* isolates (Hughes et al., 2014), including Michigan isolates from the same field (Oudman et al., *in prep*). Therefore, sexual reproduction is

likely occurring among *F. brasiliense* in Michigan. It is unknown if *F. brasiliense* was recently introduced to Michigan or if it was only recently detected. However, only one *F. brasiliense* isolate has been reported in the U.S. prior to 2014 from an unknown host in California (Aoki et al., 2005). Since *F. brasiliense* is a successful pathogen of soybeans and dry beans, it is unlikely that it has spread from California to Michigan without being detected in agricultural states in between.

High quality genomes of plant pathogens allow for many hypotheses to be addressed. Recently, advances in genome quality in fungal plant pathogens has revealed a "two-speed genome" hypothesis, where core chromosomes contain genes critical for survival and reproduction, while repeat- and transposon-rich genomic regions contain rapidly evolving effector genes specific to adaptation on specific hosts (Dong et al., 2015). High quality genomes of close relatives of *F. virguliforme* and *F. brasiliense* have revealed similar concepts (Sperschneider et al., 2015). These repeat-rich regions containing effector genes are sometimes found on small DNA elements that go by many names: lineage-specific, dispensable, or mini-chromosomes. Studies in *F. oxysporum* show that these small DNA elements can be transferred from a non-pathogenic isolate and confer virulence (Vlaardingerbroek et al., 2016b; van Dam et al., 2017). These small DNA elements can be identified by obtaining high-quality genome sequences.

Recent surveys of fungal pathogens causing root rot on soybeans and dry beans identified *F. brasiliense* in Michigan, but also revealed an interesting trend. Attempting isolations from soybean roots commonly yielded *F. virguliforme* isolates and rarely yielded *F. brasiliense* isolates (Jacobs et al., *in prep*). Similarly, isolation attempts from dry bean roots commonly yielded *F. brasiliense* isolates and rarely yielded *F. virguliforme* isolates (Jacobs et al., *in prep*,

Table 6-1). This suggested a possible host preference, where *F. virguliforme* preferentially colonizes soybean and *F. brasiliense* preferentially colonizes dry bean. The objectives of this study were to 1) use reciprocal inoculations to examine level of colonization of each pathogen (*F. virguliforme* and *F. brasiliense*) on each host (soybean and dry bean) and 2) obtain high quality genome sequences with long-read technologies to examine overall genome structure and identify potential pathogenicity chromosomes.

Species	Host	Isolates	Frequency[a]
F. virguliforme	Soybean (*Glycine max*)	12	23%
F. virguliforme	Dry bean (*Phaseolus vulgaris*)	42	77%
F. brasiliense	Soybean (*Glycine max*)	235	96%
F. brasiliense	Dry bean (*Phaseolus vulgaris*)	9	4%

Table 6-1. Isolation frequencies of *F. virguliforme* and *F. brasiliense* in Michigan from soybean and dry bean hosts.
[a] Frequency represents percent of isolates from each host and sum to 100% for each species

Materials and Methods

Isolation of fungal strains

Fungal strains were isolated from soybean and dry bean roots displaying root rot symptoms collected throughout Michigan. The roots were cut into sections soaked in 5% bleach (0.4% NaOCl) for 4 minutes, then rinsed thoroughly in sterile deionized water. The root sections were dried with sterile paper towel and plated on WMS agar (2% agar, 15µg/mL metalaxyl, 300µg/mL streptomycin). Plates were incubated for seven days at room temperature and observed under a dissecting microscope sporodochium development. Macroconidia from a sporodochium were transferred and spread on fresh WMS agar using a flame-sterilized insect pin. After 24 hours, a single germinating macroconidium was aseptically transferred onto full

strength potato dextrose agar (Neogen, Lansing, MI). Isolates were stored at room temperature on synthetic nutrient agar slants (1 g/L KH_2PO_4, 1 g/L KNO_3, 0.5 g/L $MgSO_4$, 0.5 g/L KCl, 0.2 g/L glucose, 0.2 g/L sucrose, 2% agar) in scintillation vials (Research Products International, Mount Prospect, IL, USA) for long-term storage.

Reciprocal inoculation experiment

Fungal inoculum was prepared as described in Wang et al., (2018) using *F. virguliforme* strain 'Mont-1' and *F. brasiliense* strain 'F-14-42'. Briefly, one fully colonized plate and one sterile plate of Nash-Snyder medium (Leslie et al., 2008) were added to a sterile blender with 100 mL sterile water and blended on low speed for 30 s. The inoculum slurry was added to waterlogged, sterile sorghum seed in a spawn bag, then sealed with a heat sealer. The inoculated sorghum was incubated for 4 weeks at room temperature and mixed by hand every other day. The inoculum was poured onto sterile paper towel in a biosafety hood and allowed to dry for 3 days. Colony forming units (CFU) were determined by adding 10 g of colonized sorghum to 100 mL sterile water, incubating at room temperature with shaking at 150 rpm for 30 minutes, then performing serial dilution plating. The CFU of *F. virguliforme* inoculum was higher than *F. brasiliense*, so 2.0 g of *F. virguliforme* and 11.5 g of *F. brasiliense* inoculum were used, resulting in a standardized 1.5 x 10^6 CFUs per pot.

Inoculum was added to 300 mL medium vermiculite in a 1064 mL (1 quart) plastic bag and homogenized. The inoculated vermiculite was poured into 355 mL paper cups (Solo Cup Company, Lake Forest, IL) containing three 7 mm holes for water drainage. Five seeds of soybean cultivar 'Williams 82' or dry bean cultivar 'Red Hawk' were sown on top of the inoculated medium vermiculite, then covered with 50 mL non-inoculated medium vermiculite.

Non-inoculated sorghum was used as a negative control. Five biological replicate cups were used per plant-inoculum-time point combination. Pots were watered with approximately 100 mL of water every other day, alternating between deionized water and half-strength Hoagland solution. After one, two, and three weeks of growth, all germinated plants from each pot were harvested, roots washed clean, and rated individually for root rot severity, as a percentage of discolored roots from 0-100. The average root rot severity of all plants in each pot are reported. Three plants were randomly selected from each pot, and the foliar and root tissues were separated, dried at 50°C for 48 hours, and dry weights collected. For 3-week inoculated plants, these root tissues were ground to a fine powder in a 50 mL cone-bottom tube using two 8 mm steel balls in a GenoGrinder 2010 (SPEX Sample Prep, Metuchen, NJ, USA). DNA was extracted from 50 mg of ground root tissues and used in qPCR to detect *F. virguliforme* and *F. brasiliense* quantities using highly specific qPCR assays (Roth et al., 2019; Wang et al., 2015). The relative abundance of *F. virguliforme* and *F. brasiliense* was calculated by taking $(Ct_{plant} + 10) - Ct_{pathogen})$, where Ct_{plant} represents the cycle at which amplification of the plant β-tubulin gene (Wang et al., 2018a) crossed the threshold, and $Ct_{pathogen}$ represents the cycle at which amplification of the pathogen crossed the threshold. This calculation can be intuitively interpreted, with high numbers indicative of high pathogen abundance.

Genome sequencing

Long-read sequencing technologies require high molecular weight DNA. Multiple protocols were used to extract high molecular weight DNA, though many failed to provide both high yield and high quality, which can be challenging for fungi (Schwessinger and Rathjen 2017; Kaur et al., 2017). Ultimately, the best protocol for the isolates in this study was developed by

plant researchers at Michigan State University described below (S. K. K. Raju, C. E. Niederhuth, *personal communication*).

First, *F. virguliforme* and *F. brasiliense* isolates were grown on half-strength PDA (Neogen, Lansing, MI) for 2-3 weeks for sporodochium development. Plates were flooded with 5 mL sterile water, and 4 mL water was re-collected into 15 mL conical tubes, now containing conidia. One hundred microliters of conidia were inoculated into 50 mL sterile PDB (Neogen) in 125 mL flasks and incubated at room temperature for 3-7 days with shaking at 100 rpm. Flasks were examined daily to evaluate the level and age of mycelia in order to collect a high volume of young (non-pigmented) mycelia. Mycelia was harvested by pouring the flasks into a Büchner funnel containing two layers of Miracloth (Millipore-Sigma, St. Louis, MO). Mycelia were washed twice with ~100 mL sterile water. Mycelia was gathered into the Miracloth and wrung to remove as much water as possible, then immediately transferred to a ceramic mortar containing liquid nitrogen. The mycelia were ground to a fine powder with a pestle and transferred to a 50 mL tube on ice using a SmartSpatula (Research Products International, Mt. Prospect, IL). Fifteen milliliters of DNA extraction buffer (100 mM Tris 1.4 M NaCl, 20 mM EDTA, 2% CTAB, 2% polyvinylpyrrolidone, 40 mg / mL Proteinase K, 0.2% β-mercaptoethanol) was added to the ground mycelia immediately and transferred to a 57°C water bath for 30 minutes, inverting frequently. The samples were brought to room temperature and 15 mL chloroform:isoamyl alcohol (24:1) (Millipore-Sigma) was added and incubated at room temperature for 10 minutes with shaking at 50 rpm. The samples were centrifuged for 30 minutes at 4,000 x *g* at 4°C and the supernatant was transferred to a new 50 mL conical tube using a wide orifice pipet tip. These steps were repeated with 15 mL of phenol:chloroform:isoamyl alcohol (25:24:1) (Millipore-Sigma) once, followed by 15 mL chloroform:isoamyl alcohol (24:1) once. After the final

centrifugation, the supernatant was removed using a wide orifice tip and one-half volume of chilled 5M NaCl was added, followed by 2.5 volumes of chilled isopropanol. The samples were inverted to mix, and a final addition of 3 mL 3M sodium acetate was added and inverted again. The samples were stored in -20°C for a minimum of 30 minutes and the DNA was pelleted by centrifugation at 4,000 x *g* for 30 minutes at 4°C. The pelleted DNA was washed twice with freshly prepared, chilled 70% ethanol using a centrifugation at maximum speed for 1 minute. After the final wash, all ethanol was removed except for 1 mL, which was gently poured from the 50 mL conical tube to a 1.5 mL tube, along with the DNA pellet. The 1.5 mL tubes containing the DNA pellet were centrifuged at maximum speed for 1 minute and the remaining ethanol was decanted. The DNA pellet was resuspended in 600 µl of 10 mM Tris (pH 8.0) by incubating it overnight at room temperature, with gentle shaking. RNA contamination was removed by adding RNase A and incubating at 37°C for 30 mins. The three chloroform:isoamyl, phenol:chloroform:isoamyl alcohol, and chloroform:isoamyl steps were repeated on a smaller scale in the 1.5 mL tubes, with a final DNA precipitation step using 0.5 volume chilled 5M NaCl and 1 volume chilled 100% ethanol. The DNA was precipitated at -20°C for 30 minutes, then centrifuged at max speed for 1 minute. The DNA pellet was washed twice with freshly prepared, chilled 70% ethanol. Finally, the DNA was resuspended in 200 µL 10 mM Tris (pH 8.0) and stored overnight at 4°C.

To determine if the DNA extractions contained high molecular weight, non-fragmented DNA, 1 µL was loaded and separated on a 1% agarose gel using 75 V for 45 minutes, stained in 1 µg / mL ethidium bromide for 45 minutes, and visualized on a Fotodyne FOTO/Analyst Investigator Eclipse (Thermo Fisher Scientific, Waltham, MA) (Fig. 6-3). Once DNA was determined to be high molecular weight, quantity was assessed using a Qubit fluorometer

(Thermo Fisher). To examine the presence of contaminants, 2 µL of DNA was assessed via a Nanodrop 1000 (Thermo Fisher) to obtain wavelength readings at 230, 260, and 280 nm (Table 6-2).

High molecular weight DNA was submitted to the MSU Research Technology Support Facility. Libraries for each sample were prepared using RBK004 rapid barcoding kit and sequenced on the GridION (Oxford Nanopore, Oxford, UK). Real-time bases were called using Guppy v1.4.3 and re-called using Albacore v2.3.3 (Oxford Nanopore). Genome assemblies were done using the canu pipeline using the 'genomeSize=50m' estimated from previously published *F. virguliforme* genomes (Srivastava et al., 2014) and the 'ovlMerThreshold=500' option to prevent the algorithm from setting an automatic kmer that is too high for the available data, causing significant increases in computation time. The N50 length for each genome was calculated with the Quality Assessment Tool for Genome Assemblies (QUAST) (Gurevich et al., 2013). Genome completeness was calculated with the benchmarking universal single-copy orthologs (BUSCO) tool, using the *F. graminearum* dataset as a reference (Simão et al., 2015). Genome assembly graphs were visualized with BANDAGE v0.8.1 to examine connections between contigs that are not intuitive from sequences alone (Wick et al., 2015). Whole-genome alignments were done using the 'minimap2' algorithm on the D-GENIES platform (Cabanettes and Klopp 2018).

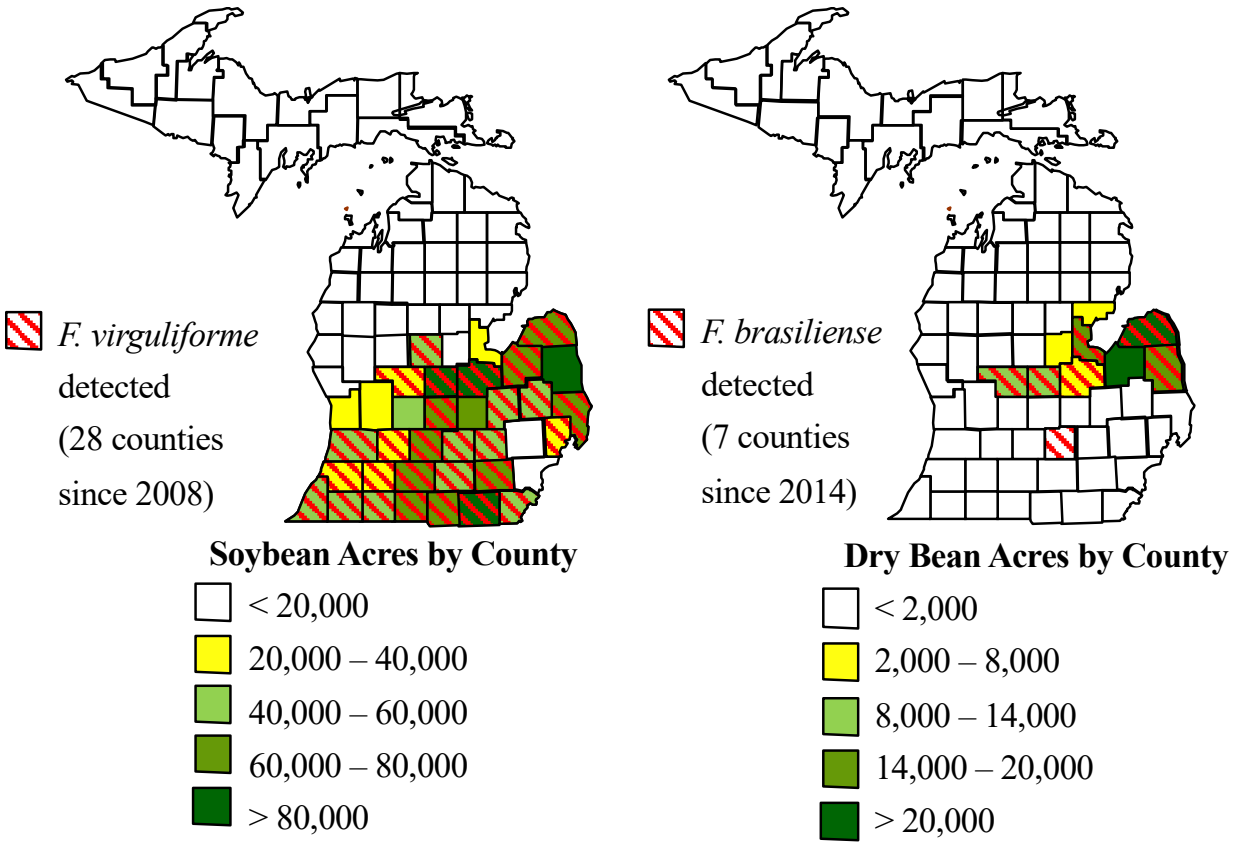

Figure 6-1. Soybean and dry bean production acreage in Michigan, and geographic distribution of *F. virguliforme* and *F. brasiliense*.

Isolate[a]	Species	Location	Host	[DNA][b]	A260 / A280[c]	A260 / A230[c]	N50[d]	Genome Size	Contigs	Coverage	BUSCO[e]	Reference
VB-2a	*F. virguliforme*	Van Buren County, MI	*Glycine max*	133	1.88	2.38	1.23	53 Mb	66	19.3 X	66.6%	This study
F-14-77	*F. virguliforme*	Ingham County, MI	*Glycine max*	86	1.92	2.46	4.61	53 Mb	22	29.3 X	73.3%	This study
DBP27R13	*F. virguliforme*	Van Buren County, MI	*Phaseolus vulgaris*	143	1.89	2.48	4.43	53 Mb	25	39.1 X	77.6%	This study
DBP30R5	*F. virguliforme*	Van Buren County, MI	*Phaseolus vulgaris*	146	1.90	2.41	0.66	53 Mb	148	19.7 X	63.6%	This study
Mont-1	*F. virguliforme*	Piatt County, IL	*Glycine max*	NA	NA	NA	0.07	51 Mb	3,098	20 X	99.2%	Srivastava et al., 2014
F-15-158	*F. brasiliense*	Saginaw County, MI	*Phaseolus vulgaris*	73	1.89	2.35	4.25	55 Mb	40	28.7 X	75.7%	This study
F-16-137	*F. brasiliense*	Saginaw County, MI	*Phaseolus vulgaris*	192	1.80	2.28	3.20	53 Mb	37	17.6 X	64.2%	This study
F-16-21	*F. brasiliense*	Montcalm County, MI	*Glycine max*	114	1.83	2.43	1.20	53 Mb	67	12.4 X	57.6%	This study
F-16-59	*F. brasiliense*	Montcalm County, MI	*Glycine max*	296	1.74	2.25	3.69	54 Mb	43	26.5 X	73.3%	This study
NRRL 31757	*F. brasiliense*	Distrito Federal, Brasilia, Brazil	*Glycine max*	NA	NA	NA	0.01	49 Mb	22,229	150 X	87.4%	Huang et al., 2016

Table 6-2. Isolate information, DNA extraction metadata, and assembly assessments for isolates sequenced in this study.

[a] Isolates in this study were collected by Dr. J. Wang, Dr. M. Chilvers, and J. Jacobs.

[b] DNA concentration in nanograms per microliter

[c] Absorbance ratios at 230, 260, and 280 nm, indicative of DNA quality and purity

[d] N50 of raw corrected contigs, in Mbp, calculated with QUAST

[e] Percent of universal single-copy orthologs detected in each genome

Results

Both *F. virguliforme* and *F. brasiliense* caused significantly higher root rot on soybean and dry bean compared to the non-inoculated sorghum (Fig. 6-2 A, $P < 0.10$). However, neither pathogen caused significant reduction in dry weights of roots nor shoots (Fig 6-2 B, C). Pathogen quantification did not suggest a host preference, as *F. brasiliense* colonized both soybean and dry bean significantly more than *F. virguliforme* did (Fig. 6-2 D).

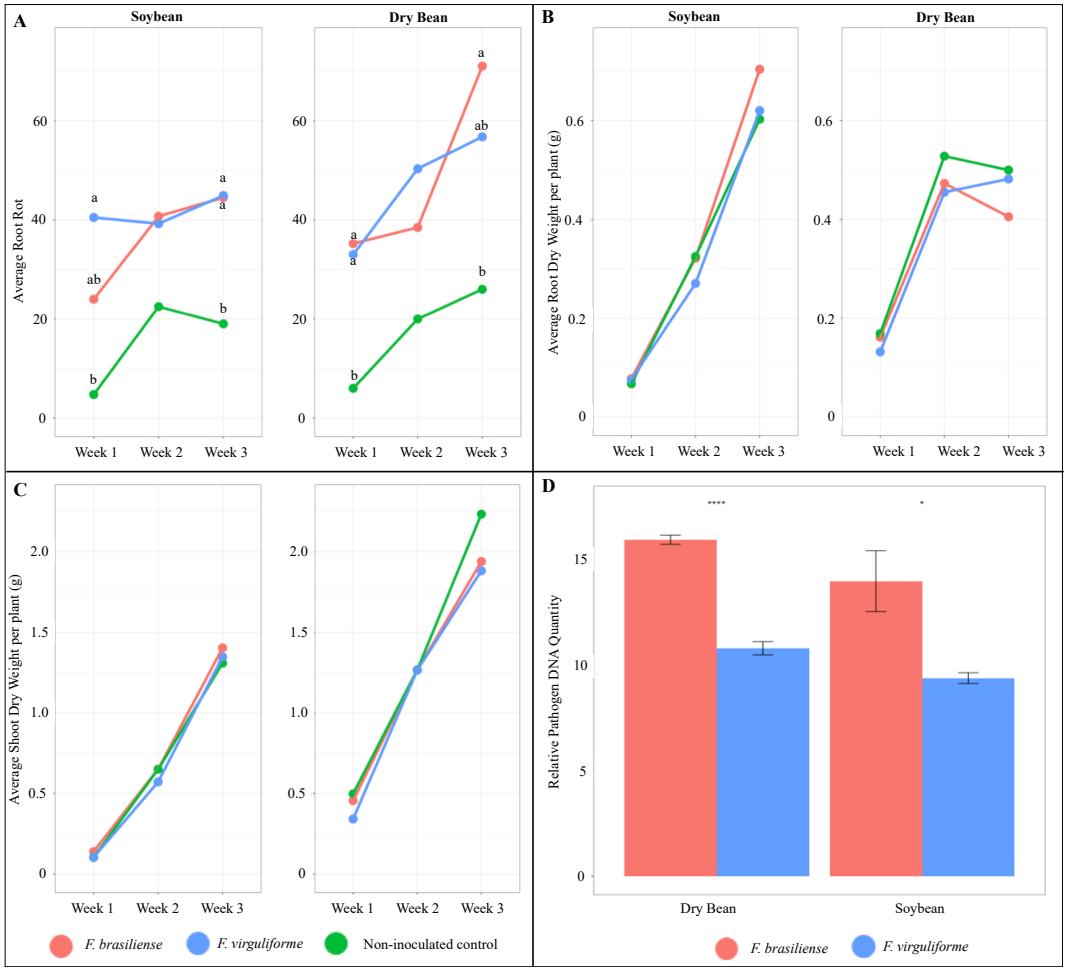

Figure 6-2. Results of factorial inoculation experiment with *F. virguliforme* and *F. brasiliense* on soybean and dry bean. Pathogen inoculation had an overall significant effect on root rot ($P < 0.05$) and these effects are plotted over time (**A**). No effect of pathogen on root dry weight or shoot dry weight were observed (**B**, **C**). *Fusarium brasiliense* was significantly higher in abundance in both soybean and dry bean roots compared to *F. virguliforme* (**D**).
**** = $P < 0.001$; * = $P < 0.05$

High quality high molecular weight DNA was successfully obtained from purified fungal mycelia (Fig. 6-3, Table 6-2). Compared to the best existing *F. virguliforme* and *F. brasiliense* genomes, the genomes developed here had lower BUSCO scores, but a larger estimated genome size, larger contig N50 values, and fewer contigs (Table 6-2). In addition, BANDAGE plots of genome assemblies developed in this study indicate near-complete genomes, with few problematic regions (Fig. 6-4).

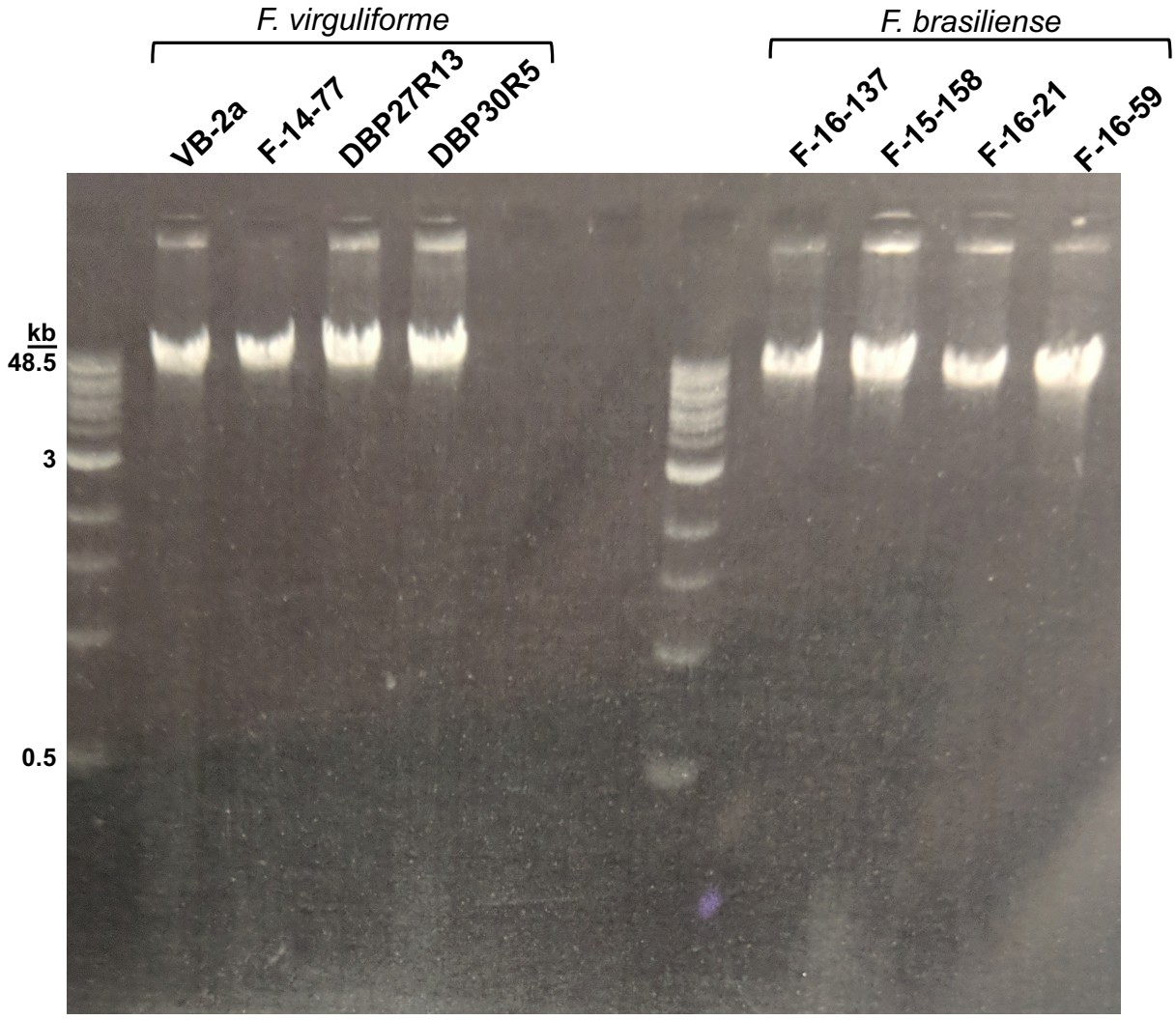

Figure 6-3. High molecular weight DNA extractions for *F. virguliforme* and *F. brasiliense* used in whole-genome sequencing with long-read Nanopore technology.

Genome-wide comparisons of each species within and across hosts revealed significant similarities in genome structure within *F. virguliforme* isolates (Fig. 6-5 A). In contrast, *F. brasiliense* isolates had unique structural variations, even if they were collected from the same host (Fig. 6-5 B). Finally, soybean isolates of *F. virguliforme* and *F. brasiliense* seem to have very similar genome structures, while dry bean isolates appear more to have more structural variation (Fig. 6-5 C).

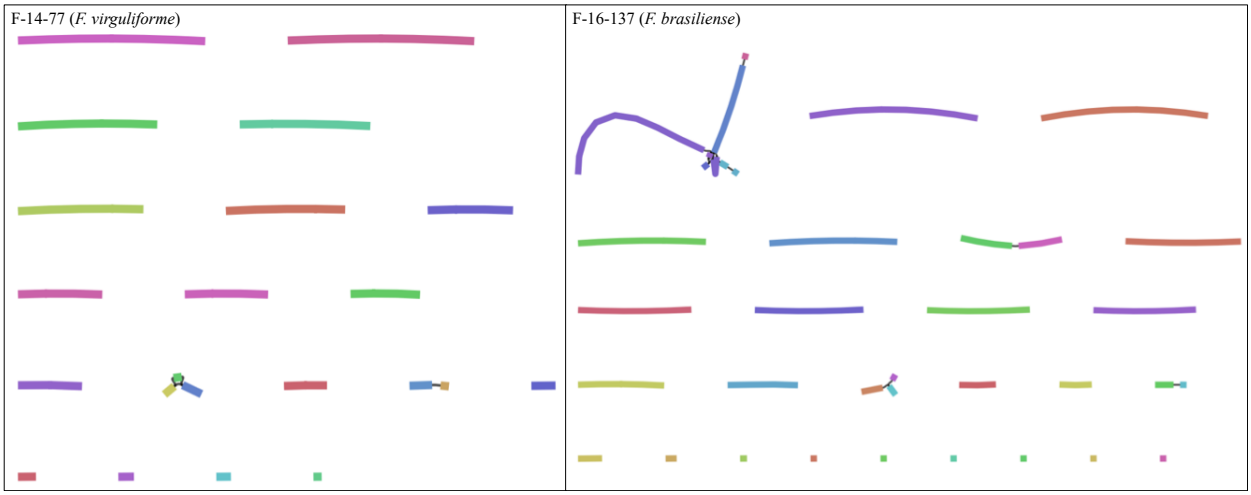

Figure 6-4. Visual representation of a *F. virguliforme* and *F. brasiliense* genome assembly in this study using BANDAGE. Isolate F-14-77 consists of 22 contigs and has very few regions of sequence complexity that needs to be resolved. Isolate F-16-137 consists of 37 contigs and has one region of strong sequence complexity that could be resolved through additional sequencing efforts.

Discussion

Both *F. virguliforme* and *F. brasiliense* are capable of infecting soybean and dry bean, and the factorial growth chamber experiment in this study indicated that significant root rot occurred in both plants due to both pathogens (Fig. 6-1). However, isolation frequencies in Michigan root rot surveys suggest a potential host preference (Table 6-1). Quantification of pathogen DNA in root systems did not support this host preference hypothesis, as *F. brasiliense* colonized soybean and dry bean roots significantly more than *F. virguliforme* (Fig. 6-2 D).

Therefore, the isolation frequencies of *F. virguliforme* from soybean and *F. brasiliense* from dry bean is more likely due to the overlapping acreage of soybean and dry bean (Fig. 6-1, Table 6-1). In addition, the smaller range of *F. brasiliense* could be due to a more recent introduction, while *F. virguliforme* has been present and spreading for a longer period of time.

Since its discovery in 1971 in Arkansas, *F. virguliforme* has spread to all soybean producing areas of the U.S. (Hartman et al., 2015). Isolates of *F. brasiliense* have been collected from symptomatic soybeans in Brazil since at least 1992, but was not formally named its own species since 2005 (Aoki et al., 2005). The recent discovery of *F. brasiliense* in Michigan (Jacobs et al., 2018; Wang et al., 2018b), coupled with the significant root rot and colonization in soybean and dry bean (Fig. 6-2) suggests that if *F. brasiliense* continues to spread, soybeans and dry beans may be faced with a significant risk of root rot and SDS. A qPCR assay for *F. brasiliense* has been developed and validated and should be widely deployed to actively monitor the spread of *F. brasiliense* (Roth et al., 2019). It remains to be seen whether *F. virguliforme* management strategies like crop rotation (Leandro et al., 2018), fungicide seed treatments (Kandel et al., 2016, 2018), and genetic resistance (Chang et al., 2018) will also be effective against *F. brasiliense*.

Genome quality can be assessed in many ways. High-quality genomes for *Fusarium* plant pathogens like *F. graminearum*, *F. oxysporum*, *F. fujikuroi*, and *F. verticillioides* (Cuomo et al., 2007; Jeong et al., 2013; King et al., 2015; Ma et al., 2010), but the quality of the *F. virguliforme* and *F. brasiliense* are lower (Huang et al., 2016; Srivastava et al., 2014). First, the number of contiguous sequences from current assemblies are over 3000, making it impossible to determine if pathogenicity chromosomes associated with host range exist as they do in *F. oxysporum* (Ma et al,. 2010; Sperschneider et al., 2015; van Dam et al., 2017; Vlaardingerbroek et al., 2016a,

2016b). Additionally, neither *F. virguliforme* or *F. brasiliense* genomes are annotated with RNA-seq data, so gene prediction algorithms are not guided, and important genes involved in pathogenicity or fungicide resistance may be incorrect or missed altogether. Despite this drawback, benchmarking using single copy ortholog (BUSCO) analyses suggest that both existing genomes are relatively complete, having over 87% of the core single-copy orthologs found in *F. graminearum* (Table 6-2). The genome assemblies generated in this study have a significant reduction in contigs because we used Nanopore's long-read technology (Table 6-2). However, a formal karyotype is needed to determine how close these assemblies are to being chromosome-level.

The most commonly cited flaw of Nanopore sequencing are the high error rates. Therefore, it was interesting to see BUSCO scores that were all > 57% and as high as 77% (Table 6-2). The best genome assemblies often use hybrid approaches with long-read technologies for scaffolding and generating contigs, along with sequencing-by-synthesis technologies like Illumina that can correct sequence errors and allow stronger confidence in gene predictions and BUSCO analyses. Incorporating Illumina-type sequencing data to these genome assemblies should provide the best genome assemblies for these species to date.

An investigation by Hughes et al. (2014) showed that global *F. virguliforme* isolates only have a single mating type, while *F. brasiliense* isolates have both. Therefore, it was not surprising to see the strong conservation of genome structure within *F. virguliforme* isolates that are likely asexually reproducing (Fig. 6-5 A). Likewise, the structural variation seen in *F. brasiliense* is not very surprising as these isolates are likely sexually reproducing (Fig. 6-5 B), since both mating types of *F. brasiliense* isolates have been identified in the same Michigan field (Oudman et al., *in prep*). However, the strong conservation of genome structure between *F.*

virguliforme and *F. brasiliense* soybean isolates is surprising, though the conservation is not seen in dry bean isolates (Fig 6-5 C). Without chromosome-level assemblies, lineage specific pathogenicity chromosomes cannot be confirmed or refuted. However, the strong conservation between soybean and dry bean isolates of *F. virguliforme* suggests that there are no soybean- or dry bean-specific pathogenicity chromosomes. Instead, it is more likely that both pathogens are equally capable of infecting both hosts given the right environment.

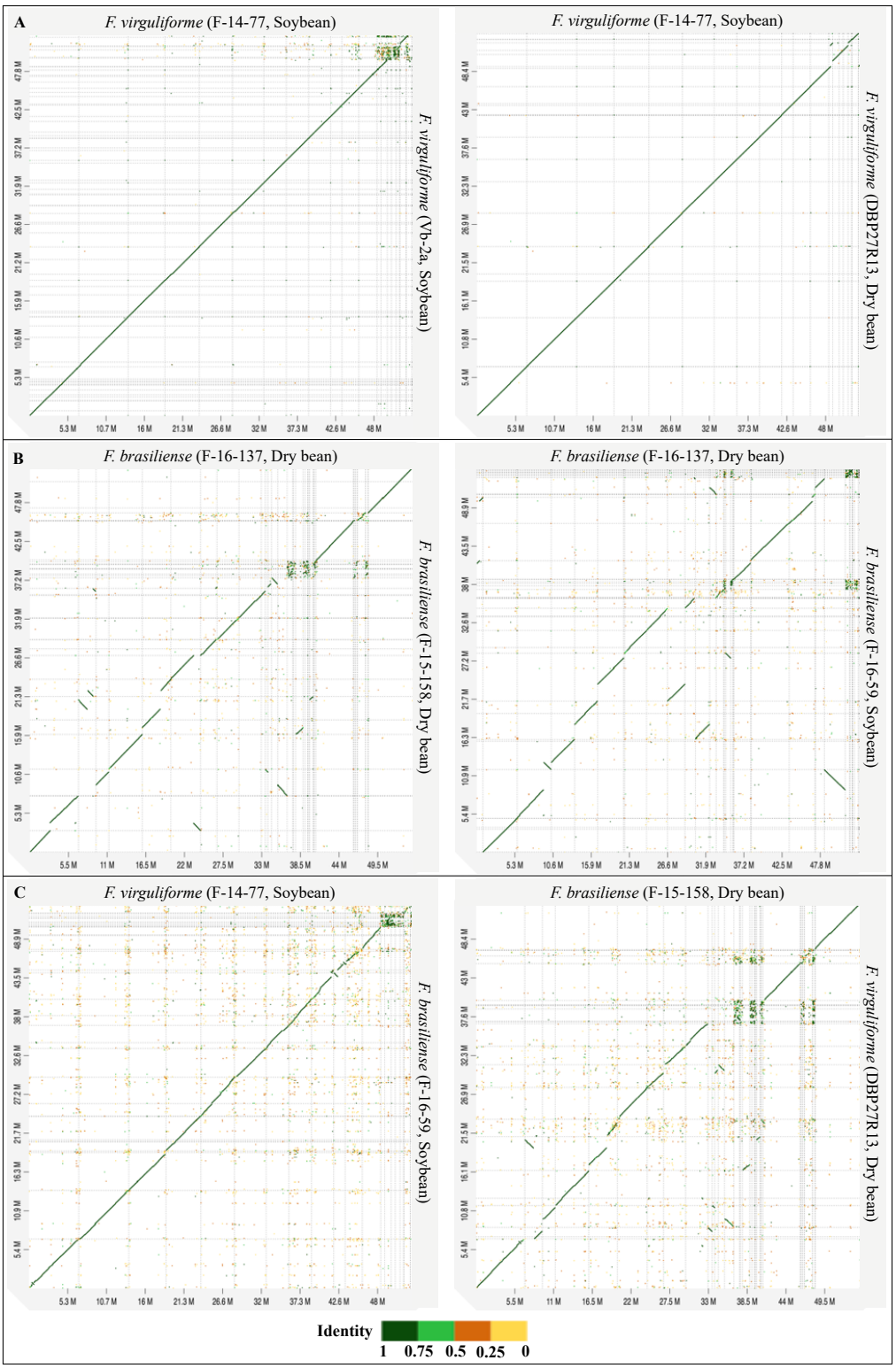

Figure 6-5. **Whole genome alignments using the 'minimap2' algorithm, plotted with D-GENIES.** *Fusarium virguliforme* isolates appear clonal across hosts (**A**), while *F. brasiliense* shows some variation in genome structure across both hosts (**B**). Comparisons between *F. virguliforme* and *F. brasiliense* within hosts show more conservation for soybean than for dry bean (**C**).

Acknowledgements

The authors would like to thank Z. Noel, B. Schwessinger, S. K. K. Raju, C. E. Niederhuth, and E. Patterson for helpful comments and suggestions regarding high molecular weight DNA extractions, genome sequencing, genome assemblies, and assessing genome quality. This work was funded in part by the Michigan Soybean Promotion Committee, the United Soybean Board, the North Central Soybean Research Program, the Syngenta Agricultural Scholarship, and the Turk Endowed Fellowship Award.

CHAPTER 7: Towards a mechanistic understanding of two SDS effector proteins: FvTox1 and FvNIS1

By

Mitchell G. Roth

This work presented in this chapter is unpublished.

Abstract

Fusarium virguliforme causes soybean sudden death syndrome (SDS) in the U.S., but also establishes relationships with other agronomically important crops and common field weeds without causing above-ground symptoms. In soybean, the soil-borne pathogen infects roots causing initial root rot symptoms, later followed by foliar symptoms marked by interveinal chlorosis and necrosis collectively known as SDS symptoms. These SDS symptoms are thought to be caused by effector proteins that enter xylem during the root infection, since *F. virguliforme* remains in the roots throughout infection. Two effector proteins, FvTox1 and FvNIS1, have been identified as important factors in foliar SDS development, but their modes of action remain unknown. Here, we explored FvTox1 and FvNIS1 production in two heterologous systems to test their ability to induce SDS-like symptoms in stem-cut assays. Neither FvTox1 nor FvNIS1 alone were able to induce SDS symptoms at the protein concentrations tested. However, transient expression of *FvTox1* and *FvNIS1* in tobacco revealed that FvNIS1 can cause a hypersensitive response, while FvTox1 causes no reproducible symptoms. Finally, we propose multiple mechanisms that alternate hosts may employ to evade SDS-like symptoms.

Introduction

Fusarium virguliforme is a soil-borne Ascomycete that is responsible for causing sudden death syndrome (SDS) in soybean. With severe infections, SDS can cause 100% yield loss, and is considered one of the top five most yield limiting diseases of soybean in the U.S. (Allen et al., 2017; Hartman et al., 2015; Koenning and Wrather 2010). Infection occurs in the soybean root and the plant symptoms it induces are two-fold, starting with root rot and later causing interveinal chlorosis and necrosis of the foliar tissues. To date, the pathogen has not been

isolated from above-ground tissues (Roy et al., 1989), so foliar symptoms are thought to be caused by pathogen secretion of phytotoxic effector proteins into the xylem. Once secreted into the host, these proteins translocate from the roots to the leaves and induce SDS foliar symptoms through currently unknown mechanisms. A study by Abeysekara and Bhattacharyya (2014) found fungal-derived proteins in the xylem sap of soybeans infected by *F. virguliforme* to support this hypothesis. Three effector proteins have been identified, but only two have been characterized (Brar et al., 2011; Chang et al., 2016a; Jin et al., 1996; Pudake et al., 2013). These two characterized effectors were named FvTox1 and FvNIS1. Both contain predicted N-terminal secretion signals, and knocking out either of these genes in *F. virguliforme* reduces its ability to induce SDS symptoms of soybeans in stem-cut and inoculation assays (Chang et al., 2016a; Pudake et al., 2013).

Management practices for *F. virguliforme* include long-term crop rotations (Leandro et al., 2018), fungicide seed treatments (Kandel et al., 2016, 2018), and genetic resistance, though genetic resistance is partial and controlled by complex QTLs (Chang et al., 2018). Exploring the molecular mechanisms of effector-induced SDS development could reveal specific mechanisms that could be targeted in breeding or transgenic efforts to improve soybean genetic resistance to SDS. *Agrobacterium*-mediated transformation of soybean is historically very challenging, which makes transient expression assays commonly used to study effector function impossible (Yamada et al., 2012). Though transient expression assays in somatic soybean embryos have been reported (Nishizawa et al., 2006), transient expression in actively growing soybean leaves has not been reported. To circumvent these apparent limitations, researchers studying soybean SDS have developed a protocol to artificially induce foliar SDS in soybeans without live *F. virguliforme* cells. This “stem-cut” assay utilizes soybean plantlets cut just above the soil line

and spent, filter-sterilized *F. virguliforme* liquid cultures, called cell-free culture filtrates, which significantly increases soybean cell death (Li et al., 1999; Xiang et al., 2015). Cell-free culture filtrates from *fvtox1* and *fvnis1* knockout mutants show significantly less foliar SDS symptoms, suggesting that FvTox1 and FvNIS1 play a role in SDS development but are not necessary for SDS (Chang et al., 2016a; Pudake et al., 2013). If FvTox1 or FvNIS1 are sufficient to produce SDS symptoms, purified FvTox1 or FvNIS1 protein would induce SDS-like symptoms in stem-cut assays. It is important to determine the mechanism by which FvTox1 and FvNIS1 trigger SDS symptoms so that scientists can accurately predict new ways to intervene and generate soybean cultivars resistant to SDS.

To study pathogen effector function, the *Agrobacterium-Nicotiana* model system is often employed. Tobacco, *Nicotiana benthamiana*, is very susceptible to *Agrobacterium tumefaciens* transformation and therefore can be used to study the effect of pathogen gene expression *in planta* (Sparkes et al., 2006). However, non-host resistance is the most robust form of plant resistance to microbial pathogens because it includes a broad spectrum of genetic mechanisms (Senthil-Kumar and Mysore 2013). *Fusarium virguliforme* is capable of infecting the roots of at least 15 other common field crops and weed species (Kolander et al., 2012), but no reports have investigated whether tobacco is a host for *F. virguliforme*. Therefore, using tobacco to study *F. virguliforme* effector function provides convenient methods, but results may not be directly applicable to soybean.

The major objective of this study was to investigate the molecular mechanisms of FvTox1- and FvNIS1-induced SDS symptoms. Three approaches were used; 1) heterologous expression of effectors using the model yeast *Pichia pastoris* for purification and use in stem-cut assays, 2) heterologous expression of effectors using the model bacterium *E. coli* for purification

and use in stem-cut assays, and 3) transient expression of effector genes in tobacco using *A. tumefaciens*-mediated transformation.

Materials and Methods

Heterologous expression in Pichia pastoris

The model yeast *Pichia pastoris* has been used for heterologous production of proteins in multiple plant-pathogen related studies (Kemen et al., 2005; Lacerda et al., 2016; Liu et al., 2016). This model yeast has a strong methanol inducible promoter, AOX1, which can be cloned upstream of a gene-of-interest and induced in *Pichia* cultures with the addition of methanol (*Pichia* Expression Kit User Guide 2014). Briefly, *FvTox1* and *FvNIS1* cDNAs were obtained using RT-PCR from isolated total RNA. The cDNA was amplified using modified primers to incorporate a KpnI cut site upstream of the genes and an ApaI cut site downstream of the genes. For full-length *FvTox1* and *cFvTox1*, the primer sequences were 5' CCA CCA GGT ACC GGT ATG AAG TCC ACA TTC ACC CTT GCG 3' and 5' CCA CCA GGG CCC CTG TGG GTT GCG CAC ACA GTT G 3'. For cFvNIS1, the primer sequences were 5' CCA CCA GGT ACC GGT ATG CGC TTC TCC CTC GCC C 3' and 5' CCA CCA GGG CCC CTG GCT GGC CTT GTA CTC CTT GC 3'. All three genes were individually cloned into pPICZ-A, which contains the AOX-1 promoter and the *BleoR* gene, conferring resistance to Zeocin (Pichia expression vectors for selection on Zeocin and purification of recombinant proteins 2010). These constructs were linearized by digestion with the restriction SacI-HF (New England Biolabs, Ipswich, MA) and transformed into *Pichia pastoris* strain X-33 using electroporation according to the *Pichia* provider protocol (ThermoFisher Scientific, Waltham, MA). Transformed *Pichia* were incubated on YPDS plates containing 100 µg / µL Zeocin for 2 days at 30°C in the dark. Putative

transformants were confirmed for the presence of *FvTox1* and *FvNIS1* using PCR with the primers AOX-1-F (5' GAC TGG TTC CAA TTG ACA AGC 3') and AOX-1-R (5' GCA AAT GGC ATT CTG ACA TCC 3').

Transformed *Pichia* isolates containing either FvTox1 or FvNIS1 were grown in liquid culture to log phase, then diluted to an OD_{600} of 1 in methanol medium in a baffled flask, according to the manufacturer protocol (Pichia Expression Kit User Guide 2014). One milliliter of culture was collected at regular time intervals of 0, 6, 12, 24, 36, 48, 60, 72, 84, and 96 hours, and methanol was added every 24 hours to maintain a final concentration of approximately 0.5% methanol in the culture (Pichia Expression Kit User Guide 2014). Since FvTox1 and FvNIS1 are predicted secreted proteins, 1 mL of collected cells were pelleted, and the cells and supernatant were analyzed separately. Amicon Ultra-15 spin filters were used to concentrate any proteins present in the supernatant according to manufacturer protocol (Millipore-Sigma, St. Louis, MO).

Heterologous expression in Escherichia coli

For expression of *FvTox1* and *FvNIS1* in *E. coli*, custom gene sequences were ordered using gBlocks Gene Fragments (Integrated DNA Technologies, Coralville, IA). Two versions of each cDNA was ordered, one with the secretion signal (FvTox1-full, FvNIS1-full) and one without the predicted secretion signal (FvTox1-noSS, FvNIS1-noSS). Each gene construct was codon optimized for expression in *E. coli* and a 6X-HIS tag and SUMO tag were fused to the N-terminus of each gene. The 6X-HIS tag is intended for affinity chromatography purification and the SUMO tag was added to aid solubility (Kuo et al., 2014). After successful expression of the fusion protein, the HIS- and SUMO-tag can be cleaved *in vivo* by incubating with Ulp1 protease (Kuo et al., 2014). These custom gene fragments were cloned into pET11-b downstream of the

strong T7 promoter and transformed into *E. coli* strain BL21 DE3 using heat-shock transformation. Successful transformants were selected on LB agar containing 50 µg / mL carbenicillin (Research Products International, Mt. Prospect, IL). Transgenic *E. coli* cells were grown to an OD_{600} of 0.6 in 100 mL LB broth at 37°C. These cells were induced to express the proteins of interest by adding IPTG to a final concentration of 5 mM and transferring the cultures to a 15°C shaking incubator to aid solubility. After a 14 h incubation, the cells were pelleted, resuspended in 50 mM sodium-phosphate buffer with 50 mM NaCl (pH 8) or 50 mM HEPES buffer with 300 mM NaCl (pH 8), and lysed twice at 4°C in a high pressurize homogenizer (Constant Systems LTD, UK). The cell lysate was centrifuged at 20,000 x *g* for 30 minutes to pellet insoluble materials like DNA, lipids, and insoluble proteins. The supernatant containing soluble protein was mixed with SDS loading dye (250 mM Tris-HCl, 30% glycerol, 0.1 g / mL SDS, 0.33 mg / mL bromophenol blue, 0.05% β-mercaptoethanol), boiled at 98°C for 15 minutes, and separated on a 4-20% gradient polyacrylamide gel (Bio-Rad Laboratories, Hercules, CA). The gels were stained for 1 hour in Coomassie blue (0.1 mg / mL Coomassie blue, 50% methanol, 40% water, 10% glacial acetic acid). The gels were destained in sterile water, with 2-minute microwave bursts until background Coomassie blue stain was removed. The predicted molecular weight of all four protein constructs of interest ranged between 26.5 and 32.3 kDa.

Attempts at purifying soluble HIS-tagged proteins were performed using Ni-NTA charged resin (ThermoFisher). Briefly, concentrated cell lysate was added to 1 mL Ni-NTA in a 5 mL plastic centrifuge column (ThermoFisher). The column was washed twice with 5 mL of 50 mM HEPES buffer containing 300 mM NaCl and 20 mM imidazole. The proteins bound to the Ni-NTA column were eluted with 3 mL of the same wash buffer, but now containing 300mM

imidazole. Due to low yields and non-specific binding of non-target proteins to the Ni-NTA column, eluted protein was not used in the stem cut assay, but rather total soluble protein from induced and non-induced *E. coli* cells.

High salt conditions, like 300 mM NaCl, allowed protein solubility but can cause chlorosis in soybean (Pantalone et al., 1997). To ensure that soybean stem-cut phenotypes were due to the presence of FvTox1 or FvNIS1 instead of high salt concentrations, the 4 mL of soluble proteins were subjected to buffer exchange using a desalting column (Bio-Rad) and re-collected in 5 mL sterile water. Five milliliters of soluble protein in 300 mM salt or 5 mL of soluble protein in sterile water were diluted with 20 mL sterile water in a 50 mL conical tube and sealed with parafilm. Three-week old soybean stems (variety 'Williams 82') were cut at the soil line, and the cotyledons and primary leaves were removed, leaving a single trifoliate leaf. The stems were used to puncture the parafilm of the 50 mL conical tubes containing protein samples, and the plants were incubated in a growth chamber at 25°C. Trifoliate leaves were harvested and imaged after 7 days of incubation.

Transient expression in Nicotiana

Full-length *FvTox1* cDNA was PCR amplified with the primers 5' CAC CAT GAA GTC CAC ATT CAC CCT TGC G 3' and 5' CTG TGG GTT GCG CAC ACA G 3', while full length FvNIS1 cDNA was PCR amplified with the primers 5' CAC CAT GCG CTT CTC CCT CGC C 3' and 5' CTG GCT GGC CTT GTA CTC CTT G 3'. These primers incorporated a 'CACC' motif that allowed for Gateway cloning of the blunt PCR fragments into pENTR/SD/D-TOPO (ThermoFisher). The pENTR plasmids containing FvTox1-full or FvNIS1-full were transformed into *E. coli* DH5α competent cells via heat-shock transformation and selected for on LB agar

containing 50 µg / mL kanamycin. Successful transformants were grown overnight in 5 mL LB broth, and pENTR plasmids were purified using a GeneJET Plasmid Miniprep Kit (ThermoFisher). pENTR vectors containing *FvTox1* and *FvNIS1* inserts were digested with ApoI to degrade the Kanamycin resistance gene. The linear pENTR construct containing the gene of interest was gel extracted and purified using a Wizard SV Gel and PCR Clean-up Kit (Promega Corporation, Madison, WI). The gene of interest in the linear pENTR construct was transferred into pEAQ-HT-DEST3 (Sainsbury et al., 2009) using the Gateway LR Clonase II kit (ThermoFisher) and transformed into *E. coli* DH5α cells via heat shock, and selected on LB agar amended with 50 µg / mL kanamycin. Successful insertion of FvTox1 or FvNIS1 into pEAQ-HT-DEST3 was confirmed via PCR and Sanger sequencing, then transformed into *Agrobacterium tumefaciens* strain GV3101 using the freeze-thaw method (Weigel and Glazebrook 2006) and selected on LB agar amended with 20 µg / mL rifampicin, 10 µg / mL gentamycin, and 50 µg / mL kanamycin. Genes inserted into the pEAQ-HT-DEST3 incorporate a 6X-HIS tag on the C-terminus of a protein of interest. Constructs lacking the secretion signal (FvTox1-noSS, FvNIS1-noSS) were not used in *Agrobacterium* infiltration.

Agrobacterium isolates containing the desired vector were streaked onto LB agar amended with rifampicin, gentamycin, and kanamycin and incubated at room temperature for 2 days to generate a lawn of bacteria. The cells were harvested by scraping the LB agar with a 1 mL pipet tip and resuspending the cells in 900 µL infiltration buffer (10 mM MES buffer, 10 mM $MgCl_2$, 100 µM acetosyringone dissolved in DMSO, pH 5.8). The cells were diluted to an optical density at 600nm (OD_{600}) of 0.6 with infiltration buffer and incubated in the dark for 2 h with gentle shaking. Three-week old *N. benthamiana* plants were wounded with an insect pin, and the *A. tumefaciens* cells were infiltrated into the wound using a 1 mL syringe. The plants

were incubated in a greenhouse for 7 days. Infiltration buffer with no *A. tumefaciens* cells was used as a negative control and *A. tumefaciens* containing the *AvrRpt2* or *AvrB* gene was used as a positive control known to induce the hypersensitive response (HR). Three 4 mm diameter leaf punches were taken each day for 6 days for RT-PCR confirmation of transgene expression, which was highest at 2 days post infiltration (data not shown). Therefore, infiltrations were repeated and 20, 10 mm diameter leaf punches were taken 2 days post infiltration for protein extraction and co-immunoprecipitation (co-IP) using PureProteome Nickel Magnetic Beads or PureProteome Protein A/G Magnetic Beads (Millipore-Sigma) with mouse IgG1 monoclonal anti-6X-antibodies (ThermoFisher).

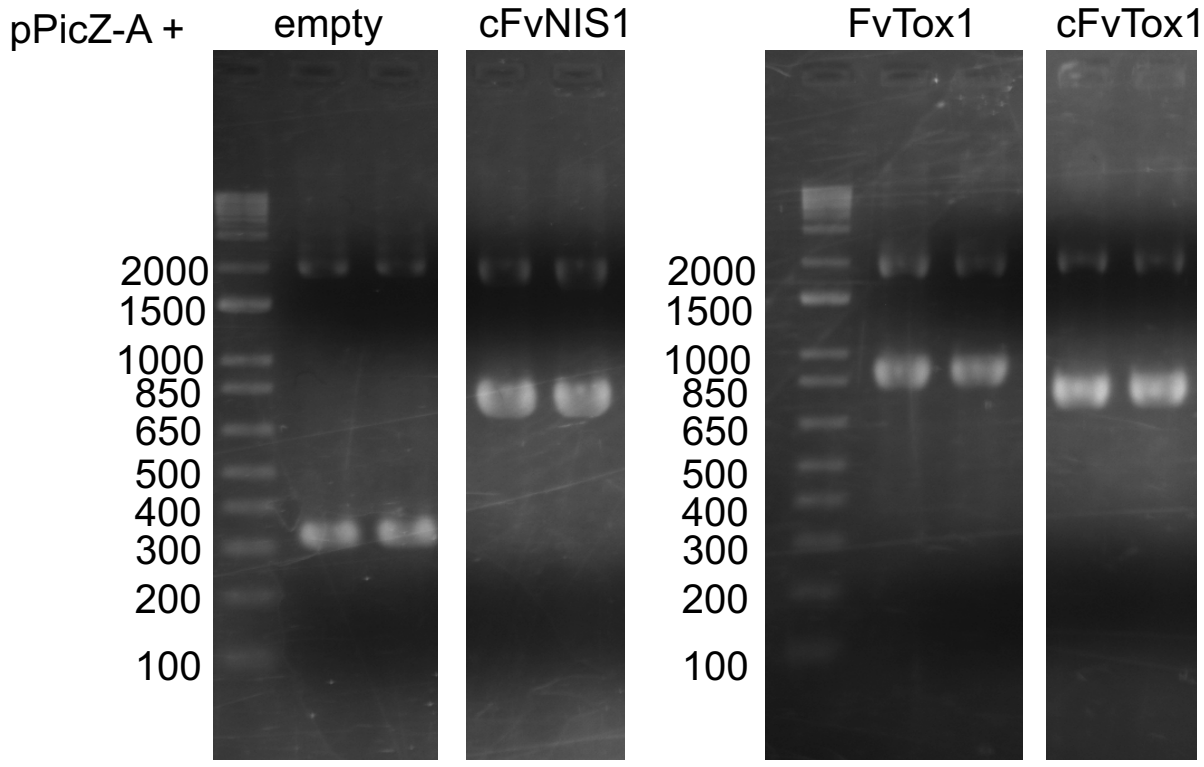

Figure 7-1. Gel electrophoresis of DNA amplified from representative *Pichia pastoris* strains transformed with linearized pPICZ-A constructs containing one of three gene constructs of interest.

Results

Heterologous expression in Pichia pastoris

Pichia pastoris cells were successfully transformed with linear pPICZ-A DNA constructs containing full length FvTox1 or intron-less cDNA versions of FvTox1 and FvNIS1 (cFvTox1, cFvNIS1, Fig. 7-1). The expected sizes of the empty pPicZ-A vector, cFvNIS1, FvTox1, and cFvTox1 amplicons were 325, 727, 931, and 820 bp, respectively. However, a DNA fragment approximately 2 kb in length was observed in all *Pichia* transformants indicating that the genes of interest were inserted randomly in the *Pichia* genome and did not replace the native *AOX1* gene. Screening these isolates for protein expression upon induction with methanol indicated that neither FvTox1 nor FvNIS1 were produced in the supernatant (Fig. 7-2). In addition, no obvious signs of FvTox1 protein expression was observed at any time point inside cells that would have suggested a failure to secrete the protein (Fig. 7-3). Instead, this observation suggested that *Pichia* was not expressing these genes of interest at all. However, RT-PCR at 96 hours post-induction did show some mRNA expression in some *Pichia* isolates (Fig. 7-4). However, significant protein production was never observed using transgenic *Pichia pastoris* cells, so this method was abandoned for further study of FvTox1 and FvNIS1.

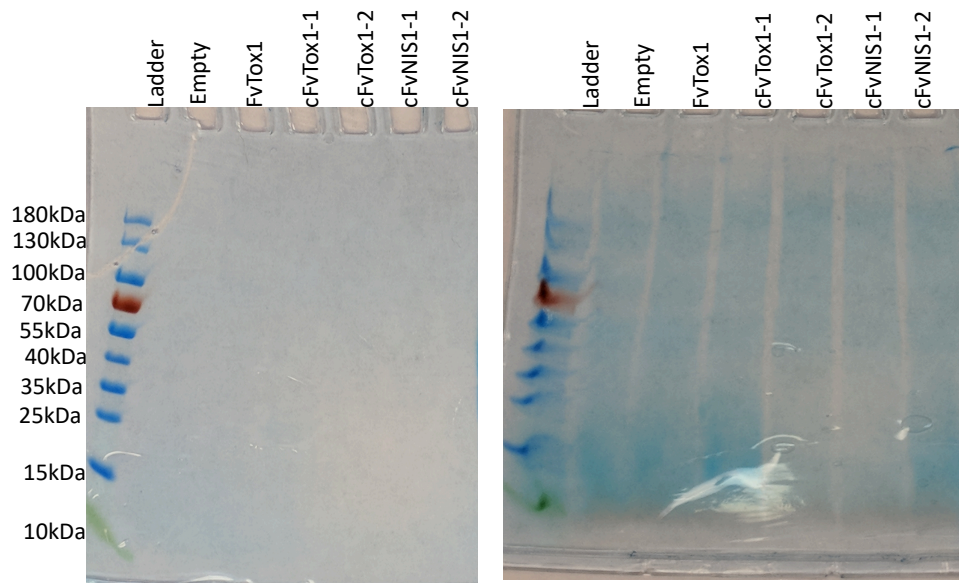

Figure 7-2. Gel electrophoresis of protein extracted from the supernatant of methanol-induced *Pichia pastoris* strains after 96 hours. One strain of *P. pastoris* containing FvTox1 was tested, while two *P. pastoris* strains each containing cFvTox1 or cFvNIS1 were tested for protein expression and are indicated by "-1" or "-2". Left, protein from *P. pastoris* supernatant. Right, protein from *P. pastoris* supernatant after a 1:50 concentration with spin filters.

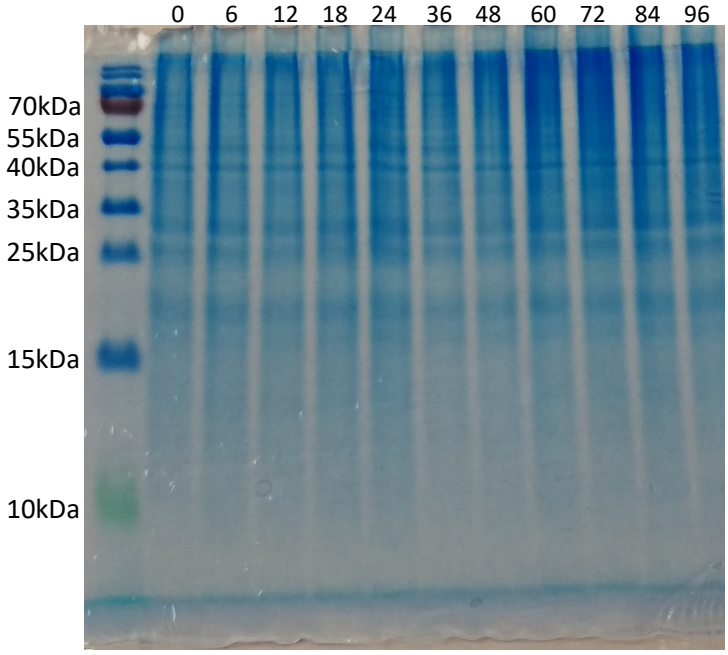

Figure 7-3. Gel electrophoresis of protein extracted from the cell pellets of methanol-induced *Pichia pastoris* strain cFvTox1-1 over time. The protein profile does not change over time, suggesting no induction of heterologous protein expression due to the presence of methanol.

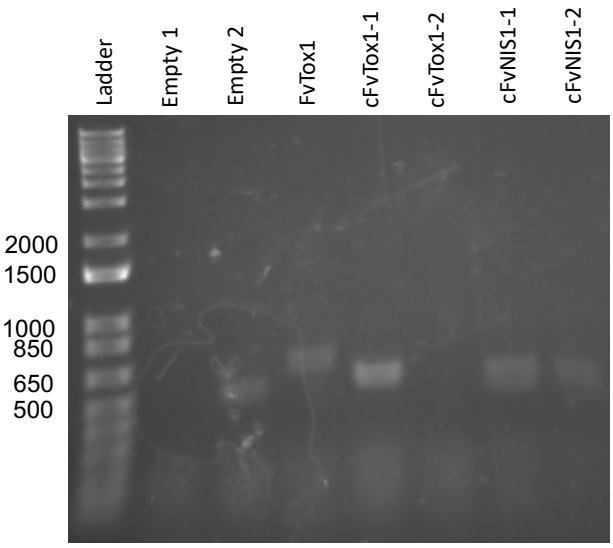

Figure 7-4. Gel electrophoresis of amplified cDNA after RNA extraction from the cell pellets of methanol-induced *Pichia pastoris* strains after 96 hours. Lane "Empty 1" is cDNA from *P. pastoris* containing the empty pPICZ-A vector amplified with FvTox1 primers, while "Empty 2" is the same cDNA amplified with FvNIS1 primers.

Heterologous expression in Escherichia coli

Escherichia coli cells were successfully transformed with pET11-b containing one of four transgenic constructs (Fig. 7-5). The addition of IPTG induced cells to express and produce the proteins of interest; however, these proteins were found to be insoluble in sodium phosphate buffer (Fig. 7-6 A). Buffer optimization suggested that three of the four proteins were highly soluble in 50 mM HEPES with 300 mM NaCl (Fig. 7-6 B, C). In all instances, protein production was specific upon induction with IPTG (Fig. 7-6 D), though in some instances the observed size of the protein constructs (35-40 KDa) was larger than the predicted molecular weight (Fig. 7-6 D).

Many native *E. coli* proteins were soluble that were not of interest to us. Therefore, affinity chromatography was implemented to reduce the number of non-specific proteins and purify our proteins of interest. Protein yields were significantly lower than anticipated, and

although many soluble proteins were washed away, some proteins other than the desired protein product remained after affinity chromatography (Fig. 7-7).

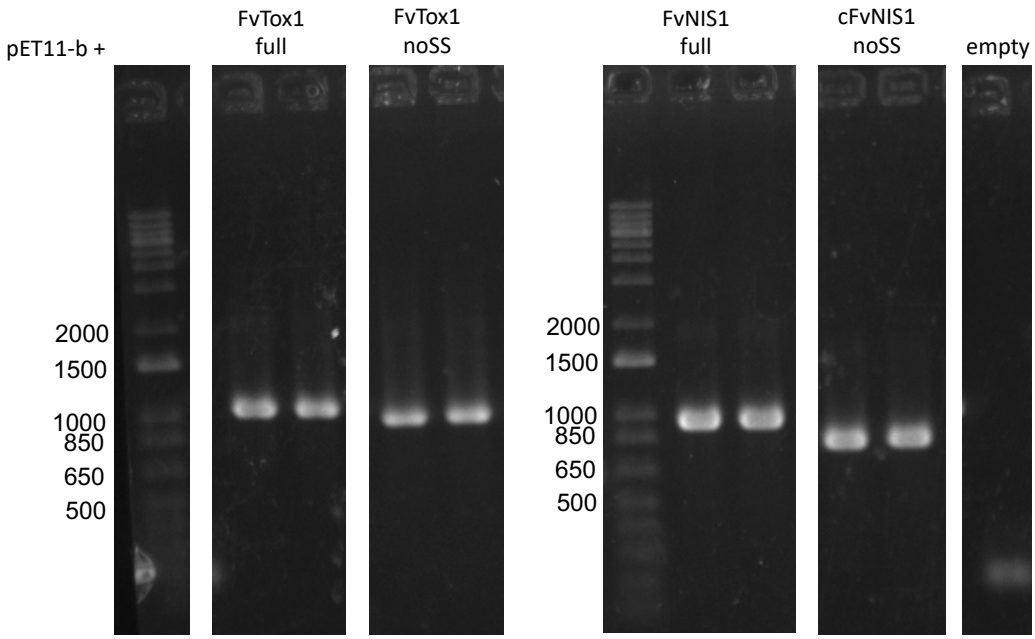

Figure 7-5. Gel electrophoresis of amplified DNA from representative *E. coli* cells transformed with pET11-b plasmids containing one of four gene constructs. "Empty" indicates amplification from the empty pET11-b plasmid using FvTox1 primers.

To determine if FvTox1 or FvNIS1 are sufficient to induce SDS, we wanted to use purified protein from induced *E. coli* cells in a stem-cut assay. Due to the low yields and non-specific purification after affinity chromatograph (Fig. 7-7), we decided to use whole-protein extract from induced and non-induced *E. coli* cells (Fig. 7-6 D). We hypothesized that it is unlikely that any native *E. coli* proteins would be able to cause SDS-like symptoms in a stem-cut assay, while heterologously produced FvTox1 or FvNIS1 may cause SDS-like symptoms. However, solubility of FvTox1 and FvNIS1 was optimal in high salt concentrations, which alone can cause SDS-like symptoms (Pantalone et al., 1997). The solubility of FvTox1 and FvNIS1 did not appear to be affected by the buffer exchange process, though yield did decrease slightly (Fig.

7-8). However, none of the three de-salted protein constructs tested were sufficient to produce SDS-like symptoms, while all high-salt conditions did induce significant chlorosis (Fig. 7-9).

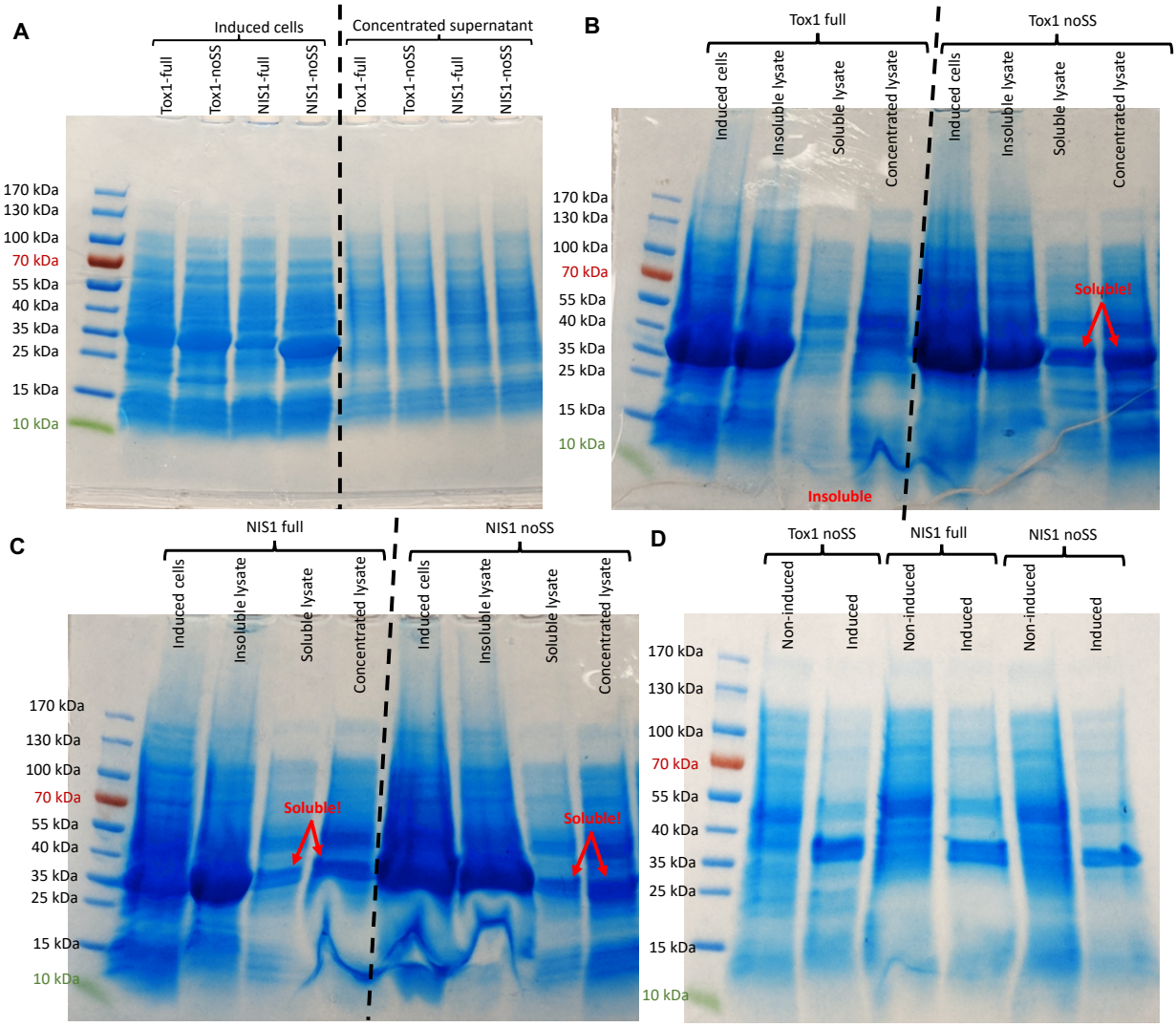

Figure 7-6. Gel electrophoresis of protein extracted from IPTG-induced *E. coli* cells transformed with pET11-b plasmids. In sodium phosphate buffer, none of the four proteins of interest were soluble (A). In HEPES buffer, Tox1 lacking the secretion signal (noSS) was soluble (B), as were both FvNIS1 constructs (C). Production of these three soluble proteins were specifically observed after the addition of the inducer, IPTG (D).

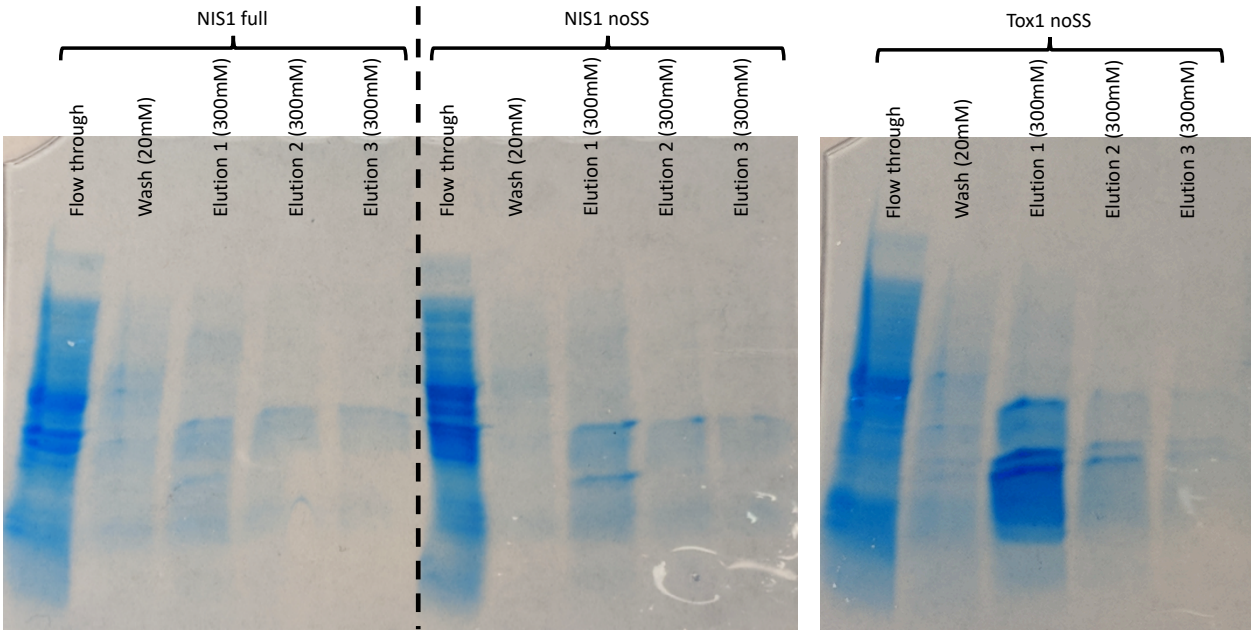

Figure 7-7. Gel electrophoresis of protein samples after purification via affinity chromatography. The "flow through" lane shows proteins that had no affinity to the column and went straight through the column. The "Wash 20 mM" lane shows proteins that had non-specific interaction with the column and were washed away in the presence of 20 mM imidazole. The "Elution 300 mM" lanes show three consecutive washes of the column with 2 mL of wash buffer containing 300 mM imidazole which releases proteins that had strong interactions with the column (i.e. 6X-HIS-tagged constructs and other proteins with strong positive charges).

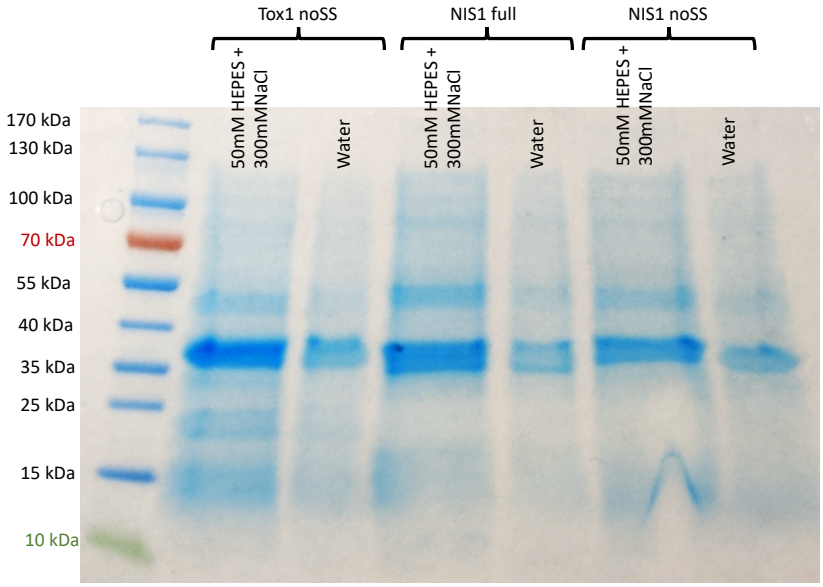

Figure 7-8. Gel electrophoresis of protein samples extracted from IPTG-induced *E. coli* cells and after exchange into water (de-salting). These protein samples were used in functional stem-cut assays.

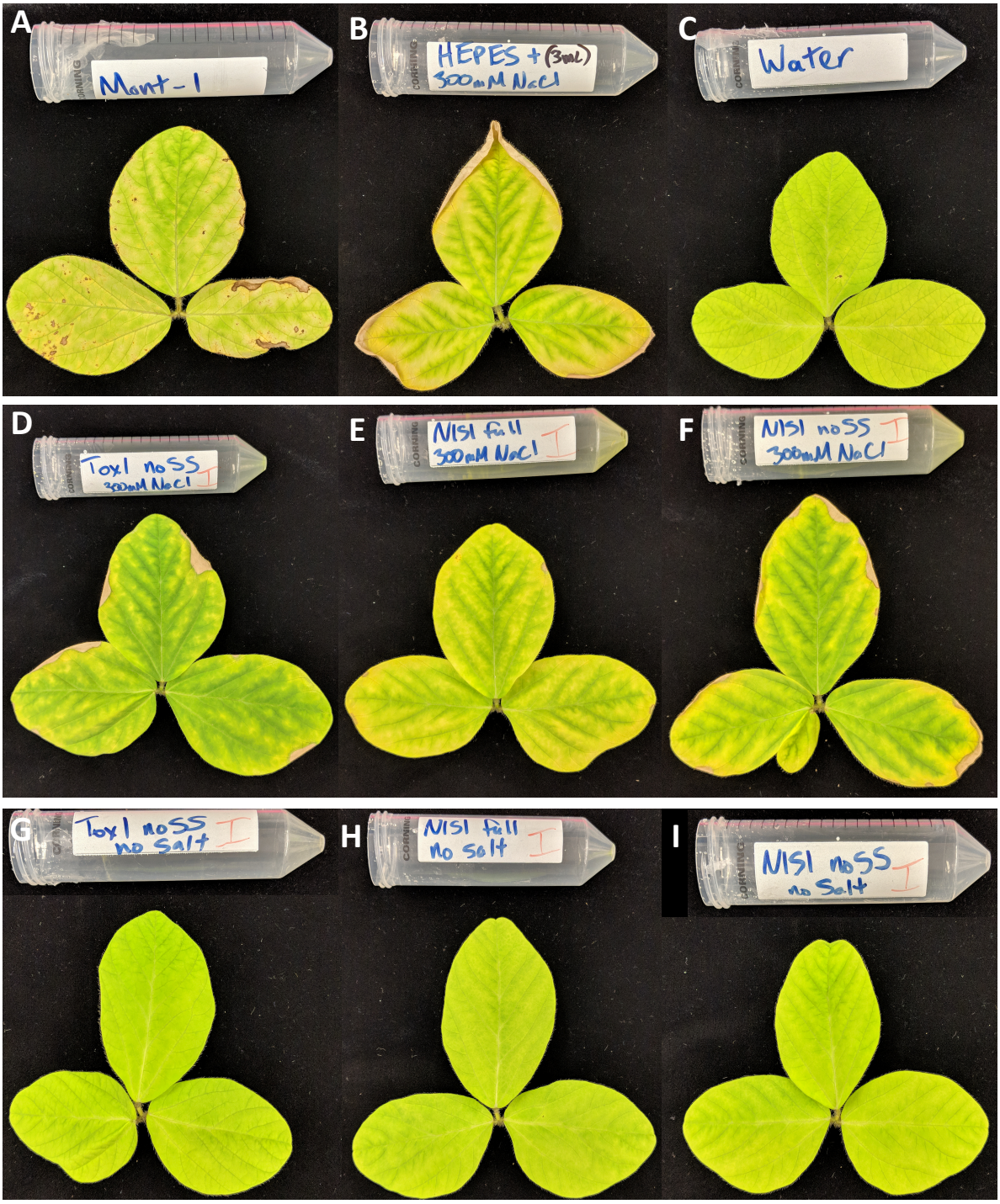

Figure 7-9. Soybean trifoliate leaves 7 days after inoculation with protein samples in stem-cut assays. "Mont-1" is the culture filtrate positive control, while "HEPES + 300 mM NaCl" and "Water" were other controls. Any protein sample containing 300 mM NaCl showed interveinal chlorosis and some necrosis along the leaf edges. De-salted protein samples did not induce significant chlorosis or necrosis, similar to the water negative control.

Transient expression in Nicotiana

Seven days after infiltration, obvious signs of chlorosis and necrosis were present in *AvrRpt2* and *FvNIS1* infiltrated regions of *N. benthamiana* leaves (Fig. 7-10 A). In contrast, very faint chlorosis was observed in some *FvTox1* infiltrations, but not all (Fig. 7-10). No symptoms were observed in buffer-infiltrated regions (Fig. 7-10). The development of HR symptoms in FvNIS1-infiltrated leaves suggested specific interactions with host proteins that trigger programmed cell death. Interestingly, *FvTox1* was able to induce chlorosis in *N. tabacum*. Co-IP experiments failed to purify any HIS-tagged FvTox1 or FvNIS1 from *N. benthamiana* using nickel based magnetic beads (Fig. 7-11 A) or anti-HIS antibodies and protein A magnetic beads (Fig. 7-11 B). Specific FvTox1 and FvNIS1 interacting proteins were not identified.

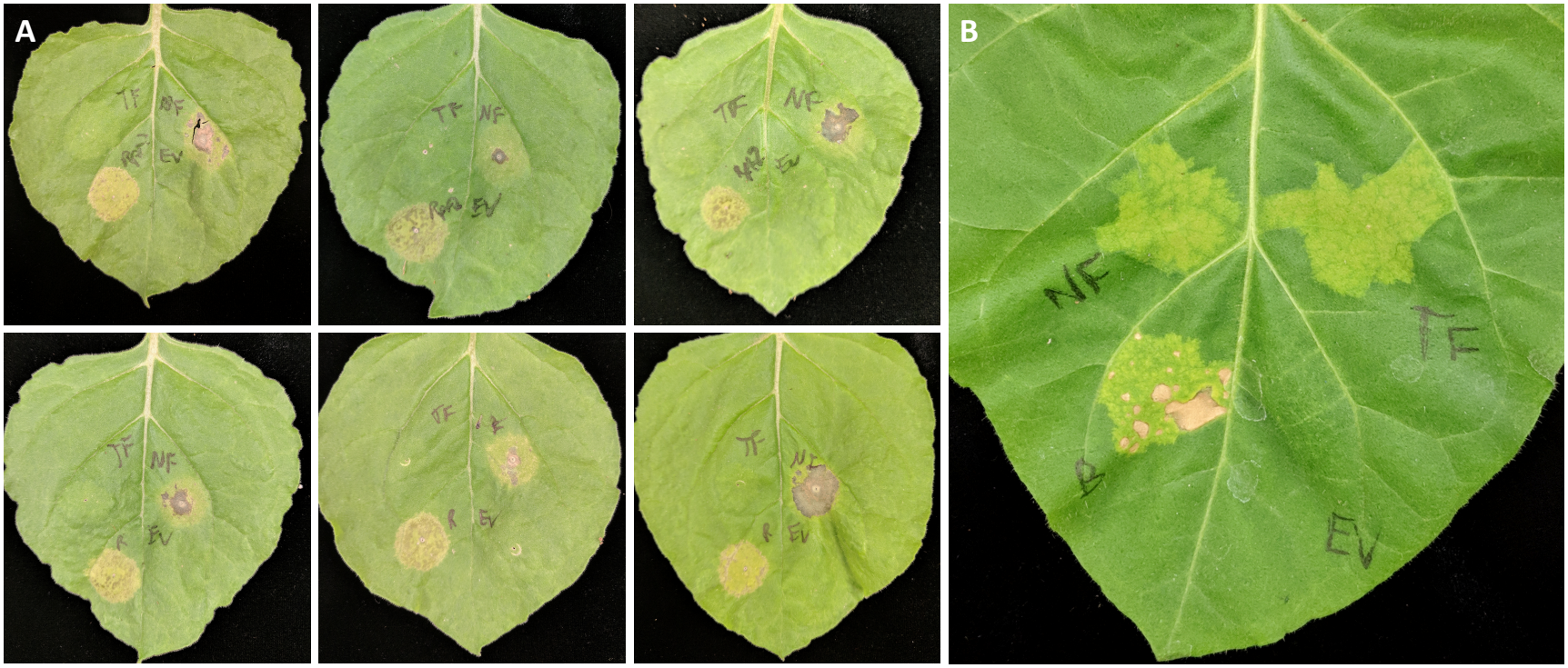

Figure 7-10. Tobacco leaves infiltrated with *Agrobacterium tumefaciens* strain GV3101. (**A**) Six leaf replicates from three *N. benthamiana* plants infiltrated with full-length FvTox1 (upper left), full-length FvNIS1 (upper right), AvrRpt2 (bottom left) or empty vector (bottom right), 10 days after infiltration. Chlorosis and spots of necrosis are frequently observed in AvrRpt2 and FvNIS1 infiltrated leaves, while no symptoms are consistently observed in FvTox1 and empty vector infiltrations. (**B**) One leaf of *N. tabacum* infiltrated with the same constructs as in (**A**), except with AvrB replacing AvrRpt2. In *N. tabacum*, FvTox1 does cause chlorosis.

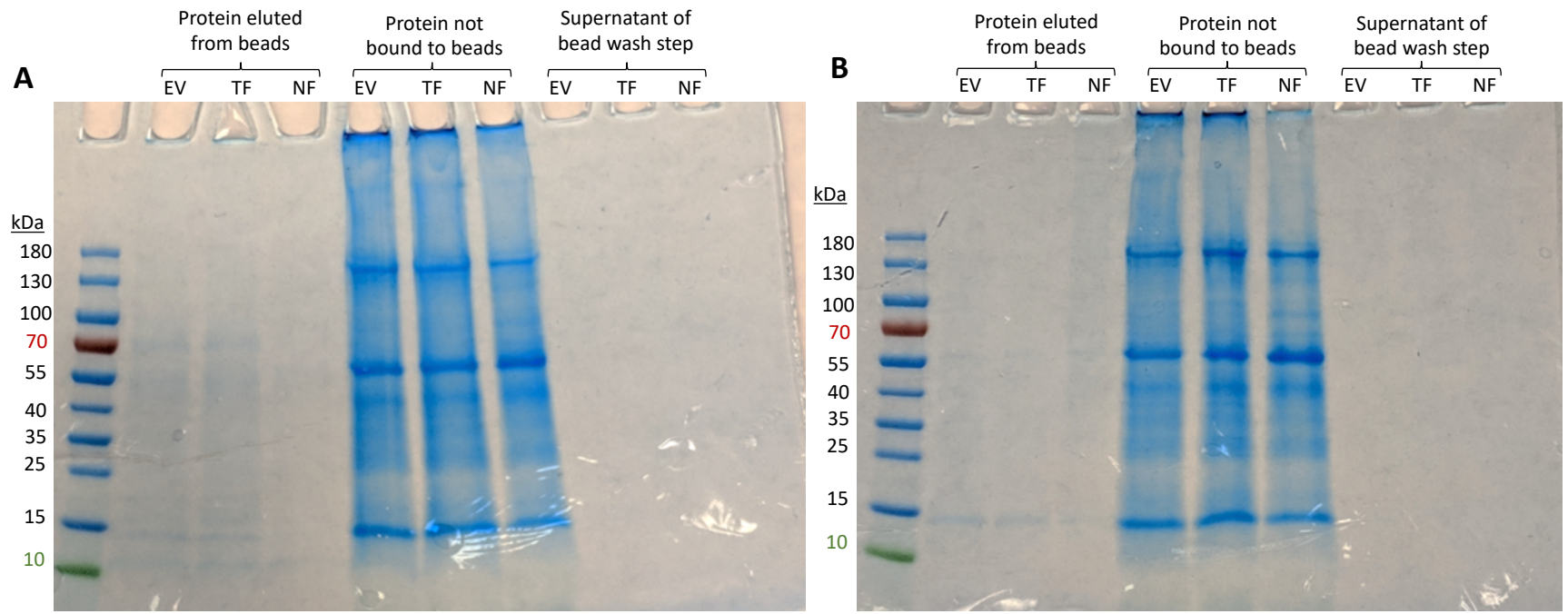

Figure 7-11. Co-immunoprecipitation (co-IP) of proteins 48 hours post *A. tumefaciens* infiltration of *N. benthamiana* leaves. (**A**) Co-IP using nickel-based magnetic beads, which have an affinity for 6X-HIS tags. (**B**) Co-IP using anti-6X-HIS antibody and protein A magnetic beads. In both co-IP experiments, protein samples from empty vector (EV), FvTox1 (TF), and FvNIS1 (NF) are identical, indicating a lack of FvTox1 or FvNIS1 expression.

Discussion

Fusarium virguliforme can infect at least 15 common plants as asymptomatic hosts yet SDS-symptoms remain specific to soybean (Kolander et al., 2012). There are multiple mechanisms by which these alternate hosts may evade the FvTox1 chlorosis inducing functions. First, it is possible that some *F. virguliforme* effectors are not expressed in other hosts, or expression is suppressed by alternate hosts. Second, effectors might be expressed in alternate hosts, but *F. virguliforme* is not able to penetrate to the xylem tissue in other hosts and release effectors as it does in soybean (Abeysekara and Bhattacharyya 2014; Navi and Yang 2008). Third, effectors could be degraded by enzymes in the xylem of non-soybean hosts. Finally, effectors may enter xylem and reach foliar tissues in alternate hosts, but their targets could be absent or highly diverged, rendering the effectors ineffective.

Multiple methods to produce large concentrations of FvTox1 and FvNIS1 were explored. Though *P. pastoris* and *E. coli* have been used in multiple heterologous expression experiments (Demain and Vaishnav, 2009; Kemen et al., 2005; Lacerda et al., 2016; Liu et al., 2016), neither system was highly productive for these two proteins. *Pichia pastoris* failed to produce any detectable protein (Fig. 7-2). Western blots are more sensitive than Coomassie staining, but western blots were not performed in this study. The *Pichia* strains in this study contained the native *AOX1* gene (Fig. 7-1), which are known as "Mut^{+}" strains, as opposed to the "Mut^{S}" strains where *AOX1* is replaced by the gene of interest. "Mut^{S}" strains grow much slower, but are known to produce significantly more protein of interest than Mut^{+} strains and could explain the low protein production (Pichia Expression Kit User Guide 2014). It has also been suggested that FvTox1 and FvNIS1 effectors may be toxic to *Pichia*, which might explain a lack of production (J. Walton, *personal communication*). *Escherichia coli* was able to produce heterologous protein

detectable through Coomassie staining, but purification methods were insufficient and resulted in very low yields. True protein quantification with Bradford assays were not performed, so the amount of protein that soybeans were exposed to in stem-cut assays is unclear (Fig. 7-8, Fig. 7-9). Therefore, there are two possible explanations for the lack of SDS-like symptoms in the stem-cut assays. First, FvTox1 and FvNIS1 may be insufficient to produce SDS-like symptoms independently. Second, the protein concentration used in this study may not have been high enough to mimic the levels produced during an active *F. virguliforme* infection of a soybean. Repeated experiments with a higher range of protein concentrations could reveal if FvTox1 and FvNIS1 are sufficient to produce SDS-like symptoms.

The *Pseudomonas syringae* effectors AvrRpt2 and AvrB induce HR in *Nicotiana benthamiana* (Bisgrove et al., 2007; Mackey et al., 2002; Kessens et al., 2014). Both do so by altering the state of RIN4, through either phosphorylation or degradation of RIN4, which is recognized by RPM1 and RPS2 respectively (Axtell et al., 2003; Axtell and Staskawicz, 2003; Mackey et al., 2002, 2003). However, many plant pathogen effectors have unknown targets and are not known to alter RIN4. Instead, recently identified leucine-rich repeat (LRR) receptor-like proteins have been implicated in recognizing effector function, though classical genetic evidence is still lacking (Swaminathan et al., 2019). The development of HR in FvNIS1 infiltrated leaves indicates that FvNIS1 interacts with or alters a specific host protein, perhaps a LRR containing receptor that triggers an immune response. An NIS1 ortholog in *Colletotrichum orbiculare* was also shown to trigger HR in *Nicotiana*, with NIS1-induced HR suppressed by *C. gloeosporioides* protein DN3 (Yoshino et al., 2012). In addition, full-length *CgNIS1* was required to induce HR in tobacco, while CgNIS1 lacking the secretion signal failed to induce HR (Yoshino et al., 2012). Infiltration of *FvTox1* constructs failed to produce reproducible chlorosis or necrosis in *N.*

benthamiana. This result is in contrast to previous findings that showed FvTox1 protein expressed from insect cell lines were able to cause two-fold reduction in chlorophyll in soybean leaf discs (Brar et al., 2011). However, FvTox1 did show chlorosis in *N. tabacum* leaves. This difference suggests that FvTox1 functions with a specific mode of action rather than a general toxicity, where the specific target is present in *N. tabacum* and absent in *N. benthamiana*. These results indicate that the target of FvNIS1 may be conserved between soybean, *N. benthamiana*, and *N. tabacum*, while the target of FvTox1 may be conserved only between soybean and *N. tabacum*.

Fusarium virguliforme is generally considered a hemibiotrophic pathogen, infecting living tissue and also persisting in dead tissue. In addition, *F. virguliforme* is quite a successful saprophyte, able to grow on water agar (data not shown), overwinter in corn and soybean residue (Navi and Yang 2016), and colonize nematodes (Donald et al., 1993; McLean and Lawrence, 1995). Finally, some may argue that *F. virguliforme* is a necrotroph because it causes cell death throughout soybean plants; root and foliar necrosis (Hartman et al., 2015). The life strategy of *F. virguliforme* is appears to transition between hemi-biotrophic, saprotrophic, and necrotrophic, which makes it a challenge to understand what roles of FvTox1 and FvNIS1 play during the host-pathogen interaction. To invade living root tissue, biotrophic pathogens release effectors to dampen plant immune signaling. To feed on dead tissues, necrotrophs purposefully induce cell death. Does *F. virguliforme* release these effectors to purposefully kill soybean plants and feed off the dead tissues in the soil? Does *F. virguliforme* release the effectors to thrive in the root system undetected, eventually causing the plant to succumb to the disease? Until a mechanistic understanding of FvTox1 and FvNIS1 exists, these questions will remain unanswered.

Acknowledgements

The authors would like to thank H.-X. Chang, J. Walton, L. Danhoff, and J. MacCready for helpful suggestions regarding heterologous expression of proteins, protein purification, and *Agrobacterium* infiltration. This work was funded in part by the Michigan Soybean Promotion Committee, the United Soybean Board, the North Central Soybean Research Program, and the Syngenta Agricultural Scholarship.

APPENDIX

APPENDIX

A list of additional manuscripts published or prepared for publication.

Kuhlgert, S., Austic, G., Zegarac, R., Osei-Bonsu, I., Hoh, D., Chilvers, M.I., **Roth, M.G.**, Bi, K., TerAvest, D., Weebadde, P., Kramer, D.M. 2016. MultispeQ Beta: a tool for large-scale plant phenotyping connected to the open PhotosynQ network. Royal Society Open Science. DOI 10.1098/rsos.160592.

All authors made substantial intellectual contributions to the work in this paper. S.K., G.A., R.Z., K.B., P.W. and D.M.K. contributed to the design, testing, programming and construction of the platform. All authors contributed to the design and implementation of the experiments. S.K., G.A., D.T., M.I.C. and D.M.K. contributed to the interpretation and analyses of the data.

Chang, H.-X., **Roth, M.G.**, Wang, D., Lightfoot, D.A., Hartman, G.L., Cianzio, S.R., Chilvers, M.I. 2018. Integration of Sudden Death Syndrome Resistance Loci in the Soybean Genome. Theoretical and Applied Genetics. https://doi.org/10.1007/s00122-018-3063-0.

HXC integrated the literature, presented the data, drafted and wrote the manuscript. MGR reviewed the data and contributed to the manuscript. DW, SRC, DAL, GLH, and MIC reviewed and contributed to the manuscript.

Wang, J., Jacobs, J.L., **Roth, M.G.**, Chilvers, M.I. 2018. Temporal dynamics of *Fusarium virguliforme* colonization of soybean roots. Plant Disease. https://doi.org/10.1094/PDIS-03-18-0384-RE.

JW, JLJ, and MGR collected and processed data. JW analyzed data, generated figures, and drafted the manuscript. JW, JLJ, MGR, and MIC contributed to the manuscript content.

Sang, H., Witte, A., Jacobs, J.L., Chang, H.-X., Wang, J., **Roth, M.G.**, and Chilvers, M.I. 2018. Fluopyram sensitivity and functional characterization of SdhB in the *Fusarium solani* species complex causing soybean sudden death syndrome. Frontiers in Microbiology. DOI 10.3389/fmicb.2018.02335.

HS, AW, JJ, H-XC, and MIC designed the research. HS and AW performed the experiments and analyzed the data. JJ, JW, H-XC, and MGR provided input on the experiments. HS and MIC wrote the manuscript. AW, JJ, JW, H-XC, and MGR edited the manuscript.

Strock, C.F., Schneider, H.M., Galindo-Castañeda, T., Hall, B.T., Van Gansbeke, B., Mather, D.E., **Roth, M.G.**, Chilvers, M.I., Guo, X., Brown, K., and Lynch, J.P. Laser Ablation Tomography for Visualization of Root Colonization by Edaphic Organisms. Journal of Experimental Botany. *Submitted 11/14/18*.

Conceived the idea: JPL. Designed the experiments: CFS, TGC, KMB and JPL. Conducted experiments and collected data: CFS, TGC, XG, HMS. Analyzed data: CFS. Interpreted data: CFS, HMS, TCG, BVG, DEM, MR, MC. Wrote the manuscript: CFS, HMS and TGC with participation of JPL, KMB, BTH, BVG, DEM, MR, MC, XG.

Roth, M.G., Sang, H., Oudman, K., Jacobs, J.L., Griffin, A., and Chilvers, M.I. Diagnostic qPCR Assay to Detect *Fusarium brasiliense*, a causal agent of soybean Sudden Death Syndrome and Root Rot of Dry Bean. Plant Disease. *Accepted 2/27/19.*

MGR, JLJ, and MIC formalized the objectives of the project. MGR designed primers, probes, and reaction conditions. MGR, KAO, AG, and HS used and validated the method. MGR analyzed data and generated figures. MGR and MIC wrote the manuscript.

*McCoy, A.G., ***Roth, M.G.**, *Shay, R., *Noel, Z.A., Jayawardana, M.A., Longley, R.W., Bonito, G., and Chilvers, M.I. Next Generation Sequencing Identification of Fungal Communities Within the Tar Spot Complex of Corn in Michigan. Phytobiomes. *Submitted 3/9/19*.

AGM, MGR, RS, MAJ, GB, and MIC planned experiments. AGM, MGR, RS, and MAJ and collected and processed samples. RWL performed PCR and constructed libraries. AGM submitted raw sequences to Sequence Read Archives. MGR and ZAN analyzed data and generated figures. AGM, RS, MGR, ZAN, and MAJ wrote the manuscript. * indicates co-first authors.

Roth, M. G. and Chilvers, M. I. A Protoplast Generation and Transformation Method for Soybean Sudden Death Syndrome Causal Agents *Fusarium virguliforme* and *F. brasiliense*. Fungal Biology and Biotechnology. *Accepted 4/21/19*.

MGR and MIC developed the ideas to generate this protocol. MGR designed primers and plasmids, performed the experiments, and acquired all images. MGR and MIC wrote and revised the manuscript, approving of the final draft.

Noel, Z.A., Sang, H., **Roth, M.G.**, and Chilvers, M.I. Convergent evolution of C239S mutation in *Pythium* spp. β-tubulin coincides with inherent insensitivity to ethaboxam. Phytopathology. *Submitted 4/5/19*.

ZAN and MIC outlined objectives for this project. ZAN performed all experiments, collected data, and analyzed data. HS and MGR provided insight and guidance for experimental procedures. ZAN wrote the manuscript with contributions from HS, MGR, and MIC.

Roth, M. G., Noel, Z. A., Wang, J. Warner, F. Byrne, A. M. and Chilvers, M. I. Predicting Soybean Yield and Sudden Death Syndrome Development using At-planting Risk Factors. Phytopathology. *Accepted 4/28/19*.

MGR, JW, and MIC designed the experiment, MGR, JW, FW, and AMB collected data, MGR and ZAN analyzed data and generated figures, MGR, ZAN, and MIC wrote the manuscript.

Roth, M.G., Jacobs, J.L., Napieralski, S., Byrne, A.M., Warner. F., Chilvers, M.I. Effect of Fluopyram on *Heterodera glycines* development in Soybean. *Submitted 4/29/19.*

AMB and MIC formalized the objectives of this project. JLJ, SN, AMB, and FW performed all experiments and collected all data. MGR analyzed all data and wrote the manuscript, with contributions from JLJ, SN, AMB, FW, and MIC.

REFERENCES

REFERENCES

Abeysekara, N. S., and Bhattacharyya, M. K. 2014. Analyses of the xylem sap proteomes identified candidate *Fusarium virguliforme* proteinacious toxins. PLoS One. 9:e93667.

Abeysekara, N. S., Swaminathan, S., Desai, N., Guo, L., and Bhattacharyya, M. K. 2016. The plant immunity inducer pipecolic acid accumulates in the xylem sap and leaves of soybean seedlings following *Fusarium virguliforme* infection. Plant Sci. 243:105–114.

Ahmed, D., and Shahab, S. 2018. Studies on interaction of *Meloidogyne incognita* (Kofoid and White) Chitwood and *Fusarium solani* (Mart.) Sacc forming a disease complex in lentil (*Lens culinaris* Medik.). Arch. Phytopathol. Plant Prot. 51:338–348.

Albuquerque, P., and Casadevall, A. 2012. Quorum sensing in fungi - a review. Med. Mycol. 50:337–345.

Alexander, D. L. J., Tropsha, A., and Winkler, D. A. Beware of R^2: simple, unambiguous assessment of the prediction accuracy of QSAR and QSPR models. J. Chem. Inf. Model. 55:1316-1322.

Allen, T. W., Bradley, C. A., Sisson, A. J., Byamukama, E., Chilvers, M. I., Coker, C. M., Collins, A. A., Damicone, J. P., Dorrance, A. E., Dufault, N. S., Esker, P. D., Faske, T. R., Giesler, L. J., Grybauskas, A. P., Hershman, D. E., Hollier, C. A., Isakeit, T., Jardine, D. J., Kelly, H. M., Kemerait, R. C., Kleczewski, N. M., Koenning, S. R., Kurle, J. E., Malvick, D. K., Markell, S. G., Mehl, H. L., Mueller, D. S., Mueller, J. D., Mulrooney, R. P., Nelson, B. D., Newman, M. A., Osborne, L., Overstreet, C., Padgett, G. B., Phipps, P. M., Price, P. P., Sikora, E. J., Smith, D. L., Spurlock, T. N., Tande, C. A., Tenuta, A. U., Wise, K. A., and Wrather, J. A. 2017. Soybean yield loss estimates due to diseases in the United States and Ontario, Canada, from 2010 to 2014. Plant Heal. Prog. 18:19–27.

Alston, D. G., and Schmitt, D. P. 1988. Development of *Heterodera glycines* life stages as influenced by temperature. J. Nematol. 20:366–72.

Anand, S. C., Matson, K. W., and Sharma, S. B. 1995. Effect of soil temperature and pH on resistance of soybean to *Heterodera glycines*. J. Nematol. 27:478–482.

Antico, C.J., Colon, C., Banks, T., and Ramonell, K.M. 2012. Insights into the role of jasmonic acid-mediated defenses against necrotrophic and biotrophic fungal pathogens. Front. Biol. 7: 48-56.

Aoki, T., O'Donnell, K., and Geiser, D. M. 2014. Systematics of key phytopathogenic *Fusarium* species: current status and future challenges. J. Gen. Plant Pathol. 80:189–201.

Aoki, T., O'Donnell, K., and Scandiani, M. M. 2005. Sudden death syndrome of soybean in South America is caused by four species of *Fusarium*: *Fusarium brasiliense* sp. nov., *F cuneirosrum* sp. nov., *F. tucumaniae*, and *F. virguliforme*. Mycoscience. 46:162–183.

Aoki, T., O'Donnell, K., Homma, Y., and Lattanzi, A. R. 2003. Sudden-death syndrome of soybean is caused by two morphologically and phylogenetically distinct species within the *Fusarium solani* species complex - *F. virguliforme* in North America and *F. tucumaniae* in South America. Mycologia. 95:660–684.

Aoki, T., Scandiani, M. M., and O'Donnell, K. 2012a. Phenotypic, molecular phylogenetic, and pathogenetic characterization of *Fusarium crassistipitatum* sp. nov., a novel soybean sudden death syndrome pathogen from Argentina and Brazil. Mycoscience. 53:167–186.

Aoki, T., Tanaka, F., Suga, H., Hyakumachi, M., Scandiani, M. M., and O'Donnell, K. 2012b. *Fusarium azukicola* sp. nov., an exotic azuki bean root-rot pathogen in Hokkaido, Japan. Mycologia. 104:1068–1084.

Armenteros, J. J. A., Tsirigos, K. D., Sønderby, C. K., Petersen, T. N., Winther, O., Brunak, S., von Heijne, G., and Nielsen, H. 2019. SignalP 5.0 improves signal peptide predictions using deep neural networks. Nat. Biotechnol. 37:420–423.

Avery, L., and You, Y.-J. 2005. *C. elegans* feeding. In WormBook: The online review of *C. elegans* biology, Pasadena, CA. https://www.ncbi.nlm.nih.gov/books/NBK116080/.

Axtell, M. J., and Staskawicz, B. J. 2003. Initiation of RPS2-specified disease resistance in *Arabidopsis* is coupled to the AvrRpt2-directed elimination of RIN4. Cell. 112:369–377.

Axtell, M. J., Chisholm, S. T., Dahlbeck, D., and Staskawicz, B. J. 2003. Genetic and molecular evidence that the *Pseudomonas syringae* type III effector protein AvrRpt2 is a cysteine protease. Mol. Microbiol. 49:1537–1546.

Back, M. A., Haydock, P. P. J., and Jenkinson, P. 2002. Disease complexes involving plant parasitic nematodes and soilborne pathogens. Plant Pathol. 51:683–697.

Backholm, M., Ryu, W. S., and Dalnoki-Veress, K. 2013. Viscoelastic properties of the nematode *Caenorhabditis elegans*, a self-similar, shear-thinning worm. Proc. Natl. Acad. Sci. 110:4528–4533.

Bajwa, S. G., Rupe, J. C., and Mason, J. 2017. Soybean disease monitoring with leaf reflectance. Remote Sens. 9:1–14.

Baker, S. E., Kroken, S., Inderbitzin, P., Asvarak, T., Li, B., Shi, L., Yoder, O. C., and Turgeon, B. G. 2006. Two polyketide synthase-encoding genes are required for biosynthesis of the polyketide virulence factor, T-toxin, by *Cochliobolus heterostrophus*. Mol. Plant-Microbe Interact. 19:139–149.

Bez, N. 2000. On the use of Lloyd's index of patchiness. Fish. Oceanogr. 9:372–376

Biere, A., and Goverse, A. 2016. Plant-mediated systemic interactions between pathogens, parasitic nematodes, and herbivores above- and belowground. Annu. Rev. Phytopathol. 54:499–527.

Bisgrove, S. R., Simonich, M. T., Smith, N. M., Sattler, A., and Innes, R. W. 2007. A disease resistance gene in *Arabidopsis* with specificity for two different pathogen avirulence genes. Plant Cell. 6:927–933.

Bluhm, B. H., Zhao, X., Flaherty, J. E., Xu, J.-R., and Dunkle, L. D. 2007. RAS2 regulates growth and pathogenesis in *Fusarium graminearum*. Mol. Plant-Microbe Interact. 20:627–636.

Boenisch, M. J., and Schäfer, W. 2011. *Fusarium graminearum* forms mycotoxin producing infection structures on wheat. BMC Plant Biol. 11:110.

Brar, H. K., and Bhattacharyya, M. K. 2012. Expression of a single-chain variable-fragment antibody against a *Fusarium virguliforme* toxin peptide enhances tolerance to sudden death syndrome in transgenic soybean plants. Mol. Plant-Microbe Interact. 25:817–824.

Brar, H. K., Swaminathan, S., and Bhattacharyya, M. K. 2011. The *Fusarium virguliforme* toxin FvTox1 causes foliar sudden death syndrome-like symptoms in soybean. Mol. Plant-Microbe Interact. 24:1179–88.

Bray, R. J., and Curtis J. T. 1957. An ordination of the upland forest communities of southern Wisconsin. Ecol. Monogr. 27:4 325-349.

Brzostowski, L. F., Schapaugh, W. T., Rzodkiewicz, P. A., Todd, T. C., and Little, C. R. 2014. Effect of host resistance to *Fusarium virguliforme* and *Heterodera glycines* on sudden death syndrome disease severity and soybean yield. Plant Heal. Prog. 15:1–8.

Cabanettes, F., and Klopp, C. 2018. D-GENIES: dot plot large genomes in an interactive, efficient and simple way. PeerJ. 6:e4958.

Carroll, A. M., Sweigard, J. A., and Valent, B. 1994. Improved vectors for selecting resistance to hygromycin. Fungal Genet. Newsl. 41:22.

Catlett, N. L., Lee, B.-N., Yoder, O. C., and Turgeon, B. G. 2003. Split-marker recombination for efficient targeted deletion of fungal genes. Fungal Genet. Newsl. 50:9–11.

Chang, H.-X., Domier, L. L., Radwan, O., Yendrek, C. R., Hudson, M. E., and Hartman, G. L. 2016a. Identification of multiple phytotoxins produced by *Fusarium virguliforme* including a phytotoxic effector (FvNIS1) associated with sudden death syndrome foliar symptoms. Mol. Plant-Microbe Interact. 29:96–108.

Chang, H.-X., Yendrek, C. R., Caetano-Anolles, G., and Hartman, G. L. 2016b. Genomic characterization of plant cell wall degrading enzymes and *in silico* analysis of xylanases and polygalacturonases of *Fusarium virguliforme*. BMC Microbiol. 16:1–12.

Chang, H.-X., Roth, M. G., Wang, D., Cianzio, S. R., Lightfoot, D. A., Hartman, G. L., and Chilvers, M. I. 2018. Integration of sudden death syndrome resistance loci in the soybean genome. Theor. Appl. Genet. 131:757-773.

Chitrampalam, P., and Nelson, B. 2016. Multilocus phylogeny reveals an association of agriculturally important *Fusarium solani* species complex (FSSC) 11, and clinically important FSSC 5 and FSSC 3 + 4 with soybean roots in the north central United States. Antonie van Leeuwenhoek, Int. J. Gen. Mol. Microbiol. 109:335–347.

Ciuffetti, L. M., Manning, V. A., Pandelova, I., Betts, M. F., and Martinez, J. P. 2010. Host-selective toxins, Ptr ToxA and Ptr ToxB, as necrotrophic effectors in the *Pyrenophora tritici-repentis*-wheat interaction. New Phytol. 187:911–919.

Coleman, J. J. 2016. The *Fusarium solani* species complex: Ubiquitous pathogens of agricultural importance. Mol. Plant Pathol. 17:146–158.

Cuomo, C. A., Güldener, U., Xu, J.-R., Trail, F., Turgeon, B. G., Pietro, A. D., Walton, J. D., Ma, L.-J., Baker, S. E., Rep, M., Adam, G., Antoniw, J., Baldwin, T., Calvo, S., Chang, Y.-L., DeCaprio, D., Gale, L. R., Gnerre, S., Goswami, R. S., Hammond-Kosack, K., Harris, L. J., Hilburn, K., Kennell, J. C., Kroken, S., Magnuson, J. k, Mannhaupt, G., Mauceli, E., Mewes, H.-W., Mitterbauer, R., Muehlbauer, G., Münsterkötter, M., Nelson, D., O'Donnell, K., Ouellet, T., Qi, W., Quesneville, H., Roncero, M. I. G., Seong, K.-Y., Tetko, I. V, Urban, M., Cees, W., Ward, T. J., Yao, J., Birren, B. W., and Kistler, H. C. 2007. The *Fusarium graminearum* genome reveals a link between localized polymorphism and pathogen specialization. Science. 317:1400–1402.

Czymmek, K. J., Fogg, M., Powell, D. H., Sweigard, J., Park, S. Y., and Kang, S. 2007. *In vivo* time-lapse documentation using confocal and multi-photon microscopy reveals the mechanisms of invasion into the *Arabidopsis* root vascular system by *Fusarium oxysporum*. Fungal Genet. Biol. 44:1011–1023.

Davis, E. L., and Tylka, G. L. 2005. Soybean cyst nematode disease. Plant Heal. Instr. DOI: 10.1094/PHI-I-2000-0725-01

de Farias Neto, A. L., Hashmi, R., Schmidt, M., Carlson, S. R., Hartman, G. L., Li, S., Nelson, R. L., and Diers, B. W. 2007. Mapping and confirmation of a new sudden death syndrome resistance QTL on linkage group D2 from the soybean genotypes PI 567374 and "Ripley." Mol. Breed. 20:53–62.

De Loof, A., Marchal, E., Rivera-Perez, C., Noriega, F. G., and Schoofs, L. 2015. Farnesol-like endogenous sesquiterpenoids in vertebrates: The probable but overlooked functional

"inbrome" anti-aging counterpart of juvenile hormone of insects? Front. Endocrinol. (Lausanne). 5:1–10.

Del Ponte, E. M., Godoy, C. V., Li, X., and Yang, X. B. 2006. Predicting severity of Asian soybean rust epidemics with empirical rainfall models. Phytopathology. 96:797–803.

Demain, A. L., and Vaishnav, P. 2009. Production of recombinant proteins by microbes and higher organisms. Biotechnol. Adv. 3:297–306.

Diaz Arias, M. M. 2012. *Fusarium* species infecting soybean roots: Frequency, aggressiveness, yield impact and interaction with the soybean cyst nematode. Graduate Theses and Dissertations. Paper 12314.

Donald, P. A., Niblack, T. L., and Wrather, J. A. 1993. First report of *Fusarium solani* blue isolate, a causal agent of sudden death syndrome of soybeans, recovered from soybean cyst nematode eggs. Plant Dis. 77:647.

Endo, B. Y. 1986. Histology and ultrastructural modification induced by cyst nematodes. In Cyst Nematodes, New York: Plenum Press. ISBN: 978-1-4613-2251-1

Epskamp, S. 2017. semPlot: Path diagrams and visual analysis of various SEM packages' output. Available at: https://CRAN.R-project.org/package=semPlot.

Faith, D. P., Minchin, P. R., Belbin, L. 1987. Compositional dissimilarity as a robust measure of ecological distance. Vegetatio. 69:57-68.

Fehr, W. R., Caviness, C. E., Burmood, D. T., and S., P. J. 1971. Stage of development description for soybeans, *Glycine max* (L.) Merrill. Crop Sci. 11:929–931.

Flor, H. H. 1946. Genetics of pathogenicity in Melampsora lini. J. Agric. Res. 73:335–357.

Flor, H. H. 1971. Current status of the gene-for-gene concept. Annu. Rev. Phytopathol. 9:275–296.

Freed, G. M., Floyd, C. M., and Malvick, D. K. 2017. Effects of pathogen population levels and crop-derived nutrients on development of soybean sudden death syndrome and growth of *Fusarium virguliforme*. Plant Dis. 101:434–441.

Gaffoor, I., Brown, D. W., Plattner, R., Proctor, R. H., Qi, W., and Trail, F. 2005. Functional analysis of the polyketide synthase genes in the filamentous fungus *Gibberella zeae* (anamorph *Fusarium graminearum*). Eukaryot. Cell. 4:1926–1933.

Gao, X., Jackson, T. A., Hartman, G. L., and Niblack, T. L. 2006. Interactions between the soybean cyst nematode and *Fusarium solani* f. sp. *glycines* based on greenhouse factorial experiments. Phytopathology. 96:1409–15.

Gaspar, A. P., Mueller, D. S., Wise, K. A., Chilvers, M. I., Tenuta, A. U., and Conley, S. P. 2017. Response of broad-spectrum and target-specific seed treatments and seeding rate on soybean seed yield, profitability, and economic risk. Crop Sci. 57:1–12.

Gibson, D. G., Young, L., Chuang, R.-Y., Venter, J. C., Hutchison III, C. A., and Smith, H. O. 2009. Enzymatic assembly of DNA molecules up to several hundred kilobases. Nat. Methods. 6:343–345.

Giraldo, M. C., and Valent, B. 2013. Filamentous plant pathogen effectors in action. Nat. Rev. Microbiol. 11:800–814.

Golbraikh, A., and Tropsha, A. Beware of q2! J. Mol. Graph. Model. 20:269-276.

Gongora-Canul, C. C., and Leandro, L. F. S. 2011. Effect of soil temperature and plant age at time of inoculation on progress of root rot and foliar symptoms of soybean sudden death syndrome. Plant Dis. 95:436–440.

Gurevich, A., Saveliev, V., Vyahhi, N., and Tesler, G. 2013. QUAST: quality assessment tool for genome assemblies. Bioinformatics. 29:1072–1075.

Hallen-Adams, H. E., Cavinder, B. L., and Trail, F. 2011. *Fusarium graminearum* from expression analysis to functional assays. In Fungal Genomics, eds. Jin-Rong Xu and Burton H Bluhm. Humana Press. ISBN: 978-1-61779-040-9.

Hartman, G. L., Chang, H.-X., and Leandro, L. F. 2015. Research advances and management of soybean sudden death syndrome. Crop Prot. 73:60–66.

Hershman, D. E., Hendrix, J. W., Stuckey, R. E., Bachi, P. R., and Henson, G. 1990. Influence of planting date and cultivar on soybean sudden death syndrome in Kentucky. Plant Dis. 74:761–766.

Hillnhütter, C., Albersmeier, A., Berdugo, C. A., and Sikora, R. A. 2011. Synergistic damage by interactions between *Ditylenchus dipsaci* and *Rhizoctonia solani* (AG 2-2IIIB) on sugar beet. J. Plant Dis. Prot. 118:127–133.

Hornby, J. M., Jensen, E. C., Lisec, A. D., Tasto, J. J., Shoemaker, R., Dussault, P., and Nickerson, K. W. 2001. Quorum sensing in the dimorphic fungus *Candida albicans* is mediated by farnesol. Appl. Environ. Microbiol. 67:2982–2992.

Howard, R. J., and Valent, B. 1996. Breaking and entering: Host penetration by the fungal rice blast pathogen *Magnaporthe grisea*. Annu. Rev. Microbiol. 50:491–512.

Howard, R. J., Ferrari, M. A., Roach, D. H., and Money, N. P. 1991. Penetration of hard substrates by a fungus employing enormous turgor pressures. Proc. Natl. Acad. Sci. 88:11281–11284.

Huang, X., Das, A., Sahu, B. B., Srivastava, S. K., Leandro, L. F., O'Donnell, K., and Bhattacharyya, M. K. 2016. Identification of highly variable supernumerary chromosome segments in an asexual pathogen. PLoS One. 11:e0158183.

Hughes, T. J., Kurtzweil, N. C., Diers, B. W., and Grau, C. R. 2004. Resistance to brown stem rot in soybean germ plasm with resistance to the soybean cyst nematode. Plant Dis. 88:761–768.

Hughes, T. J., O'Donnell, K., Sink, S., Rooney, A. P., Scandiani, M. M., Luque, A., Bhattacharyya, M. K., and Huang, X. 2014. Genetic architecture and evolution of the mating type locus in fusaria that cause soybean sudden death syndrome and bean root rot. Mycologia. 106:686–697.

Hussey, R. S., and Grundler, F. M. 1998. Nematode parasitism of plants. In Physiology and biochemistry of free-living and plant-parasitic nematodes, Oxford: CAB International Press. ISBN: 085199-231-5.

Islam, K. T., Bond, J. P., and Fakhoury, A. M. 2017a. FvSNF1, the sucrose non-fermenting protein kinase gene of *Fusarium virguliforme*, is required for cell-wall-degrading enzymes expression and sudden death syndrome development in soybean. Curr. Genet. 63:723–738.

Islam, K. T., Bond, J. P., and Fakhoury, A. M. 2017b. FvSTR1, a striatin orthologue in *Fusarium virguliforme*, is required for asexual development and virulence. Appl. Microbiol. Biotechnol. 101:6431–6445.

Ithal, N., Recknor, J., Nettleton, D., Hearne, L., Maier, T., Baum, T. J., and Mitchum, M. G. 2007a. Parallel genome-wide expression profiling of host and pathogen during soybean cyst nematode infection of soybean. Mol. Plant-Microbe Interact. 20:293–305.

Ithal, N., Recknor, J., Nettleton, D., Maier, T., Baum, T. J., and Mitchum, M. G. 2007b. Developmental transcript profiling of cyst nematode feeding cells in soybean roots. Mol. Plant-Microbe Interact. 20:510–525.

Ivanov, S., and Harrison, M. J. 2014. A set of fluorescent protein-based markers expressed from constitutive and arbuscular mycorrhiza-inducible promoters to label organelles, membranes and cytoskeletal elements in *Medicago truncatula*. Plant J. 80:1151–1163.

Jacobs, J. L., Oudman, K., Sang, H., and Chilvers, M. I. 2018. First report of *Fusarium brasiliense* causing root rot of dry bean in the United States. Plant Dis. 102:2035.

Jenkins, W. R. 1964. A rapid centrifugal-flotation technique for separating nematodes from soil. Plant Dis. Reports. 48:692.

Jeong, H., Lee, S., Choi, G. J., Lee, T., and Yun, S. H. 2013. Draft genome sequence of *Fusarium fujikuroi* B14, the causal agent of the bakanae disease of rice. Genome Announc. 1:e00035-13.

Ji, J., Scott, M. P., and Bhattacharyya, M. K. 2006. Light is essential for degradation of ribulose-1,5-bisphosphate carboxylase-oxygenase large subunit during sudden death syndrome development in soybean. Plant Biol. 8:597–605.

Jin, H., Hartman, G. L., Nickell, C. D., and Widholm, J. M. 1996a. Characterization and purification of a phytotoxin produced by *Fusarium solani*, the causal agent of soybean sudden death syndrome. Phytopathology. 86:277–282.

Jin, H., Hartman, G. L., Nickell, C. D., and Widholm, J. M. 1996b. Phytotoxicity of culture filtrate from *Fusarium solani*, the causal agent of sudden death syndrome of soybean. Plant Dis. 80:922–927.

Kandel, Y. R., Haudenshield, J. S., Srour, A. Y., Islam, K. T., Fakhoury, A. M., Santos, P., Wang, J., Chilvers, M. I., Hartman, G. L., Malvick, D. K., Floyd, C. M., Mueller, D. S., and Leandro, L. F. S. 2015. Multilaboratory comparison of quantitative PCR assays for detection and quantification of *Fusarium virguliforme* from soybean roots and soil. Phytopathology. 105:1601–1611.

Kandel, Y. R., Wise, K. A., Bradley, C. A., Chilvers, M. I., Tenuta, A. U., and Mueller, D. S. 2016. Fungicide and cultivar effects on sudden death syndrome and yield of soybean. Plant Dis. 100:1339–1350.

Kandel, Y. R., Wise, K. A., Bradley, C. A., Chilvers, M. I., Byrne, A. M., Tenuta, A. U., Faghihi, J., Wiggs, S. N., and Mueller, D. S. 2017. Effect of soybean cyst nematode resistance source and seed treatment on population densities of *Heterodera glycines*, sudden death syndrome, and yield of soybean. Plant Dis. 101:2137-2143.

Kandel, Y. R., Mueller, D. S., Legleiter, T., Johnson, W. G., Young, B. G., and Wise, K. A. 2018. Impact of fluopyram fungicide and preemergence herbicides on soybean injury, population, sudden death syndrome, and yield. Crop Prot. 106:103–109.

Kaur, S., Pham, Q. A., and Epstein, L. 2017. High quality DNA from *Fusarium oxysporum* conidia suitable for library preparation and long read sequencing with PacBio. DOI: dx.doi.org/10.17504/protocols.io.i8ichue.

Kazi, S., Shultz, J., Afzal, J., Johnson, J., Njiti, V. N., and Lightfoot, D. A. 2008. Separate loci underlie resistance to root infection and leaf scorch during soybean sudden death syndrome. Theor. Appl. Genet. 116:967–977.

Kemen, E., Hahn, M., Mendgen, K., Voegele, R. T., Hempel, U., Rafiqi, M., and Kemen, A. C. 2005. Identification of a protein from rust fungi transferred from haustoria into infected plant cells. Mol. Plant-Microbe Interact. 18:1130–1139.

Kessens, R., Ashfield, T., Kim, S. H., and Innes, R. W. 2014. Determining the GmRIN4 requirements of the soybean disease resistance proteins Rpg1b and Rpg1r using a *Nicotiana glutinosa*-based agroinfiltration system. PLoS One. 9:e108159.

Khan, M. W., and Pathak, K. N. 1993. Nematodes as vectors of bacterial and fungal plant pathogens. In Nematode Interactions, ed. M W Khan. Bury St Edmunds, p. 251–272. ISBN: 978-94-011-1488-2.

King, R., Urban, M., Hammond-Kosack, M. C. U., Hassani-Pak, K., and Hammond-Kosack, K. E. 2015. The completed genome sequence of the pathogenic ascomycete fungus *Fusarium graminearum*. BMC Genomics. 16:544.

Koenning, S. R., and Wrather, J. A. 2010. Suppression of soybean yield potential in the continental United States by plant diseases from 2006 to 2009. Plant Heal. Prog. DOI: 10.1094/PHP-2010-1122-01-RS.

Kolander, T. M., Bienapfl, J. C., Kurle, J. E., and Malvick, D. K. 2012. Symptomatic and asymptomatic host range of *Fusarium virguliforme*, the causal agent of soybean sudden death syndrome. Plant Dis. 96:1148–1153.

Kuhlgert, S., Austic, G., Zegarac, R., Osei-Bonsu, I., Hoh, D., Chilvers, M. I., Roth, M. G., Bi, K., TerAvest, D., Weebadde, P., and Kramer, D. M. 2016. MultispeQ Beta: a tool for large-scale plant phenotyping connected to the open PhotosynQ network. R. Soc. Open Sci. 3:160592.

Kuhn, M. 2018. caret: Classification and regression training. Available at: https://CRAN.R-project.org/package=caret.

Kuo, D., Nie, M., and Courey, A. J. 2014. SUMO as a solubility tag and *in vivo* cleavage of SUMO fusion proteins with Ulp1. In Protein Affinity Tags: Methods and Protocols, eds. Richard J Giannone and Andrew B Dykstra. New York, NY: Springer New York, p. 71–80.

Kutner, M. H., Nachtsheim, C. J., Neter, J., and Li, W. Multicollinearity and its effects. In: Applied Linear Statistical Models, 5th edition. p. 278-293.

Lacerda, A. F., Del Sarto, R. P., Silva, M. S., de Vasconcelos, E. A. R., Coelho, R. R., dos Santos, V. O., Godoy, C. V., Seixas, C. D. S., da Silva, M. C. M., and Grossi-de-Sa, M. F. 2016. The recombinant pea defensin Drr230a is active against impacting soybean and cotton pathogenic fungi from the genera *Fusarium*, *Colletotrichum* and *Phakopsora*. 3 Biotech. 6:1–10.

Leandro, L. F. S., Eggenberger, S., Chen, C., Williams, J., Beattie, G. A., and Liebman, M. 2018. Cropping system diversification reduces severity and incidence of soybean sudden death syndrome caused by *Fusarium virguliforme*. Plant Dis. 102:1748-1758.

Leslie, J. F., Summerell, B. A., and Bullock, S. 2008. The *Fusarium* laboratory manual. Hoboken, NJ: Wiley. ISBN: 978-0-813-81919-8

Li, S., Hartman, G. L., and Widholm, J. M. 1999. Viability staining of soybean suspension-cultured cells and a seedling stem cutting assay to evaluate phytotoxicity of *Fusarium solani* f. sp. *glycines* culture filtrates. Plant Cell Reports. 18:375-380.

Li, S., Hartman, G. L., and Chen, Y. 2009. Evaluation of aggressiveness of *Fusarium virguliforme* isolates that cause soybean sudden death syndrome. J. Plant Pathol. 91:77–86.

Li, X., Beeson IV, W. T., Phillips, C. M., Marletta, M. A., and Cate, J. H. D. 2012. Structural basis for substrate targeting and catalysis by fungal polysaccharide monooxygenases. Structure. 20:1051–1061.

Lightfoot, D. A. 2015. Two decades of molecular marker-assisted breeding for resistance to soybean sudden death syndrome. Crop Sci. 55:1460–1484.

Liu, Z., Gao, Y., Kim, Y. M., Faris, J. D., Shelver, W. L., de Wit, P. J. G. M., Xu, S. S., and Friesen, T. L. 2016. SnTox1, a *Parastagonospora nodorum* necrotrophic effector, is a dual-function protein that facilitates infection while protecting from wheat-produced chitinases. New Phytol. 211:1052–1064.

Liu, Z., Zhang, Z., Faris, J. D., Oliver, R. P., Syme, R., McDonald, M. C., McDonald, B. A., Solomon, P. S., Lu, S., Shelver, W. L., Xu, S., and Friesen, T. L. 2012. The cysteine rich necrotrophic effector SnTox1 produced by *Stagonospora nodorum* triggers susceptibility of wheat lines harboring Snn1. PLoS Pathog. 8: e1002467.

Lloyd, M. 1967. Mean crowding. J. Anim. Ecol. 36:1-30.

Luckew, A. S., Leandro, L. F., Bhattacharyya, M. K., Nordman, D. J., Lightfoot, D. A., and Cianzio, S. R. 2013. Usefulness of 10 genomic regions in soybean associated with sudden death syndrome resistance. Theor. Appl. Genet. 126:2391–2403.

Luo, Y., Hildebrand, K., Chong, S. K., Myers, O., and Russin, J. S. 2000. Soybean yield loss to sudden death syndrome in relation to symptom expression and root colonization by *Fusarium solani* f. sp. *glycines*. Plant Dis. 84:914–920.

Ma, L.-J., van der Does, H. C., Borkovich, K. A., Coleman, J. J., Daboussi, M.-J., Di Pietro, A., Dufresne, M., Freitag, M., Grabherr, M., Henrissat, B., Houterman, P. M., Kang, S., Shim, W.-B., Woloshuk, C., Xie, X., Xu, J.-R., Antoniw, J., Baker, S. E., Bluhm, B. H., Breakspear, A., Brown, D. W., Butchko, R. A. E., Chapman, S., Coulson, R., Coutinho, P. M., Danchin, E. G. J., Diener, A., Gale, L. R., Gardiner, D. M., Goff, S., Hammond-Kosack, K. E., Hilburn, K., Hua-Van, A., Jonkers, W., Kazan, K., Kodira, C. D., Koehrsen, M., Kumar, L., Lee, Y.-H., Li, L., Manners, J. M., Miranda-Saavedra, D., Mukherjee, M., Park, G., Park, J., Park, S.-Y., Proctor, R. H., Regev, A., Ruiz-Roldan, M. C., Sain, D., Sakthikumar, S., Sykes, S., Schwartz, D. C., Turgeon, B. G., Wapinski, I., Yoder, O.,

Young, S., Zeng, Q., Zhou, S., Galagan, J., Cuomo, C. A., Kistler, H. C., and Rep, M. 2010. Comparative genomics reveals mobile pathogenicity chromosomes in *Fusarium*. Nature. 464:367-373.

MacCready, J. S., Schossau, J., Osteryoung, K. W., and Ducat, D. C. 2017. Robust Min-system oscillation in the presence of internal photosynthetic membranes in cyanobacteria. Mol. Microbiol. 103:483–503.

Mackey, D., Belkhadir, Y., Alonso, J. M., Ecker, J. R., and Dangl, J. L. 2003. *Arabidopsis* RIN4 is a target of the type III virulence effector AvrRpt2 and modulates RPS2-mediated resistance. Cell. 112:379–389.

Mackey, D., Holt III, B. F., Wiig, A., and Dangl, J. L. 2002. RIN4 interacts with *Pseudomonas syringae* type III effector molecules and is required for RPM1-mediated resistance in *Arabidopsis*. Cell. 108:743–754.

Manning, V. A., and Ciuffetti, L. M. 2005. Localization of Ptr ToxA produced by *Pyrenophora tritici-repentis* reveals protein import into wheat mesophyll cells. Plant Cell. 17:3203–3212.

Manning, V. A., Hardison, L. K., and Ciuffetti, L. M. 2007. Ptr ToxA interacts with a chloroplast-localized protein. Mol. plant-microbe Interact. 20:168–177.

Mansouri, S. 2012. Electrophoretic karyotype variation among Fusarium virguliforme isolates. In: IDENTIFICATIN AND CHARACTERIZATION OF PATHOGENICITY GENES IN FUSARIUM VIRGULIFORME, THE CAUSAL AGENET OF SUDDEN DEATH SYNDROME (SDS) IN SOYBEAN. Available at: https://opensiuc.lib.siu.edu/dissertations/573/.

Mansouri, S., Van Wijk, R., Rep, M., and Fakhoury, A. M. 2009. Transformation of *Fusarium virguliforme*, the causal agent of sudden death syndrome of soybean. J. Phytopathol. 157:319–321.

Marburger, D., Conley, S., Esker, P., MacGuidwin, A., and Smith, D. 2014. Relationship between *Fusarium virguliforme* and *Heterodera glycines* in commercial soybean fields in Wisconsin. Plant Heal. Prog. 15:11–18.

Martin, M. J., Riedel, R. M., and Rowe, R. C. 1982. *Verticillium dahliae* and *Pratylenchus penetrans*: Interactions in the early dying complex of potato in Ohio. Phytopathology. 72:640-644.

Marquez, N., Giachero, M. L., Gallou, A., Debat, H. J., Declerck, S., and Ducasse, D. A. 2019. Transcriptome analysis of mycorrhizal and nonmycorrhizal soybean plantlets upon infection with *Fusarium virguliforme*, one causal agent of sudden death syndrome. Plant Pathol. 68:470–480.

McLean, K. S., and Lawrence, G. W. 1993. Interrelationship of *Heterodera glycines* and *Fusarium solani* in sudden death syndrome of soybean. J. Nematol. 25:434–439.

McLean, K. S., and Lawrence, G. W. 1995. Development of *Heterodera glycines* as affected by *Fusarium solani*, the causal agent of sudden death syndrome of soybean. J Nematol. 27:70–77.

Meksem, K., Doubler, T. W., Chancharoenchai, K., Njiti, V. N., Chang, S. J. C., Rao Arelli, A. P., Cregan, P. E., Gray, L. E., Gibson, P. T., and Lightfoot, D. A. 1999. Clustering among loci underlying soybean resistance to *Fusarium solani*, SDS and SCN in near-isogenic lines. Theor. Appl. Genet. 99:1131–1142.

Menke, J., Weber, J., Broz, K., and Kistler, H. C. 2013. Cellular development associated with induced mycotoxin synthesis in the filamentous fungus *Fusarium graminearum*. PLoS One. 8:e63077.

Mila, A. L., Carriquiry, A. L., and Yang, X. B. 2004. Logistic regression modeling of prevalence of soybean *Sclerotinia* stem rot in the north-central region of the United States. Phytopathology. 94:102–110.

Mitchum, M. G., Hussey, R. S., Baum, T. J., Wang, X., Elling, A. A., Wubben, M., and Davis, E. L. 2013. Nematode effector proteins: An emerging paradigm of parasitism. New Phytol. 199:879–894.

Muhammed, M., Coleman, J. J., and Mylonakis, E. 2012a. *Caenorhabditis elegans*: A nematode infection model for pathogenic fungi. In Host-Fungus Interactions: Methods and Protocols, eds. Alexandra C Brand and Donna M MacCallum. Totowa, NJ: Humana Press, p. 447–454.

Muhammed, M., Fuchs, B. B., Wu, M. P., Breger, J., Coleman, J. J., and Mylonakis, E. 2012b. The role of mycelium production and a MAPK-mediated immune response in the *C. elegans*-*Fusarium* model system. Med. Mycol. 50:488–496.

Navi, S. S., and Yang, X. B. 2008. Foliar symptom expression in association with early infection and xylem colonization by *Fusarium virguliforme* (formerly *F. solani* f. sp. *glycines*), the causal agent of soybean sudden death syndrome. Plant Heal. Prog. DOI:10.1094/PHP-2008-0222-01-RS.

Navi, S. S., and Yang, X. B. 2016. Impact of crop residue and corn-soybean rotation on the survival of *Fusarium virguliforme* a causal agent of sudden death syndrome of soybean. J. Plant Pathol. Microbiol. 7:1–7.

Niblack, T. L., Arelli, P. R., Noel, G. R., Opperman, C. H., Orf, J. H., Schmitt, D. P., Shannon, J. G., and Tylka, G. L. 2002. A revised classification scheme for genetically diverse populations of *Heterodera glycines*. J. Nematol. 34:279–88.

Niblack, T. L., Lambert, K. N., and Tylka, G. L. 2006. A model plant pathogen from the kingdom animalia: *Heterodera glycines*, the soybean cyst nematode. Annu. Rev. Phytopathol. 44:283–303.

Nishizawa, K., Kita, Y., Kitayama, M., and Ishimoto, M. 2006. A red fluorescent protein, DsRed2, as a visual reporter for transient expression and stable transformation in soybean. Plant Cell Rep. 25:1355–1361.

Njiti, V. N., Johnsona, J. E., Torto, T. A., Gray, L. E., and Lightfoot, D. A. 2001. Inoculum rate influences selection for field resistance to soybean sudden death syndrome in the greenhouse. Crop Sci. 41:1726–1731.

Noble, W. S. 2009. How does multiple testing correction work? Nature Biotech. 27:1135-1137.

Noel, G. R., and Edwards, D. I. 1996. Population development of *Heterodera glycines* and soybean yield in soybean-maize rotations following introduction into a noninfested field. J. Nematol. 28:335–342.

Noon, J. B., Hewezi, T., Maier, T. R., Simmons, C., Wei, J.-Z., Wu, G., Llaca, V., Deschamps, S., Davis, E. L., Mitchum, M. G., Hussey, R. S., and Baum, T. J. 2015. Eighteen new candidate effectors of the phytonematode *Heterodera glycines* produced specifically in the secretory esophageal gland cells during parasitism. Phytopathology. 105:1362–1372.

Nychka, D., Furrer, R., Paige, J., and Sain, S. 2017. fields: Tools for spatial data. doi: 10.5065/D6W957CT.

O'Brien, R. M. 2007. A caution regarding rules of thumb for variance inflation factors. Qual Quant. 41:673–690.

Oksanen, J., Blanchet, F. G., Friendly, M., Kindt, R., Legendre, P., McGlinn, D., Minchin, P. R., O'Hara, R. B., Simpson, G. L., Solymos, P., Stevens, M. H. H., Szoecs E., and Wagner H. 2018. vegan: Community ecology package. Available at: https://CRAN.R-project.org/package=vegan

Pantalone, V. R., Kenworthy, W. J., Slaughter, L. H., and James, B. R. 1997. Chloride tolerance in soybean and perennial *Glycine* accessions. Euphytica. 97:235–239.

Peberdy, J. F. 1979. Fungal protoplasts: Isolation, reversion, and fusion. Annu. Rev. Microbiol. 33:21–39.

Pichia Expression Kit User Guide. 2014. Pichia Expression Kit. Available at: https://www.thermofisher.com/document-connect/document-connect.html?url=https%3A%2F%2Fassets.thermofisher.com%2FTFS-Assets%2FLSG%2Fmanuals%2Fpich_man.pdf&title=UGljaGlhIEV4cHJlc3Npb24gS2l0.

Pichia expression vectors for selection on Zeocin and purification of recombinant proteins. 2010. pPICZ A, B, and C. Available at: https://www.thermofisher.com/document-connect/document-connect.html?url=https%3A%2F%2Fassets.thermofisher.com%2FTFS-Assets%2FLSG%2Fmanuals%2Fppiczalpha_man.pdf&title=cFBJQ1phbHBoYSBBLCBCIGFuZCBD.

Pincus, Z., Mazer, T. C., and Slack, F. J. 2016. Autofluorescence as a measure of senescence in *C. elegans*: Look to red, not blue or green. Aging. 8:889–898.

Pudake, R. N., Swaminathan, S., Sahu, B. B., Leandro, L. F., and Bhattacharyya, M. K. 2013. Investigation of the *Fusarium virguliforme fvtox1* mutants revealed that the FvTox1 toxin is involved in foliar sudden death syndrome development in soybean. Curr. Genet. 59:107–117.

Qi, M., Link, T. I., Müller, M., Hirschburger, D., Pudake, R. N., Pedley, K. F., Braun, E., Voegele, R. T., Baum, T. J., and Whitham, S. A. 2016. A small cysteine-rich protein from the Asian soybean rust fungus, *Phakopsora pachyrhizi*, suppresses plant immunity. PLoS Pathog. 12:1–29.

Radwan, O., Liu, Y., and Clough, S. J. 2011. Transcriptional analysis of soybean root response to *Fusarium virguliforme*, the causal agent of sudden death syndrome. Mol. Plant-Microbe Interact. 24:958–972.

Ramamoorthy, V., Govindaraj, L., Dhanasekaran, M., Vetrivel, S., Kumar, K. K., and Ebenezar, E. 2015. Combination of driselase and lysing enzyme in one molar potassium chloride is effective for the production of protoplasts from germinated conidia of *Fusarium verticillioides*. J. Microbiol. Methods. 111:127–134.

Rep, M., Van Der Does, H. C., Meijer, M., Van Wijk, R., Houterman, P. M., Dekker, H. L., De Koster, C. G., and Cornelissen, B. J. C. 2004. A small, cysteine-rich protein secreted by *Fusarium oxysporum* during colonization of xylem vessels is required for I-3-mediated resistance in tomato. Mol. Microbiol. 53:1373–1383.

Riga, E., Welacky, T., Potter, J., Anderson, T., Topp, E., and Tenuta, A. 2001. The impact of plant residues on the soybean cyst nematode, *Heterodera glycines*. Can. J. Plant Pathol. 23:168–173.

Rosseel, Y. 2012. lavaan: An R package for structural equation modeling. Journal of Statistical Software, 48(2), 1-36.

Rossman, D. R., Byrne, A. M., and Chilvers, M. I. 2018. Profitability and efficacy of soybean seed treatment in Michigan. Crop Prot. 114:44-52.

Roth, M. G., Noel, Z. A., Wang, J., Warner, F., Byrne, A. M., and Chilvers, M. I. 2019a. Predicting soybean yield and sudden death syndrome development using at-planting risk factors. Phytopathology. *Submitted*.

Roth, M. G. and Chilvers, M. I. 2019b. Protoplast generation and transformation methods for soybean sudden death syndrome causal agents *Fusarium virguliforme* and *F. brasiliense*. Fungal Biol. Biotechnol. *Submitted*.

Roth, M. G., Oudman, K. A., Griffin, A., Jacobs, J. L., Sang, H., and Chilvers, M. I. 2019c. Diagnostic qPCR assay to detect *Fusarium brasiliense*, a causal agent of soybean sudden death syndrome and root rot of dry bean. Plant Dis. *Accepted*.

Rowe, R. C., Riedel, R. M. and Martin, M. J. 1985. Synergistic interactions between *Verticillium dahliae* and *Pratylenchus penetrans* in potato early dying disease. Phytopathology. 75:412-418.

Roy, K. W., Hershman, D. E., Rupe, J. C., and Abney, T. S. 1997. Sudden death syndrome of soybean. Plant Dis. 81:1100–1111.

Roy, K. W., Lawrence, G. W., Hodges, H. H., McLean, K. S., and Killebrew, J. F. 1989. Sudden death syndrome of soybean: *Fusarium solani* as incitant and relation of *Heterodera glycines* to disease severity. Phytopathology. 79:191–197.

Rupe, J. C. 1989. Frequency and pathogenicity of *Fusarium solani* recovered from soybeans with sudden death syndrome. Plant Dis. 73:581–584.

Rupe, J. C., Sabbe, W. E., Robbins, R. T., and Gbur, E. E. 1993. Soil and plant factors associated with sudden-death syndrome of soybean. J. Prod. Agric. 6:218–221.

Sahu, B. B., Baumbach, J. L., Singh, P., Srivastava, S. K., Yi, X., and Bhattacharyya, M. K. 2017 Investigation of the *F. virguliforme* transcriptomes induced during infection of soybean roots suggests that enzymes with hydrolytic activities could play a major role in root necrosis. PLoS One. 12:e0169963.

Sainsbury, F., Thuenemann, E. C., and Lomonossoff, G. P. 2009. PEAQ: Versatile expression vectors for easy and quick transient expression of heterologous proteins in plants. Plant Biotechnol. J. 7:682–693.

Sang, H., Witte, A., Jacobs, J. L., Chang, H.-X., Wang, J., Roth, M. G., and Chilvers, M. I. 2018. Fluopyram sensitivity and functional characterization of SdhB in the *Fusarium solani* species complex causing soybean sudden death syndrome. Front. Microbiol. 9:1–12.

Scherm, H., and Yang, X. B. 1996. Development of sudden death syndrome of soybean in relation to soil temperature and soil water matric potential. Phytopathology. 86:642–649.

Scherm, H., Yang, X. B., and Lundeen, P. 1998. Soil variables associated with sudden death syndrome in soybean fields in Iowa. Plant Dis. 82:1152–1157.

Scherm, H. and Yang, X. B. 1999. Risk assessment for sudden death syndrome of soybean in the north-central United States. Agric. Syst. 59:301-310.

Schindelin, J., Arganda-Carreras, I., Frise, E., Kaynig, V., Longair, M., Pietzsch, T., Preibisch, S., Rueden, C., Saalfeld, S., Schmid, B., Tinevez, J. Y., White, D. J., Hartenstein, V., Eliceiri, K., Tomancak, P., and Cardona, A. 2012. Fiji: An open-source platform for biological-image analysis. Nat. Methods. 9:676–682.

Schoffelmeer, E. A. M., Klis, F. M., Sietsma, J. H., and Cornelissen, B. J. C. 1999. The cell wall of *Fusarium oxysporum*. Fungal Genet. Biol. 27:275–282.

Schwessinger, B., and Rathjen, J. P. 2017. Extraction of high molecular weight DNA from fungal rust spores for long read sequencing. Methods Mol. Biol. 1659:49–57.

Semighini, C. P., Murray, N., and Harris, S. D. 2008. Inhibition of *Fusarium graminearum* growth and development by farnesol. FEMS Microbiol. Lett. 279:259–264.

Senthil-Kumar, M., and Mysore, K. S. 2013. Nonhost resistance against bacterial pathogens: retrospectives and prospects. Annu. Rev. Phytopathol. 51:407–427.

Shannon, P., Markiel A., Ozier O., Baliga N. S., Wang J. T., Ramage D., Amin N., Schwikowski B., and Ideker T. 2003. Cytoscape: a software environment for integrated models of biomolecular interaction networks. Genome Res. 13:2498-504.

Shultz, J. L., Ali, S., Ballard, L., and Lightfoot, D. A. 2007. Development of a physical map of the soybean pathogen *Fusarium virguliforme* based on synteny with *Fusarium graminearum* genomic DNA. BMC Genomics. 8:262.

Shurtleff, M. C., and Averre III, C. W. 2000. Diagnosing plant diseases caused by nematodes. St. Paul, MN: APS Press. ISBN: 978-0890542545.

Simão, F. A., Waterhouse, R. M., Ioannidis, P., Kriventseva, E. V, and Zdobnov, E. M. 2015. BUSCO: assessing genome assembly and annotation completeness with single-copy orthologs. Bioinformatics. 31:3210–3212.

Singh, G. 2010. The Soybean: Botany, Production and Uses. ed. Guriqbal Singh. London: CAB International. ISBN: 9781845936440.

Sipes, S., B., Schmitt, P., D., Barker, and R., K. 1992. Fertility of three parasitic biotypes of *Heterodera glycines*. Phytopathology. 82:999–1001.

Soetaert, K. 2017. plot3D: Plotting multi-dimensional data. Available at: https://CRAN.R-project.org/package=plot3D.

Sparkes, I. A., Runions, J., Kearns, A., and Hawes, C. 2006. Rapid, transient expression of fluorescent fusion proteins in tobacco plants and generation of stably transformed plants. Nat. Protoc. 1:2019–2025.

Sperschneider, J., Gardiner, D. M., Thatcher, L. F., Lyons, R., Singh, K. B., Manners, J. M., and Taylor, J. M. 2015. Genome-wide analysis in three *Fusarium* pathogens identifies rapidly evolving chromosomes and genes associated with pathogenicity. Genome Biol. Evol. 7:1613–1627.

Srivastava, S. K., Huang, X., Brar, H. K., Fakhoury, A. M., Bluhm, B. H., and Bhattacharyya, M. K. 2014. The genome sequence of the fungal pathogen *Fusarium virguliforme* that causes sudden death syndrome in soybean. PLoS One. 9:e81832.

Srour, A. Y., Gibson, D. J., Leandro, L. F. S., Malvick, D. K., Bond, J. P., and Fakhoury, A. M. 2017. Unraveling microbial and edaphic factors affecting the development of sudden death syndrome in soybean. Phytobiomes. 1:91-101.

Srour, A., Afzal, A. J., Blahut-Beatty, L., Hemmati, N., Simmonds, D. H., Li, W., Liu, M., Town, C. D., Sharma, H., Arelli, P., and Lightfoot, D. A. 2012. The receptor like kinase at Rhg1-a/Rfs2 caused pleiotropic resistance to sudden death syndrome and soybean cyst nematode as a transgene by altering signaling responses. BMC Genomics. 13:1–18.

Stergiopoulos, I., and de Wit, P. J. G. M. 2009. Fungal effector proteins. Annu. Rev. Phytopathol. 47:233–263.

Swaminathan, S., Abeysekara, N. S., Knight, J. M., Liu, M., Dong, J., Hudson, M. E., Bhattacharyya, M. K., and Cianzio, S. R. 2018. Mapping of new quantitative trait loci for sudden death syndrome and soybean cyst nematode resistance in two soybean populations. Theor. Appl. Genet. 131:1047–1062.

Swaminathan, S., Das, A., Assefa, T., Knight, J. M., Da Silva, A. F., Carvalho, J. P. S., Hartman, G. L., Huang, X., Leandro, L. F., Cianzo, S. R., and Bhattacharyya, M. K. 2019. Genome wide association study identifies novel single nucleotide polymorphic loci and candidate genes involved in soybean sudden death syndrome resistance. PLoS One. 14:e0212071.

Takken, F., and Rep, M. 2010. The arms race between tomato and *Fusarium oxysporum*. Mol. Plant Pathol. 11:309–314.

Tan, R., Collins, P. J., Wang, J., Wen, Z., Boyse, J. F., Laurenz, R. G., Gu, C., Jacobs, J. L., Song, Q., Chilvers, M. I., and Wang, D. 2019. Different loci associated with root and foliar resistance to sudden death syndrome (*Fusarium virguliforme*) in soybean. Theor. Appl. Genet. 132:501–513

Tewoldemedhin, Y. T., Lamprecht, S. C., Geldenhuys, J. J., and Kloppers, F. J. 2014. First report of soybean sudden death syndrome caused by *Fusarium virguliforme* in South Africa. Plant Dis. 98:569–569.

Tewoldemedhin, Y. T., Lamprecht, S. C., Vaughan, M. M., Doehring, G., and O'Donnell, K. 2017. Soybean SDS in South Africa is caused by *Fusarium brasiliense* and a novel undescribed *Fusarium* sp. Plant Dis. 101:150–157.

Tylka, G. L. 2016. Understanding soybean cyst nematode HG types and races. Plant Heal. Prog. 17:149–151.

Uri, N. D. 2000. Perceptions on the use of no-till farming in production agriculture in the United States: An analysis of survey results. Agric. Ecosyst. Environ. 77:263–266.

USDA. 2019. World Agricultural Supply and Demand Estimates. Available at: https://www.usda.gov/oce/commodity/wasde/wasde0219.pdf.

van Dam, P., Fokkens, L., Ayukawa, Y., van der Gragt, M., ter Horst, A., Brankovics, B., Houterman, P. M., Arie, T., and Rep, M. 2017. A mobile pathogenicity chromosome in *Fusarium oxysporum* for infection of multiple cucurbit species. Sci. Rep. 7:1–15.

Varden, F. A., De la Concepcion, J. C., Maidment, J. H. R., and Benfeld, M. J. 2017. Taking the stage: effectors in the spotlight. Curr. Opin. Plant Biol. 38:25–33.

Venables, W. N., and Ripley, B. D. 2002. Modern applied statistics with S. Fourth Edition. Springer, New York. ISBN 0-387-95457-0.

Vick, C. M., Bond, J. P., Chong, S. K., and Russin, J. S. 2006. Response of soybean sudden death syndrome to tillage and cultivar. Can. J. Plant Pathol. 28:77–83.

Vick, C. M., Chong, S. K., Bond, J. P., and Russin, J. S. 2003. Response of soybean sudden death syndrome to subsoil tillage. Plant Dis. 87:629–632.

Vlaardingerbroek, I., Beerens, B., Rose, L., Fokkens, L., Cornelissen, B. J. C., and Rep, M. 2016a. Exchange of core chromosomes and horizontal transfer of lineage-specific chromosomes in *Fusarium oxysporum*. Environ. Microbiol. 18:3702–3713.

Vlaardingerbroek, I., Beerens, B., Schmidt, S. M., Cornelissen, B. J. C., and Rep, M. 2016b. Dispensable chromosomes in *Fusarium oxysporum* f. sp. *lycopersici*. Mol. Plant Pathol. 17:1455–1466.

Vu, V. Q. 2011. ggbiplot: A ggplot2 based biplot. Available at: http://github.com/vqv/ggbiplot.

Wang, X., Meyers, D., Yan, Y., Baum, T., Smant, G., Hussey, R., and Davis, E. 1999. *In planta* localization of a β-1,4-endoglucanase secreted by *Heterodera glycines*. Mol. Plant. Microbe. Interact. 12:64–67.

Wang, J., Niblack, T. L., Tremain, J. A., Wiebold, W. J., Tylka, G. L., Marett, C. C., Noel, G. R., Myers, O., and Schmidt, M. E. 2003. Soybean cyst nematode reduces soybean yield without causing obvious aboveground symptoms. Plant Dis. 87:623–628.

Wang, B., Swaminathan, S., and Bhattacharyya, M. K. 2015. Identification of *Fusarium virguliforme* FvTox1-interacting synthetic peptides for enhancing foliar sudden death syndrome resistance in soybean. PLoS One. 10:e0145156.

Wang, J., Jacobs, J. L., Byrne, J. M., and Chilvers, M. I. 2015. Improved diagnoses and quantification of *Fusarium virguliforme*, causal agent of soybean sudden death syndrome. Phytopathology. 105:378–387.

Wang, J., Bradley, C. A., Stenzel, O., Pedersen, D. K., Reuter-Carlson, U., and Chilvers, M. I. 2017. Baseline sensitivity of *Fusarium virguliforme* to fluopyram fungicide. Plant Dis. 101:576–582.

Wang, J., Jacobs, J. L., Roth, M. G., and Chilvers, M. I. 2018a. Temporal dynamics of *Fusarium virguliforme* colonization of soybean roots. Plant Dis. 103:19–27.

Wang, J., Sang, H., Jacobs, J. L., Oudman, K. A., Hanson, L. E., and Chilvers, M. I. 2018b. Soybean sudden death syndrome causal agent *Fusarium brasiliense* present in Michigan. Plant Dis. DOI: 10.1094/PDIS-08-18-1332-RE.

Weems, J. D., Haudenshield, J. S., Bond, J. P., Hartman, G. L., Ames, K. A., and Bradley, C. A. 2015. Effect of fungicide seed treatments on *Fusarium virguliforme* infection of soybean and development of sudden death syndrome. Can. J. Plant Pathol. 37:435–447.

Weigel, D., and Glazebrook, J. 2006. Transformation of *Agrobacterium* using the freeze-thaw method. Cold Spring Harb. Protoc. DOI: 10.1101/pdb.prot4666.

Wen, Z., Tan, R., Yuan, J., Bales, C., Du, W., Zhang, S., Chilvers, M. I., Schmidt, C., Song, Q., Cregan, P. B., and Wang, D. 2014. Genome-wide association mapping of quantitative resistance to sudden death syndrome in soybean. BMC Genomics. 15:809.

Westphal, A., Li, C., Xing, L., McKay, A., and Malvick, D. 2014. Contributions of *Fusarium virguliforme* and *Heterodera glycines* to the disease complex of sudden death syndrome of soybean. PLoS One. 9:1–13.

Wheeler, D. L., Scott, J., Dung, J. K. S., and Johnson, D. A. 2019. Evidence of a trans-kingdom plant disease complex between a fungus and plant-parasitic nematodes. PLoS One. 14:e0211508.

Wick, R. R., Schultz, M. B., Zobel, J., and Holt, K. E. 2015. Bandage: interactive visualisation of *de novo* genome assemblies. Bioinformatics. 31:3350–3352.

Wiemann, P., Brown, D. W., Kleigrewe, K., Bok, J. W., Keller, N. P., Humpf, H. U., and Tudzynski, B. 2010. FfVel1 and fflae1, components of a *velvet*-like complex in *Fusarium fujikuroi*, affect differentiation, secondary metabolism and virulence. Mol. Microbiol. 77:972–994.

Wiemann, P., Willmann, A., Straeten, M., Kleigrewe, K., Beyer, M., Humpf, H. U., and Tudzynski, B. 2009. Biosynthesis of the red pigment bikaverin in *Fusarium fujikuroi*: Genes, their function and regulation. Mol. Microbiol. 72:931–946.

Willbur, J. F., Fall, M. L., Bloomingdale, C., Byrne, A. M., Chapman, S. A., Magarey, R. D., McCaghe, M. M., Bueller, B. D., Russo, J. M., Schlegel, J., Chilvers, M. I., Mueller, D. S., Kabbage, M., and Smith, D. L. 2018a. Weather-based models for assessing the risk of *Sclerotinia sclerotiorum* apothecial presence in soybean (*Glycine max*) fields. Plant Dis. 102:73–84.

Willbur, J. F., Fall, M. L., Byrne, A. M., Chapman, S. A., McCaghey, M. M., Mueller, B. D., Schmidt, R., Chilvers, M. I., Mueller, D. S., Kabbage, M., Giesler, L. J., Conley, S. P., and Smith, D. L. 2018b. Validating *Sclerotinia sclerotiorum* apothecial models to predict *Sclerotinia* stem rot in soybean (*Glycine max*) fields. Plant Dis. 102:2592–2601.

Wolpert, T. J., Dunkle, L. D., and Ciuffetti, L. M. 2002. Host-selective toxins and avirulence determinants: What's in a name? Annu. Rev. Phytopathol. 40:251–285.

Wrather, A., and Koenning, S. 2009. Effects of diseases on soybean yields in the United States 1996 to 2007. Plant Heal. Prog. DOI:10.1094/PHP-2009-0401-01-RS.

Xiang, Y., Scandiani, M. M., Herman, T. K., and Hartman, G. L. 2015. Optimizing conditions of a cell-free toxic filtrate stem cutting assay to evaluate soybean genotype responses to *Fusarium* species that cause sudden death syndrome. Plant Dis. 99:502–507.

Xing, L., and Westphal, A. 2013. Synergism in the interaction of *Fusarium virguliforme* with *Heterodera glycines* in sudden death syndrome of soybean. J. Plant Dis. Prot. 120:209–217.

Yamada, T., Takagi, K., and Ishimoto, M. 2012. Recent advances in soybean transformation and their application to molecular breeding and genomic analysis. Breed. Sci. 61:480–494.

Yoshino, K., Irieda, H., Sugimoto, F., Yoshioka, H., Okuno, T., and Takano, Y. 2012. Cell death of *Nicotiana benthamiana* is induced by secreted protein NIS1 of *Colletotrichum orbiculare* and is suppressed by a homologue of CgDN3. Mol. Plant-Microbe Interact. 25:625–636.

Young, L. D. 1996. Yield loss in soybean caused by *Heterodera glycines*. Suppl. to J. Nematol. 28:604–607.

Zhang, Y., Choi, Y.-E., Zou, X., and Xu, J.-R. 2011. The FvMK1 mitogen-activated protein kinase gene regulates conidiation, pathogenesis, and fumonisin production in *Fusarium verticillioides*. Fungal Genet. Biol. 48:71–79.